PHASE BEHAVIOR AND THERMAL PROPERTIES OF POLYELECTROLYTE COMPLEXES

A Dissertation

by

YANPU ZHANG

Submitted to the Office of Graduate and Professional Studies of
Texas A&M University
in partial fulfillment of the requirements for the degree of

DOCTOR OF PHILOSOPHY

Chair of Committee,	Jodie L. Lutkenhaus
Committee Members,	Zhengdong Cheng
	Yossef Elabd
	Svetlana A. Sukhishvili
Head of Department,	M. Nazmul Karim

May 2018

Major Subject: Chemical Engineering

ABSTRACT

Polyelectrolyte complexes (PECs) are formed by mixing oppositely charged polyelectrolyte solutions together. They have numerous applications in industry and advanced material areas. PECs are receiving increasing attention because of their stimuli-responsive behaviors to external conditions, such as ionic strength, pH, and temperature. In this dissertation, the phase behavior and thermal properties of PECs are explored.

The influence of polycation/polyanion mixing ratio and ionic strength on the phase behavior of PECs in aqueous state are investigated. The PECs consist of poly(diallyldimethylammonium chloride) (PDADMAC) and poly(sodium 4-styrenesulfonate) (PSS). PECs are formed by mixing PDADMA and PSS solutions together rapidly. It then takes minutes to days for the primary PECs to aggregate and precipitate. Turbidity and hydrodynamic size of PECs are recorded at different times. The results mark the colloidally stable, unstable, and solution boundaries and establish a phase diagram based on the mixing ratio and salt concentration. Molecular dynamic (MD) simulations are also performed to investigate the microscopic structure and effective charge distribution of PECs. PECs transit from colloidally stable to unstable when the mixing ratio reaches stoichiometric condition. Salt screening effect becomes stronger with increasing salt concentration, which induces the phase change from unstable to solution states.

The thermal properties of PECs containing weak polyelectrolytes, poly(allylamine hydrochloride) (PAH) and poly(acrylic acid) (PAA), are investigated using modulated differential scanning calorimetry (DSC). The properties of PECs are significantly

influenced by complexation pH. As pH increases, PAA mol% within PECs decreases and PAA degree of ionization increases. Modulated DSC results show that hydrated PECs undergo a glass-transition-like thermal event. The glass transition temperature (T_g) decreases with increasing water content or decreasing pH. All T_g collapse into one master curve when plotted against the ratio of water to intrinsic ion pair (polycation-polyanion). The effect of water-solvent mixtures on T_g is also examined, including 1-propanol and propanediols. T_g only depends on water content, implying that organic solvents exhibit no plasticization effect. The results suggest that water works as nontraditional plasticizer to PECs by reducing the electrostatic attractions of intrinsic ion pairs.

Thermal behaviors of PDADMAC–PSS complexes are investigated using modulated DSC and all-atom MD simulations. T_g of hydrated PECs decreases with increasing salt doping level or with increasing water content. The ratio of water to intrinsic ion pair influences T_g in PDADMAC–PSS system, following a linear relationship $1/T_g \sim \ln\left(\frac{n_{\text{water}}}{n_{\text{intrinsic ion pair}}}\right)$. The activation energy obtained from this van't Hoff plot is close to the value of restructuring one hydrogen bond. MD simulations of PDADMA−PSS directly observed the intrinsic and extrinsic ion pairs separately, showing that the T_g was connected to a decrease in hydrogen bonds between water−PSS at intrinsic ion pairs. The results imply an underlying mechanism for the glass transition: water plasticizes the PECs by weakening intrinsic ion pairing, and water surrounding the intrinsic ion pair facilitates the sliding motion and relaxation of polyelectrolytes within the assembly. This finding impacts current interpretations of relaxation dynamics in charged assemblies and points to water's important contribution at the molecular level.

ACKNOWLEDGEMENTS

I would like to express deep appreciation to my research advisor, Dr. Jodie L. Lutkenhaus, for the support and patient mentoring she had given me throughout my Ph.D. program. She trained and guided me to become an independent researcher in the academic field. She is an excellent mentor that I will always remember and follow. I have learned so much things from her, including conducting research, mentoring students, writing papers, and giving presentations. I also would like to thank my collaborator, Dr. Maria Sammalkorpi. With her contribution to our research project, we made huge progress and publish several papers.

I would like to thank Dr. Yossef Elabd, Dr. Svetlana Sukhishvili and Dr. Zhengdong Cheng for taking their time to serve on my committee, and for their valuable suggestions and guidance in completing my research. They helped me through the committee meeting every year and the preliminary exam.

I also would like to show gratitude for my lab members, my collaborators at Aalto University, and the undergraduate students I mentored at Texas A&M. They were very helpful in the lab. I would like to thank all the colleagues and members I work with, in Chemical Engineering Graduate Student Association and Society of Plastic Engineers.

Many thanks to all my friends at Texas A&M, and China Hong Dancing Society. I am so fortunate to meet many great people and make friends with them. They give me the courage to overcome the frustrations and failures encountered in the research. I will always remember the enjoyable time we have. Finally, I want to thank my family for their always support. Their love gives me courage and confidence to pursuit my dream. I would

like to thank my husband, Dr. Shaohong Liu. He always supports me during my toughest times.

CONTRIBUTORS AND FUNDING SOURCES

Contributors

This work was supervised by a dissertation committee consisting of Professor Jodie L. Lutkenhaus, Professors Zhengdong Cheng and Yossef Elabd of the Department of Chemical Engineering Department, and Professor Svetlana A. Sukhishvili of the Department of Material Science and Engineering.

The molecular dynamic simulation for Chapter II and IV was provided by Professor Maria Sammalkorpi of the Department of Chemistry at Aalto University. All other work conducted for the dissertation was completed by the student independently.

Funding Sources

Graduate study and this dissertation work were supported in part by National Science Foundation under Grant Number 1312676 and Grant Number 1609696.

NOMENCLATURE

PEC	Polyelectrolyte complex
PEM	Polyelectrolyte multilayer
PDADMAC	Poly(diallyldimethylamonium chloride)
PSS	Poly(sodium 4-styrenesulfonate)
DSC	Differential scanning calorimetry
T_g	Glass transition temperature
T_{tr}	Thermal transition temperature
MD	Molecular dynamic
FTIR	Fourier-transform infrared spectroscopy
NAA	Neutron activation analysis spectroscopy
NMR	Nuclear magnetic resonance
DLS	Dynamic light scattering
EIS	Electrochemical impedance spectroscopy

TABLE OF CONTENTS

Page

LIST OF FIGURES

FIGURE Page

FIGURE Page

FIGURE Page

FIGURE Page

LIST OF TABLES

CHAPTER I

INTRODUCTION AND LITERATURE REVIEW

1.1 Introductory remarks

Polyelectrolyte assemblies, including polyelectrolyte complexes (PECs) and polyelectrolyte multilayers (PEMs), are formed by the molecular level interactions of oppositely charged polyelectrolytes. They have many applications in fields such as membrane separation, pharmaceutical engineering, energy storage, and sensors.[1-4] Their properties can be tunable during fabrication. After preparation, they also have sensitive responses to external stimuli, such as solvent, pH, and temperature.

There are numerous reported works focusing on the formation and internal structure of polyelectrolyte assemblies. However, the investigations about the temporal colloidal stability and thermal behaviors of PECs and PEMs are rare. So in this dissertation, the colloidal stability of PECs in aqueous media and their thermal properties were studied. The future work will discuss the thermal properties of PECs in contact with divalent electrolytes. The significance of this work includes a better understanding of the colloidal stability of PECs, thermal properties of PECs and PEMs, and key factors in controlling these behaviors.

1.2 Polyelectrolyte complexes and multilayers

1.2.1 Polyelectrolyte complexes

Polyelectrolytes, also known as polyions, are a group of polymers carrying anionic or cationic charges on each of their repeating units. Small ions, which associate with the charged groups to maintain electroneutrality, are called counterions. When dissolved in polar solvent, the ionizable groups on polyelectrolyte chains can dissociate and release small counterions into the solution, with charges staying on the polymer chains.[5] The strong electrostatic interactions arising from the charged groups result in different properties of polyelectrolyte solutions from neutral polymer solutions.

There are several types of classifications of polyelectrolytes. Based upon the charged groups, they can be classified as polycations when containing positive charges, or polyanions when bearing negatively charged groups. On the basis of their origins, polyelectrolytes are either natural material, such as DNA, polypeptide, and humic acid, or synthetic ones, including polyacrylates and polymethacrylates. From the dissociation extent of charged groups, there are strong and weak polyelectrolytes. In strong polyelectrolytes, the charged groups are all disassociated in solution regardless of pH. In the case of weak polyelectrolytes, the degree of ionization is controlled by the solution pH. In this dissertation, we study one pair of strong polyelectrolytes, poly(diallyldimethylammonium chloride) (PDADMAC) and poly(sodium 4-styrene sulfonate) (PSS), and another pair of weak polyelectrolytes, poly(allylamine hydrochloride) (PAH) and poly(acrylic acid) (PAA). The chemical structures of these polyelectrolytes are shown in Figure 1.1.

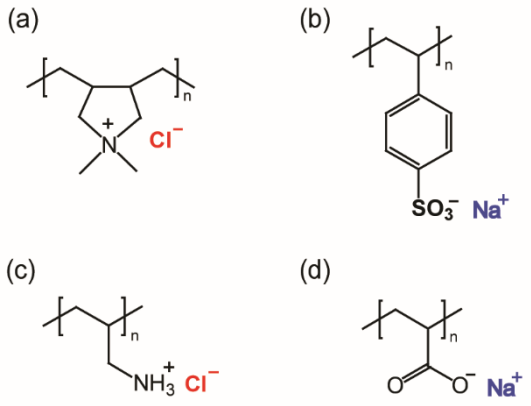

Figure 1.1. Chemical structures of (a) poly(diallyldimethylammonium chloride) (PDADMAC), (b) poly(sodium 4-styrene sulfonate) (PSS), (c) poly(allylamine hydrochloride) (PAH) and (d)poly(acrylic acid) (PAA).

Polyelectrolyte complexes (PECs) are usually formed by mixing oppositely charged polyelectrolyte solutions together. Figure 1.2 presents the formation of the PECs, with the release of counterions.[6] The PEC phase can be viewed as the dense polycation and polyanion chains held together using fluctuating electrostatic interactions.[7] The intermolecular electrostatic interactions function as physical crosslinks.[5, 8-10]

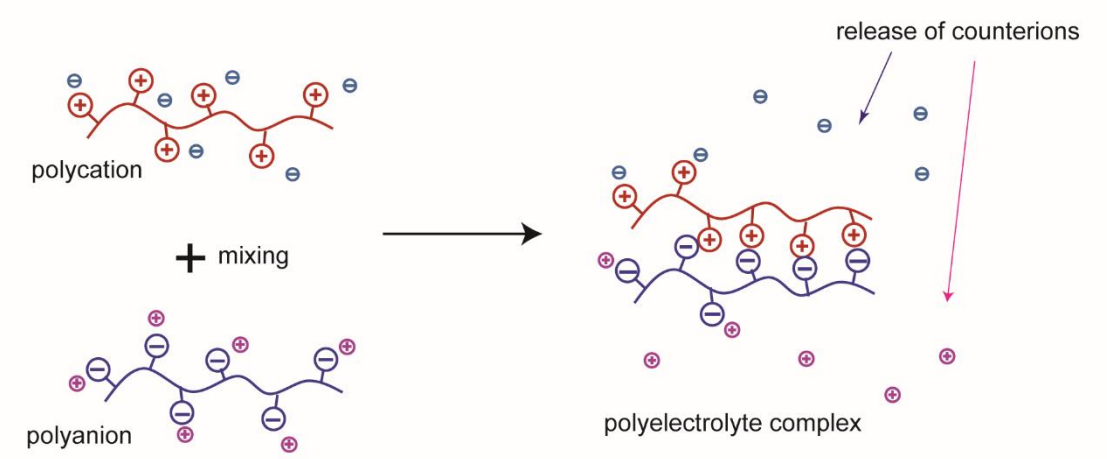

Figure 1.2. Schematic depiction of polyelectrolyte complex formation with the release of the counterions.

PEC formation process can also be presented as a reaction in Equation 1.1:[11]

$$Pol^+A^-_{aq} + Pol^-M^+_{aq} \rightarrow Pol^+Pol^-_s + M^+A^-_{aq} \qquad 1.1$$

where M^+ and A^- are counterions associating with charges on the polyelectrolyte chains. The formed solid PECs can also be dissolved in high salt concentration solution. This process is called "salt doping", the inverse reaction of Equation 1.1, represented by

$$Pol^+Pol^- + M^+A^- \rightarrow Pol^+A^- + Pol^-M^+ \qquad 1.2$$

The molecular association between polycation and polyanion repeat unites are defined as "intrinsic ion pairing," while the interactions between counterions and the polyelectrolytes refer to "extrinsic ion pairing." The intrinsic and extrinsic sites of PECs are shown in Figure 1.3.[12] The formation process of PECs is mainly an entropically driven process with only 0 to 10% contribution from enthalpic component, as studied by isothermal titration calorimetry (ITC).[11, 13] With respect to time, the stopped-flow mixing

technique with light scattering showed that the formation process of PECs was very fast and within 1 second. The order of mixing or the mixing method altered the structure of PECs, indicating the kinetic feature of the materials.[14]

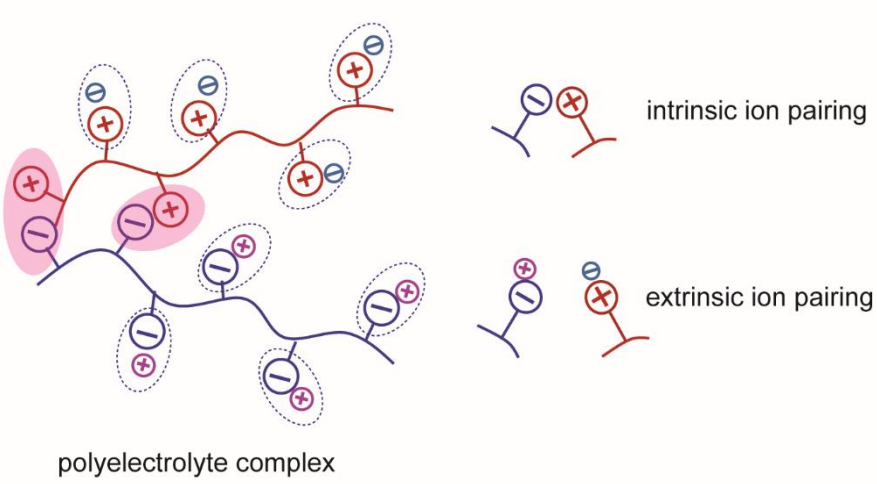

Figure 1.3. Intrinsic and extrinsic ion pairing in polyelectrolyte complexes.

The doping level y is the fraction of extrinsic ion pairing in PECs, as shown in Equation 1.3:[11]

$$y = \frac{M^+A^-}{Pol^+Pol^-} = \frac{A^-}{Pol^+} = \frac{M^+}{Pol^-} \qquad 1.3$$

Water molecules are involved when PECs are formed in aqueous solution, since the charged groups are hydrated with water molecules around them, as shown in Equation 1.4.[15] The water molecules strongly influence the physical properties of PECs since water has a dramatic plasticization effect on the materials.

$$Pol^+A^- \cdot aH_2O + Pol^-M^+ \cdot bH_2O \rightarrow Pol^+Pol^- \cdot dH_2O + zH_2O + M^+A^- \qquad 1.4$$

PEC formation and phase separation in solution has been studied intensively. The formation depends on both the chemistry of polymers, including backbone structure,[16] charge density, and degree of ionization,[17] and the formation external conditions, such as the total polyelectrolyte concentration,[18] the mixing ratio,[19] mixing order,[20] adding salt type,[21] ionic strength,[22] and pH of the solutions.[23] Different molecular interactions are involved during the formation of PECs, including electrostatic interactions, hydrogen bonding, and hydrophobic interactions.[24]

The PECs produced from aqueous solution result in various appearances: solid-like precipitate, liquid-like coacervate, and quasi-soluble polyelectrolyte solutions.[25] Solid precipitate PECs are generally prepared from strong polyelectrolytes at stoichiometric condition with medium salt concentration.[26] Coacervate, liquid phase separation, is usually yielded from weak or bio- polyelectrolytes. [7, 25] At very high salt concentration, the solid PECs could be dissolved due to salt doping, forming quasi-soluble polyelectrolyte solutions.[25] The phase diagram of PECs at varying conditions has been investigated in many types of PECs, such as PAH−PAA[25] or poly(lysine)−poly(glutamic acid).[27]

PECs can be used in the oil industry and flocculation applications.[28] Recently, PECs have been studied for soft and bio- materials because PECs doped with salt show soft and viscous liquid-like properties. Dynamic mechanical properties of poly(methacrylic acid) (PMAA)−PDADMA complexes were comparable to nucleus pulposus.[29] PECs consisting of branched poly(ethylene imine) (PEI) and PAA exhibited self-healing ability as in contact with NaCl solution and acid or base solutions.[30] PECs

could entirely disassociate in high salt concentration solutions, which further improved the processibility of the materials.[31, 32] For example, PECs consisting of PDADMA and PSS could be dissolved in 2.5 M KBr solution. The PEC solution could be used to prepare spin coating films[31] and hollow microcapsules.[32] Those template- and surfactant-free microcapsules could easily encapsulate molecules and nanoparticles.[32]

1.2.2 Polyelectrolyte multilayers

Polyelectrolyte multilayers (PEMs), also known as layer-by-layer (LbL) films, are fabricated from alternating depositions of oppositely charged polyelectrolytes on substrates, with rinsing steps in between to remove weakly bound materials.[33-35] This technique was revitalized by Decher in polyelectrolyte film preparations.[33] At first, the method was to immerse or dip a substrate into solutions. Gradually, many other methods have been developed to allow quicker PEM building process. Three different methods are shown in Figure 1.4 as (a) immersive, (b) spin, and (c) spray-fluidic assembly.[36] The thickness of PEMs can be easily controlled by the number of deposition cycles. It allows the coating on almost any shape of substrates, including plane and spherical shapes.

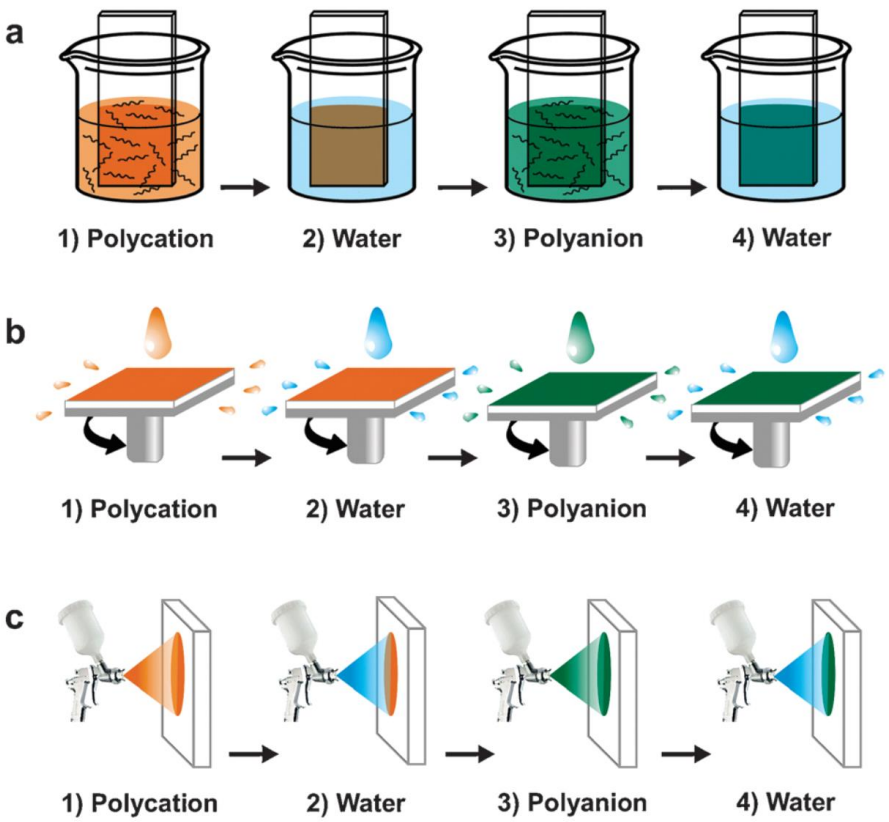

Figure 1.4. Schematic illustration of the three distinct technology categories for PEM assembly. Reprinted with permission.[36] Copyright (2012) The Royal Society of Chemistry.

The growth and internal structures of PEMs are strongly influenced by the salt concentration of assembly solutions. PDADMA/PSS films grew linearly without salt and they became exponentially growing films when assembled from 0.25 to 1.25 M NaCl solutions.[34] For the case of weak polyelectrolyte, pH dramatically changes the formation of PEMs due to the change in degree of ionization of weak polyelectrolytes. In PAH/PAA multilayer films, the precise control of the PEM thickness was realized by changing the pH of assembly solutions. When the polyelectrolyte changed from a fully charged state to

70-90% charge units, a transition of thin flat PEM to a relative thicker one occurred.[37] Using quartz-crystal microbalance with dissipation (QCM-D) and ellipsometry, five different film growth regimes were identified, which directly correlated film growth to the solutions pH.[38]

The internal structure of PEMs are fuzzy and interpenetrated, rather than perfectly stratified. The interdiffusion of polyelectrolyte during assembly account for this fuzzy structure.[33, 39] After assembly, salt ions can dope into PEMs and break intrinsic ion pairing by immersing PEMs into a high salt concentration solution. Salt doping leads to an increase of polyelectrolyte chain mobility because it induces disentanglement of PEMs. The freshly prepared, non-equilibrium PEMs could be annealed in water and salt solution at high temperatures, diminishing roughness.[40] The results showed that the interpenetration of PEMs increased by both salt and temperature.[39] The diffusion coefficient of polyelectrolyte was revealed to be influenced exponentially by the salt concentration in the annealing solution.[41] The interdiffusion of chitosan through swollen poly(ethylene oxide) (PEO) /PAA multilayer films was studied and the results showed that the PEO was replaced by chitosan during the diffusion process due to stronger electrostatic interactions between chitosan and PAA.[42]

Because PEMs has many advantages as thin films, they have been used in a wide range of applications, such as multivalent ion separation,[43] drug delivery,[44] gas barrier,[45] and tissue repairing.[46] PEMs coated with very little active biological proteins showed excellent bone repair efficacy because the nanolayered coating bridged the defects and restored the bone tissue.[46]

1.2.3 Comparison of PECs and PEMs

PECs are made by mixing polyelectrolytes in bulk solution, while PEMs are prepared by a layer-by-layer deposition process of polyelectrolyte on a substrate. PECs phase separation can lead to precipitate, coacervate, or liquid materials. Two types of growing processes have been reported in PEMs that the film thickness either increases linearly or exponentially as a function of the number of deposition steps. The molecular interactions between these two systems are the same, including electrostatic interactions, hydrogen bonding, and hydrophobic forces. The compositions are different in PECs and PEMs. PECs prepared at stoichiometric mixing ratio contain almost the same amount of polycation and polyanion, while the composition of PEMs is nonstoichiometric. Ghostine et al. reported the asymmetric growth in PDADMA/PSS multilayers.[47]

Previous research has attempted to correlate the phase behavior of PECs and growth kinetics of PEMs. Salt induced the phase separation in PECs and also changed the deposition mass of polyelectrolytes on each step during PEM assembly. Salt concentration made a rational connection between PECs and PEMs consisting of quaternized poly(4-vinylpyridine) (QPVP) and PMAA.[48] The maximum mass of PECs precipitated from QPVP−PMAA and the largest polymer deposition mass of PEMs occurred at the same salt concentration.[48]

Laugel et al. correlated the growth regimes of PEMs and the reaction enthalpy of PECs formed from the same pair of polycations and polyanions. Isothermal titration microcalorimetry results indicated that an endothermic PEC formation process correlated

to an exponential film growth. A strong exothermic process of PECs was linked to the linearly growth PEMs.[49]

Salehi et al. compared the phase behavior of PECs and growth kinetics of PEMs, using one type of polyanion, PAA, and three different types of polycations, PAH, poly(N,N-dimethylaminoethyl methacrylate) (PDMAEMA) and PDADMAC. The interaction strength or the phase behavior of PECs showed a nonmonotonic effect on the corresponding PEM growth kinetics. In addition to electrostatic interactions as the driving force, other secondary interactions, including hydrogen bonding, ion-dipole force, and hydration, exhibited a profound effect on the formation kinetic of both PECs and PEMs. The critical salt concentration rationalized part of the PEM growth behavior.[50]

1.3 Phase behavior of PECs in aqueous solution

PECs formed in aqueous solution show different phase behaviors and morphologies depending on internal and external conditions.[11] The molecular interactions or ion pairing within PECs are important since it decides the crosslinking density and mechanical properties of the materials.[51] There are two types of topologies: ladder and network, as presented in Figure 1.5.[51] A ladder structure is a sequential segment on a polyelectrolyte backbone forming ion pairs with an oppositely charged sequential polyelectrolyte. Alternating segment pairing with different polyelectrolyte chains forms a network topology. In reality, PEC structure is a mixture of both ladder and network topologies.[52] The ladder structure is likely to form a liquid-like coacervate. The network structure shows that many polyelectrolyte chains are incorporated into a dense structure, which are easily to form solid precipitates.[52]

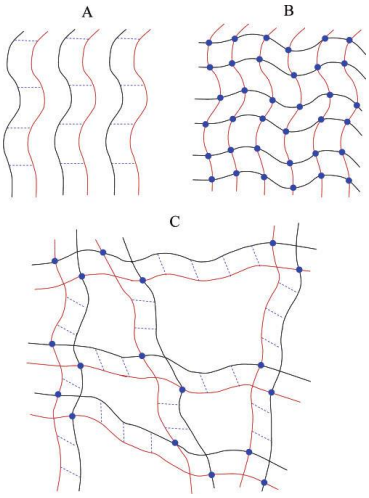

Figure 1.5. The ladder and network topologies of polyelectrolyte complexes: (a) a ladder structure, (b) a full network without ladder pairing, and (c) a mixture of networks and ladders. Reprinted with permission.[51] Copyright (2006) American Chemical Society.

It was reported that PEC formation followed a two-stage process. At the first stage, polyanion and polycation interact with each other to form primary PEC particles (molecular level). At the second stage, those primary PEC particles aggregate, leading to large secondary PEC particles (colloidal level), as presented in Figure 1.6. The secondary PEC particles could be solid-like precipitate or liquid-like coacervate. [26, 53]

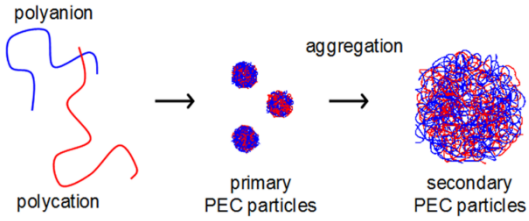

Figure 1.6. Schematic presentation of formation process of PECs. Reprinted with permission.[26] Copyright (2012) American Chemical Society.

This two-step formation model was verified in one PEC system. Isothermal titration calorimetry (ITC) was used to investigate the thermodynamic characterization between poly(L-ornithine hydrobromide) (PO) and poly(L-glutamic acid sodium salt) (PGlu). The reaction enthalpy change ΔH, entropy change $-T\Delta S$, and free energy ΔG were estimated from the ITC measurements. The two-step formation model fitted the ITC results successfully.[54]

The PECs formed in aqueous solution could be solid-like precipitates, liquid-like coacervates, or even polyelectrolyte solutions, as shown in Figure 1.7.[25] Solid PECs are usually made from strong polyelectrolytes. Mixing weak- or bio-polyelectrolyte solutions yields liquid-like coacervate.[55, 56] Different characterization methods and techniques have been exploited to study the physical properties and the formation of PECs. Optical microscopy provides direct observation of PEC particles.[7, 25, 27, 57-59] Turbidity of PEC aqueous mixture reflects the size and extent of PEC formation. Dynamic light scattering measures the size of PEC particles.[60] Static light scattering measures the mass, structural density, and radius of PEC particles.[61]

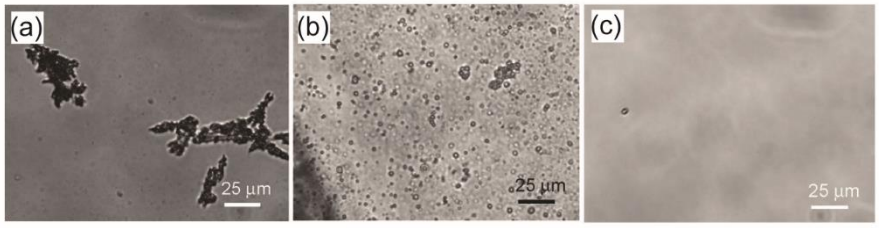

Figure 1.7. PECs prepared from PAH and PAA. Optical micrographs of (a) precipitate, (b) coacervate, and (c) solution phase. Adapted with permission.[25] Copyright (2010) American Chemical Society.

Many pioneers have explored the formation process of PECs [9, 17, 62]. It has been reported that the chemistry of polyelectrolyte, mixing ratio, salt concentration, pH, and temperature all influence the formation of PECs. Dautzenberg and coworkers studied the phase behaviors of PECs and their response to addition of salt.[9, 17, 61, 63-65] Tirrel et al. investigated the mixing ratio, ionic strength, total polymer concentration, pH, and temperature effects on the phase behavior of PECs consisting of weak polyelectrolytes or polypeptides.[7, 25, 27, 54, 57-59, 66] Cohen Stuart et al. reported the formation of micelles from polyelectrolyte and their copolymers.[67]

1.3.1. Effect of chemistry of polyelectrolyte

The chemistry properties of the ionic groups of polyelectrolyte influence the strength of ion pairing and the PEC formation. To reveal the ionic functionality effect on the strength of ion pairing, different types of PECs were tested using salt doping method. The results showed that primary amines and aromatic sulfonates formed stronger ionic pairs, whereas hydrophilic charged groups or carboxylates interacted more weakly with other polyelectrolytes.[68] It was found that PMAA formed lower level of precipitate aggregation with PDADMA as compared to PSS with PDADMA. It was because that the electrostatic attractions between cations and carboxylic ions were weaker than the attractions between cations and sulfonate charged groups. PECs prepared from PDADMA and its copolymer with acrylamide resulted in suppressed secondary aggregation because of the hydrophilic nature of acrylamide groups.[64]

The molecular weight or the chain length of polyelectrolyte affects the stability of PECs.[69] In poly(L-lysine hydrochloride) (PLys) and poly(L-glutamic acid sodium salt)

(PGA) complexes, the PECs showed larger adhesion and interfacial energy with increasing chain length, indicating that a higher interconnected structure was formed between the polypeptides.[66] In PAH−PAA system, as the PAA molecular weight decreased, the critical salt concentration required to observe the transition from precipitate to coacervate also decreased. This decreasing stability was due to the fact that the shorter polyelectrolyte chain interrupted the percolation state of intermolecular electrostatic interactions.[57]

The ternary PEC systems consisting of three types of polyelectrolytes provided another method to fine-tune the response of materials to external stimuli due to synergistic interactions among the components. The authors added a third polycation, PAH or branched PEI to the original binary coacervate system, PAA and poly(N,N-dimethylaminoethyl methacrylate) (PDMAEMA). The turbidity and rheology results showed that ternary coacervate maintained the similar trend observed in binary systems. However, the third component strongly influenced their response to external stimuli.[58]

1.3.2. Effect of stoichiometry

Mixing of oppositely charged polyelectrolyte solutions could form particle dispersion or highly aggregated precipitate depending on the stoichiometry or mixing ratio of polyelectrolytes.[60] Formed at nonstoichiometric conditions, PEC particles consist of a charge-neutralized core surrounded by a shell of excess polyelectrolyte chains, which stabilizes the particles from aggregation. The minor component is completely included in the PECs. At stoichiometric condition, neutralized particles are formed and they become destabilized and flocculate.[61]

Dautzenberg studied the formation of PECs as a function of mixing ratio using static light scattering, which measured the particle size and mass.[64] In pure water solution, as the molar mixing ratio of PSS to PDADMA increased from 0.1 to 1, the mass and size of the PEC particles slightly decreased, which was due to the decreasing excess major component bound around PEC primary particles. The decrease of the concentration of free major component altered the charge compensation by conformational changes, which also accounted for the decrease of particle size. Conversely, when in salt solution, the size of PEC particles increased with rising mixing ratio, which was ascribed to the favorable secondary aggregation as the stabilizing shell shrank.[64]

In PAH−PAA complexes, the precipitate mass of PECs increased as the mixing ratio changed from stoichiometrically unbalanced systems to stoichiometric ratio. The turbidity measurements reported the same trend.[25]

1.3.3 Effect of salt

PEC formation is sensitive to the salt concentration or ionic strength of solutions. Precipitate solid PECs were easily formed in pure water. When small amount of salt is added to the solution, the conformation of polyelectrolyte changed from stiff to coiled structure because salt screening effect reduced the electrostatic repulsion along the charged chains. The ion pairing of charged groups were likely to take place between two flexible and coiled chains, leading to less aggregation. Continuing increase of salt concentration reduced repulsion forces between primary PEC particles, leading to further secondary aggregation.[64]

The addition of salt has been shown to induce secondary aggregation, swelling or dissolution of primary PEC particles, depending on the salt concentration.[61] The response of formed PECs to subsequent addition of salt was studied in PDADMA−PSS and PDADMA−Na-poly(methacrylate) complexes. Subsequent addition of salt caused additional aggregation and macroscopic flocculation to PECs containing PSS. While for PECs containing PMA, the PECs were dissolved when NaCl concentration reached 0.6 mol/L. The diffident results were attributed to the discrepancy of internal structure and strength of ion pairing.[70]

As the salt concentration increased, the interfacial energy of PLys−PGA complexes decreased, which was explained that the increasing salt concertation resulted in weaker ionic attractions between oppositely charged groups.[66] In PO−PGlu complexes, as the salt concentration increased, both the ion pairing and complexation processes were suppressed.[54] 848

The effect of ionic strength and electrolyte type on the formation of PECs has been investigated. Požar et al. studied PECs prepared from PAH and PSS in dilute solution added a series of sodium electrolytes (NaX, X =F, Cl, Br, I, NO_3, ClO_4). The results indicated that the flocculation occurred at equal polycation/polyanion molar ratio and lower salt concentration (<0.1 mol/L). The composition of PECs strongly depended on counteranion chemistry type, which was explained that the difference of small ion distribution around PAH induced the discrepancies. Calorimetry results revealed a correlation between PEC formation enthalpy and anion hydration enthalpy.[71]

The effect of ions was also studied using dynamic simulation method. It has been reported that the increase of salt concentration induced decomplexation of DNA and polylysine. Divalent ion Ca^{2+} showed a stronger effect than monovalent Na^{+} on destabilizing DNA-polylysine because the former one had larger water binding capability and stronger electrostatic interactions.[72]

1.3.4 Effect of pH and temperature

In weak polyelectrolytes, the degree of ionization is controlled by the solution pH. The fraction of charged groups of weak polyelectrolyte affects the electrostatic interactions with oppositely charged polymers. In PAH−PAA complexes, partially ionized PAA with PAH formed a broader single solution regime than the fully charged PAA. The critical salt concentration required to dissolve PECs was lower for partially charged polyelectrolytes than fully charged polymers, which was also due to the lower charge density in the former materials.[25] In PO−PGlu complexes, as the pH increased from 7 to 8.8, the degree of ionization of PO decreased but the PGlu remained fully charged. This reduced binding sites of PO resulted in a smaller enthalpy change per PGlu in the first step of complexation.[54]

Temperature effect is weaker compared to salt concentration and pH in PO−PGlu complexes. Increasing temperature lowered the complex formation due to the decreasing number of electrostatic interactions and binding strength.[54] The temperature became significant when the total polymer concentration increasd.[7]

1.4 Thermal properties of PEMs and PECs

1.4.1 Thermal properties of PEMs

PEMs have been widely used in many applications.[1, 46, 73, 74] However, the thermal properties of PEMs is not well understood. PEMs are brittle and glassy in dry condition due to the strong electrostatic interactions.[34] When water and salt are present in the materials, PECs become soft and processable. They undergo a glass transition, indicating the plasticization effects of water and salt.[34, 35, 75] At high temperature, the polyelectrolytes gain enough thermal energy to overcome the kinetic barrier of structure rearrangements. The ideas and studies centering on thermal behaviors of polyelectrolyte assemblies, including PEMs and PECs, are still debating and not conclusive. The thermal transition event at temperature T has been named as melting transition T_m, glass transition T_g, and general thermal transition T_{tr}. In this dissertation, both T_g and T_{tr} are used they are interchangeable concepts.[34, 35, 76-80]

The temperature-dependent behavior of PEMs in aqueous solution was intensively studied by Köhler and coworkers. [81, 82] From direct size observation using microscopy, the PDADMA/PSS multilayer capsules terminated with PSS exhibited a pronounced shrinkage and finally reached into a solid sphere at a high incubation temperature, which was driven by hydrophobic forces. Conversely, capsules terminated with PDADMA swelled up to 5-fold of the initial size and ended up with rupture upon heating. This swelling behavior was driven by the electrostatic repulsion force. This glass transition temperature (T_g) for capsules was also verified using calorimetry technique. In another work, the temperature influence on internal structure of PEMs has been studied using

neutron reflectometry. The results showed that the outmost layer degenerated while the inner part of the layer became denser. The swelling and water uptake depended on the chemistry nature of terminal layer.[83]

The thermal transitions of plane PEMs, made of PDADMA/PSS, were investigated using a novel technique, quartz crystal microbalance with dissipation (QCM-D). It allowed the detection of both mass and viscoelasticity of the PEMs at different temperatures.[34, 35] In PDADMA/PSS multilayers, the glass transition temperature of PEMs terminated with PDADMA was determined from a sudden increase of the mass and dissipation, corresponding to the increased chain mobility and film swelling. The findings indicated that the linearly growing films assembled without NaCl were glassy while the exponentially growing films assembled with NaCl showed a glass transition. A trend in T_g was also observed that the T_g decreased from 56 to 49 ºC as the assembly salt concentration increased from 0.25 to 1 M.[34] T_g of PEMs consisting of weak polyelectrolytes was influenced by the assembly pH. PEMs assembled at pH 3.5, 5, and 9 underwent a glass transition event. At pH 7, the polyelectrolyte were fully charged and the film was thin and glassy, thus no thermal transition event was observed.[35] The deformation of the multilayer microtubes made of PAH/PAA occurred at the same temperature range, which confirmed the consistency of T_g in PAH/PAA system.[75]

The effect of counterion salts on the thermal properties of freestanding PEMs was studied. The T_g depended on both the electrolyte type and the water content, which was linked to the couternion's hydration shell and Donnan exclusion.[84]

1.4.2 Thermal properties of PECs

The thermal transition behavior of dry PECs is not easily detectable, due to the high density of ionic crosslinks. Huglin et al. studied the glass transition of poly[sodium(2-acrylamido-2-methylpropane sulfonate)] (PAMPSNa), poly(4-vinylpyridinium chloride) (PVPHC1), and their corresponding PECs using DSC and nuclear magnetic resonance spectroscopy (NMR). The glass transition of PECs was not determined because of the high density of ionic crosslinks.[85] PAH−PAA complexes electrospun fibers exhibited no thermal transition when tested using DSC.[86] It was also confirmed from Qian's work that T_g of PECs consisting of PDADMA and PAA increased with increasing ionic complexation degree (ICD). When ICD increased above 0.16, the T_g became undetectable, due to the depressed polymer chain mobility.[87] Imre et al. reported a T_g using calorimetry method and T_g depended on the composition of PECs. The ionic conductivity $\sigma_{dc}$of dry PDADMA−PSS complexes was recorded at a wide temperature range, from −70 to 300 ^oC, using impedance spectroscopy. The detected $\sigma_{dc}T$ was not affected by T_g.[88]

Many efforts have been made to determine thermal transition temperatures (T_{tr}) or a glass transition temperature (T_g) of hydrated PECs. Schlenoff et al. determined T_g of equilibrium hydrated PDADMA−PSS complexes using both calorimetry and dynamic mechanical analysis. T_g depended on the deformation rate, which was consistent with time/temperature superposition principle. T_g also deceased with increasing salt doping level in PECs, which was explained that salt doping decreased the number of intrinsic ion pairs and increased polymer chain mobility.[77] The thermal and humidity histories of PECs also influence their thermomechanical properties. The work performed by Peterson et al.

showed that the water or the humidity history had a strong effect on the structure and mechanical properties of PECs.[89]

All atom simulation method has been used to detect the molecular dynamics and interactions in hydrated polyelectrolytes and PECs.[90] In PDADMA−PSS complexes, as temperature increased, the number of hydrogen bonds between water and polyelectrolyte decreased. They reported that the thermal transition arose from the weakened hydrogen bond supramolecular structure with water.[78] They also explored the effects of salt on PECs. The findings showed that salt might have opposite effects on plasticization of PECs. Salt provided electrostatic screening and broke the polyelectrolyte-polyelectrolyte attractions, which facilitated the polymer chain movement. On the other hand, salt present in the PECs attracted water around it to form hydration shell, which decreased water dynamic and suppressed the water plasticization effect.[80]

1.5 Dissertation outline

Polyelectrolyte assemblies, including polyelectrolyte complexes and multilayers, have been utilized as promising materials in different application areas, including underwater adhesion,[91] synergistic bone remolding,[46] three-dimensional printing,[92, 93] separation.[94] All the potential applications require basic understanding of the physical properties of polyelectrolyte assemblies. This dissertation consist of experimental work at Texas A&M University and simulation work conducted by our collaborators at Aalto University. The experimental techniques and computational simulation methods allow more detailed and broader interpretation in this research field.

Chapter II presents the phase behavior and colloidal stability of the PECs made of PDADMA−PSS in aqueous state. We focus on the formation process of the PECs, monitoring the turbidity and hydrodynamic size of samples as a function of time. A phase diagram of PECs, which is used to exhibit stable, unstable colloid and solution phases, is established based on the mixing ratio of polycation/polyanion and salt concentration in complexation solutions.

In Chapter III, the thermal behaviors of weak polyelectrolytes PAH−PAA is studied using modulated DSC. The detected T_{tr} or T_g is controlled by both the assembly pH and water content in the PECs. Chapter IV presents the thermal properties of PECs made of strong polyelectrolytes PDADMA−PSS. T_g in this system is influenced by the salt doping level and the hydration content within the materials. One general controlling parameter, ratio of water to intrinsic ion pair, is proposed for the first time. The work also supports the hypothesis that water forms hydrogen bonds with polyelectrolytes, which facilitates the polymer chain relaxation at high temperature.

Chapter V summarizes the research results and presents possible future work. The thermal properties of PEMs will be investigated using electrochemical impedance spectroscopy in the future.

CHAPTER II

COLLOIDAL STABILITY OF PDADMA/PSS POLYELECTROLYTE COMPLEXES[1]

2.1 Introduction

Polyelectrolyte complexes (PECs) form when oppositely charged polymers are mixed together and the two interact to form a larger structure.[8] Promising applications of PECs range from industrial flocculants, coatings, and membranes to advanced material fields such as solar cells, injectable hydrogels, drug release, medical implants, chemical sensors, and lubricants.[66, 73, 95-98] PECs have been described by many works,[8, 9, 13, 17, 54, 62, 99, 100] which have shown complexation to be a largely isoenthalpic, entropy-driven process, resulting from an intricate interplay of electrostatic, van der Waals, and hydrophobic interactions. Hence, PEC formation is highly sensitive to polyelectrolyte characteristics (e.g. polymer structure and charge density) and external parameters including polyelectrolyte concentration, polyanion/polycation mixing ratio, mixing order, salt type, salt concentration, and solution pH (for weak polyelectrolytes).[16-18, 20-23, 27, 71] The resulting structure may be solid-like (complex solid) or liquid-like (complex coacervate).[7, 25, 26]

---

[1] Modified and reprinted with permission from The Royal Society of Chemistry. http://pubs.rsc.org/en/Content/ArticleLanding/2015/SM/C5SM01184A# "The influence of ionic strength and mixing ratio on the colloidal stability of PDAC/PSS polyelectrolyte complexes" by Yanpu Zhang, Erol Yildirim, Hanne S. Antila, Luis D. Valenzuela, Maria Sammalkorpi and Jodie L. Lutkenhaus, *Soft Matter*, 2015, 11, 7392–7401, Copyright 2015, The Royal Society of Chemistry

Many prior investigations have focused upon the effects of mixing ratio, ionic strength, and other external parameters on the formation or response of PECs, usually at a fixed point in time. Little attention is paid to the temporal domain, even though many PECs macroscopically change (phase separate or aggregate) over the course of minutes to days. Knowledge of PEC behavior with respect to time is expected to be significant for any industrial application proposing the formation and implementation of PECs, especially with regard to colloidal stability.

It has been shown that under certain conditions PECs aggregate, ripen, and eventually precipitate out of suspension,[7, 58, 70] although there is limited knowledge regarding the specific boundaries that govern this behavior. A recent review summarizes this issue from a theoretical point of view, describing aggregation to occur when short-range attractions (van der Waals, hydrophobic) overcome long-range electrostatic repulsion between like-charge complexes.[101] The process is generally described as the aggregation or bridging of primary PEC particles into larger secondary particles. At a critical point, the secondary particle precipitates and no longer remains suspended in the PEC solution, resulting in solid-liquid macrophase separation. This process is markedly different from coacervation, which is liquid-liquid phase separation. Dautzenberg and Jaeger reported that salt concentration and mixing ratio played a large role in whether or not PECs of poly(sodium 4-styrenesulfonate) (PSS) and polycation poly(diallyldimethylammonium chloride) (PDADMAC) and its copolymers, aggregated or flocculated, although a limited salt range was explored.[17] For nonstoichiometric ratios,

the complexes consisted of spherical particles with a neutralized core and a shell of the excess component, and for stoichiometric ratios, the shell of excess was less pronounced.

Besides colloidal stability, salt concentration and mixing ratio also have been shown to strongly influence phase behavior (solution/complex coacervate/complex solid).[7, 10, 70, 102] It is generally found that no added salt or low salt concentrations produce a complex solid, and that high salt concentrations excessively screen the polyelectrolytes to prevent complexation. Intermediate salt concentrations yield a coacervate, although the boundary between complex solid and complex coacervate is not definitive.[102] Many of these findings and others[48-50, 103] have attempted to equate the properties of PECs with that of layer-by-layer assemblies.

More recently, Schlenoff and coworkers conducted studies of PECs made from PDADMAC and PSS.[13, 77, 102, 104, 105] The addition of salt water rendered the PEC's processable by extrusion or ultracentrifugation, forming a class of materials termed "saloplastics".[29, 104, 106, 107] It was shown that salt type affected the doping and diffusion coefficients of the extruded PECs.[105] Salt doping also influenced the thermal transition of the saloplastic, as it modified the nature of the ion-pair interactions between the two oppositely charged polymers.[77] The solution/coacervate/precipitate boundary was also probed in a ternary PEC/water/salt phase diagram, in which the PECs were equilibrated by a "backwards" salt annealing method.[102] Here, the colloidal stability and temporal evolution of PECs are presented. Strong polyelectrolytes, PDADMAC and PSS are selected as the polycation and polyanion, respectively, because there is a good deal of existing literature on their PEC phase behavior.[13, 15, 17, 51, 52, 61, 63-65, 70, 102, 104, 105, 108-110] We

chose to focus upon mixing ratio and ionic strength because they have a large effect on colloidal stability at a given molecular weight and total polymer concentration. Salt type was not explored here, but has been studied extensively elsewhere.[59, 71] The ionic strength (0-3 M NaCl) and mixing ratio (20 mol% to 80 mol% PDADMAC) were varied, and the turbidity, hydrodynamic radius, and zeta potential are recorded. Under these conditions, solid-like PECs were formed for the most part. PECs showed solution behavior ranging from a stable colloidal dispersion to an unstable aggregating precipitate and eventually dissolved polymer chains. Molecular dynamic simulations on PECs of corresponding mixing ratios and salt concentrations were conducted to obtain a microscopic view and the resulting aggregation barriers that dictate their colloidal stability. The simulation findings are discussed with the experimental results.

2.2 Materials and methods

2.2.1 Materials

In this work, poly(diallyldimethylammonium chloride) (PDADMAC, Mw=200,000-350,000 g/mol, 20 wt% in water, Sigma Aldrich) was chosen as the polycation, poly(sodium 4-styrenesulfonate) (PSS, Mw=500,000 g/mol, powder, Scientific Polymer Products) was chosen as the polyanion, and both were used directly as received. Sodium chloride was used to adjust the ionic strength of the solutions. The water used in all experiments was 18.2 MΩ cm (Milli-Q) water.

2.2.2 Polyelectrolyte complex preparation

To study the effects of polycation/polyanion mixing ratio and ionic strength on the formation of PECs, the concentration of the overall repeat unit of the polyelectrolyte was held constant at 10 mM. The PDADMAC solution was always added to the PSS solution, for which both had the same adjusted ionic strength. PDADMAC or PSS stock solutions with concentrations (based on repeat unit) of 4, 6.7, 10, 13.3, 16 mM were prepared. Five combinations of PDADMAC and PSS were made, specifically with mol% PDADMAC varying from 20% to 80% (again based, on repeat unit), as shown in Table 2.1. Different amounts of NaCl were added to the stock polyelectrolyte solution to adjust the ionic strength before mixing. For each polyelectrolyte solution, the ionic strength varied from 0 to 1.0 M with an interval of 0.1 M and from 1.0-3.0 M with an interval of 0.5 M. PEC formation was carried out directly in disposable polystyrene cuvettes for UV-Vis-NIR spectroscopy and dynamic light scattering (DLS) characterization. To make PDADMA/PSS complexes, 0.75 mL PSS solution was first loaded into the cuvette; then 0.75 mL PDADMAC solution was mixed rapidly into the PSS solution using a pipette. Mixing occurred within a 1 s time span. All PECs were prepared just prior to measurements, unless otherwise indicated.

Table 2.1 PDADMA/PSS complex composition. All values are based on repeat unit.

Group	mol% PDADMAC in the PEC	PDADMAC concentration (mM)	PSS concentration (mM)
1	20	4	16
2	33	6.7	13.3
3	50	10	10
4	67	13.3	6.7
5	80	16	4

2.2.3 Turbidity measurements

A Hitachi U-4100 UV-Vis-NIR spectrophotometer (341-F) was used to measure the turbidity of PECs formed in the cuvettes. A wavelength of 750 nm was selected because both pure PDADMAC and PSS solutions do not absorb light at this wavelength. All PECs were analyzed just after preparation. The turbidity (T) of the mixture was calculated by

$$T = -\ln\left(\frac{I}{I_0}\right) \text{ [=] a.u.} \qquad 2.1$$

Where I_0 is the incident light intensity of the control solution and I is the intensity of light passed through the PEC. Turbidity was calculated in adsorption units (a.u.).[7]

2.2.4 Hydrodynamic size and zeta potential measurements

A Zetasizer Nano ZS90 (Malvern Instruments, Ltd., Worcestershire, UK) was employed to characterize the PEC hydrodynamic size and zeta potential. In the hydrodynamic size measurements, newly prepared PECs were formed in a disposable cuvette, and the size measurement was conducted immediately. For aqueous media and moderate electrolyte concentration, the Smoluchowski approximation is suitable for the PEC. The zeta potential was calculated by the Henry equation after measurement of the electrophoretic mobility. In the zeta potential measurements, disposable capillary cells (DTS1070) were used. After PECs were formed, the mixture was transferred to the capillary cell to carry out the zeta potential measurements.

2.2.5 Simulations of PECs

Classical molecular dynamics simulations in all-atom detail were performed to investigate the effective charge distribution around the complexes with and without excess salt with the motivation that electrostatic barriers dominate the colloidal stability of the PEC solution. COMPASS (Condensed-Phase Optimized Molecular Potentials for Atomistic Simulation Studies) force field, and its explicit 3-site fully flexible water model[111] within Accelrys Materials Studio software[111, 112] were used. The force field and its water model have been validated extensively for conformational and solubility properties of polymers.[113, 114] The simulations are performed in the NPT ensemble using Andersen barostat,[115] Nosé-Hoover-Langevin thermostat,[116-120] and Ewald summation with accelerated convergence of lattice sums[121, 122] for long range electrostatics.

The PDADMA/PSS complexes were modeled in compositions of 5 PSS_{40} – 1 $PDADMA_{40}$, 3 PSS_{40} – 3 $PDADMA_{40}$, and 1 PSS_{40} – 5 $PDADMA_{40}$ chains (corresponding to experimental mol% PDADMA molar fractions of 17, 50, and 83). The subscript 40 refers to the length of each polyelectrolyte chain in repeat units in the simulations. For each composition, three salt concentrations matching the experimental range were considered: no added salt (just the native counterions), 1 M excess NaCl, and 2 M excess NaCl as ions. For each composition and salt concentration, 1.1 ns simulations using three different initial configurations were run. Simulation box size is between $(7.8\ nm)^3$ and $(8.1\ nm)^3$ depending on the system resulting in density of 1.07-1.11 g/cm^3. The complex structure and the cumulative charge (charge contained within that distance) distribution were analyzed.[72, 123]

In the molecular dynamics simulations, a cut-off distance of 12.5 Å was used for the van der Waals interactions and the Ewald summation method with accelerated convergence of lattice sums[121, 122] was used. The pressure was maintained at 1 atm by using the Andersen barostat method using a piston mass of 20 a.m.u.[115] The Nosé-Hoover-Langevin method[117] which is superior in thermostatting compared to the original Nosé thermostat, was used to maintain the temperature at 300 K with Q, mass of the time-scaling coordinate ratio of 10958 $kcal/mol \cdot ps^2$.[118-120] Using this NPT ensemble setup, three different complex structures for each of the nine studied systems were relaxed for 1 ns after which data was collected for 100 ps at 5 ps intervals.

The initial configurations for the molecular dynamics simulations were initially generated within the Amorphous Cell tool in Accelrys Materials Studio Software.

Amorphous Cell builds disorganized polymer conformations by employing a sampling method developed by Theodorou.[124] In this, a force-field defined distribution of polymer backbone torsion angles with the constraint that close contacts between atoms in a cell are minimized and no overlap or ring spearing exists are used. Out of 100 different generated stable complexes, three lowest energy structures for each composition were selected for further simulations. This procedure ensures relatively low energy, representative structures for the complexes. The obtained structures were then solvated by explicit water molecules in 8 nm^3 boxes with periodic boundary conditions. Finally, to obtain the initial configuration for the molecular dynamics simulations, the resulting 27 simulation systems were minimized in energy with conjugate gradient algorithm for 5000 steps. Table 2.2 presentes detailed information about the simulated systems.

Table 2.2 Summary of simulated systems. Subscript 40 refers to the number of monomers in each PSS or PDADMA chain. Simulation box size is between $(7.8\ nm)^3$ and $(8.1\ nm)^3$ depending on the system. Na^+ and Cl^- columns show the total number of ions (counterions and excess salt). All systems are solvated by 15000 water molecules.

Simulated system	PSS/PDADMA molar ratio	Excess salt	Na^+	Cl^-	H_2O
1 PSS_{40} -5 $PDADMA_{40}$	0.167	none	40	200	15000
1 PSS_{40} -5 $PDADMA_{40}$-1 M	0.167	1 M NaCl	340	500	15000

Table 2.2 continued

Simulated system	PSS/PDADMA molar ratio	Excess salt	Na^+	Cl^-	H_2O
1 PSS_{40} -5 $PDADMA_{40}$-2 M	0.167	2 M NaCl	640	800	15000
3 PSS_{40} -3 $PDADMA_{40}$	0.500	none	120	120	15000
3 PSS_{40} -3 $PDADMA_{40}$-1 M	0.500	1 M NaCl	420	420	15000
3 PSS_{40} -3 $PDADMA_{40}$-2 M	0.500	2 M NaCl	720	720	15000
5 PSS_{40} -1 $PDADMA_{40}$	0.833	none	200	40	15000
5 PSS_{40} -1 $PDADMA_{40}$-1 M	0.833	1 M NaCl	500	340	15000
5 PSS_{40} -1 $PDADMA_{40}$-2 M	0.833	2 M NaCl	800	640	15000

2.3. Results

2.3.1 Visual inspection of PECs with time

There are a number of ways to create PECs, which brings difficulty in comparing across studies. PECs tend to exist in kinetically trapped, path-dependent states[17] in which

even the order of polyelectrolyte addition affects properties, Figure 2.1. The order of mixing is another factor that affects the PEC formation, suggestive of a kinetically trapped state. The overall trend is similar regardless of mixing order but the exact turbidity value varies, which is consistent with Chen's work.[125] Here, PDADMA was always added into PSS to eliminate the effect of this variable. For this reason, we arbitrarily chose to always mix PDADMA into PSS so as to solely focus on ionic strength and mixing ratio effects. The total concentration of the PDADMAC and PSS repeat units was kept constant at 10 mM. The NaCl concentration was varied from 0 to 3 M, and the mole percentage of PDADMAC repeat units was varied from 20 to 80 mol% (relative to the total concentration of PDADMAC and PSS repeat units). In all cases, the solution became turbid upon mixing, consistent with the formation of PECs. The resulting PECs were classified into "stable", "unstable", or "solution" states, as defined below.

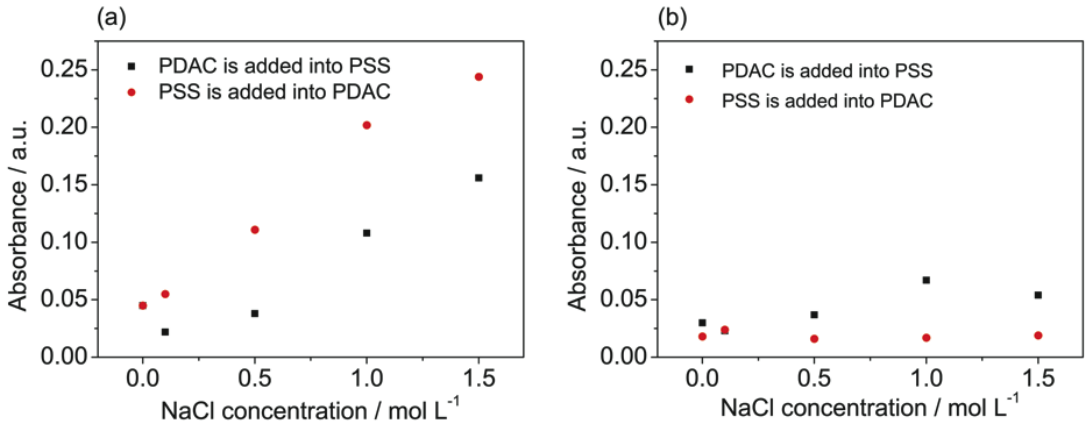

Figure 2.1. Turbidity of newly prepared complexes with different mixing order. The complex are prepared from (a) 20 mol% PDADMAC, (b) 80 mol% PDADMAC, respectively.

Figure 2.2a shows an example of stable PECs (20 mol% PDADMAC, 0.5 M NaCl). Upon mixing (0 min) the stable PECs generally had lower turbidity as compared to the unstable PECs. The mixture was left undisturbed and observed over the course of seven days, with no visible changes in appearance. For those mixtures whose turbidity or overall appearance remained constant, we assign them as "stable". Stable PECs were generally observed for highly nonstoichiometric mixing ratios (20 or 80% mol% PDADMAC) and low ionic strength, with exceptions noted later. Centrifugation of the stable PECs yielded a precipitate at the bottom of the vial, having an irregular structure, Figure 2.3 and Figure 2.4, which is consistent with a complex solid phase rather than a complex coacervate phase.

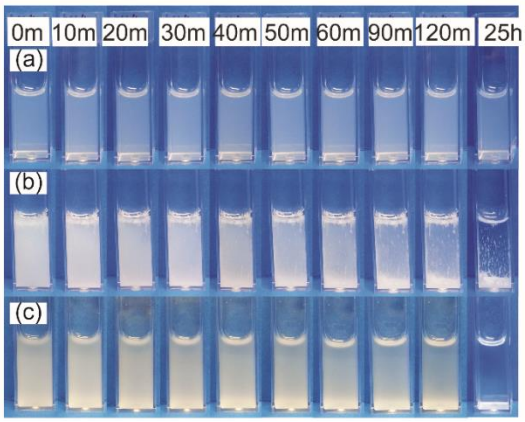

Figure 2.2. Time-lapsed digital images of PECs formed by mixing PDADMAC and PSS: (a) 20 mol% PDADMAC, 0.5 M NaCl "stable" PECs and (b) 50 mol% PDADMAC, 0.5 M NaCl "unstable" PECs and (c) 50 mol% PDADMAC, 3.0 M NaCl PECs that dissolve. Total concentration of PDADMAC and PSS repeat units (10 mM) were identical for all cases. Concentrations are on a repeat unit basis. Reprinted with permission.[60] Copyright (2015) The Royal Society of Chemistry.

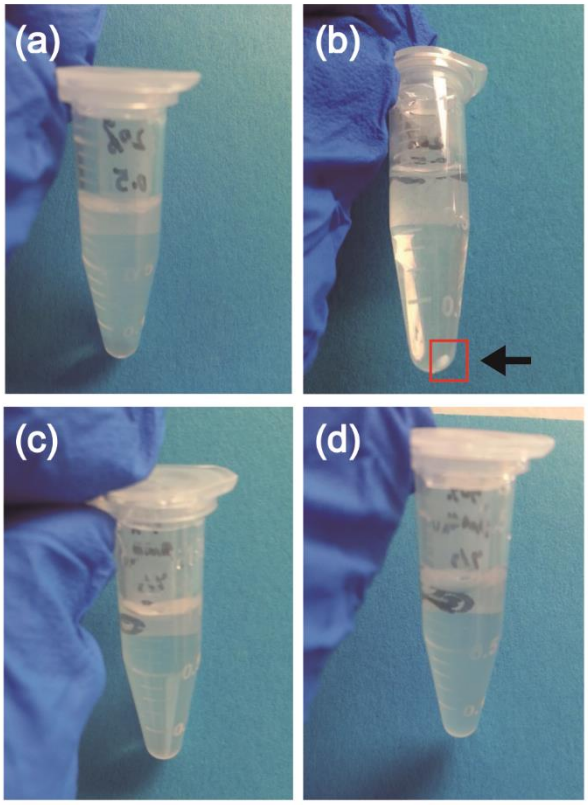

Figure 2.3. Optical images of PEC aged for 24 hs. 20 mol% PDADMAC, 0.5 M NaCl (upper panel) before (a) and after (b) centrifugation. 50 mol% PDADMAC, 3.0 M NaCl (lower panel) before (c) and after (d) centrifugation. Centrifugation parameters: 8500 rpm, 15 min. The black arrow and red square help to observe the white precipitate of complex.

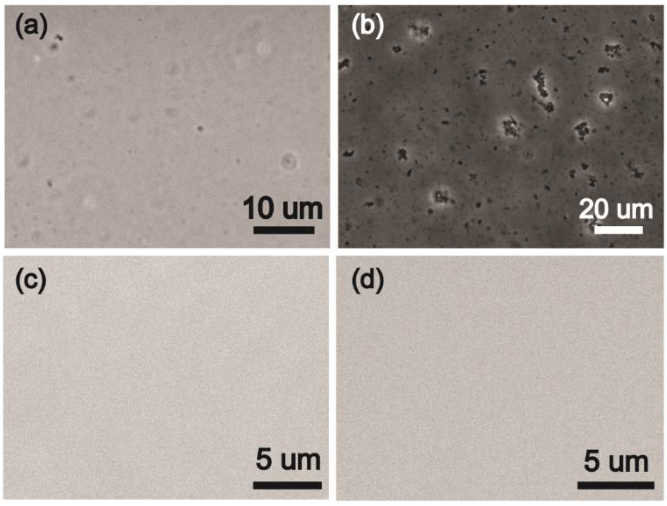

Figure 2.4. Light micrograph of PEC aged for 24hs. 20 mol% PDADMAC, 0.5 M NaCl (upper panel) without (a) and with (b) centrifuge. 50 mol% PDADMAC, 3.0 M NaCl (lower panel) without (c) and with (d) centrifuge.

Figure 2.2b shows an example of "unstable" PECs (50 mol% PDADMAC, 0.5 M NaCl.) Initially, the mixture was very turbid, followed by a gradual decrease in turbidity while a white string-like precipitate formed. The white precipitate either fell to the bottom or adhered to the walls of the cuvette. Again, the mixture was undisturbed over this time, with no centrifugation. Unstable PECs were generally observed when PDADMAC and PSS were mixed at or near 1:1 stoichiometry, or with high ionic strength.

Figure 2.2c shows an example of PECs (50 mol% PDADMAC, 3.0 M NaCl) that quickly form but then dissolve gradually over the course of time. Initially, the complex was turbid, indicating the formation of complex. In contrast to Figure 2.2b, the turbidity decreased gradually with time without any precipitate formation. At 25 h after preparation, the complex was totally clear. This behavior was generally observed at high ionic strengths

(2.5 – 3.0 M NaCl). Almost a day after mixing, centrifugation resulted in a single phase, and optical microscopy similarly showed no evidence of complex precipitate or complex coacervate formation, thus suggesting the presence of a solution phase (Figure 2.3c and Figure 2.3d). It is possible that a small fraction of coacervate phase exists such that it is not observable by these means. For simplicity, we discuss this phase as a solution.

2.3.2 Turbidity measurements

From our initial screening, it is clear that the ratio of PDADMAC to PSS repeat units and the ionic strength of the solution both play large roles in the stability of the resultant PECs. Turbidity measurements, popularly employed to investigate the properties of PECs,[7, 58] were performed on PEC mixtures both newly prepared and aged for seven days without disturbance.

Figure 2.5a shows a turbidity map of newly prepared PECs as a function of composition and salt concentration. In terms of composition, the turbidity was lowest at highly nonstoichiometric PDADMA/PSS ratios (20 or 80 mol% PDADMAC). As for salt, the turbidity was lowest when the NaCl concentration was low or equal to zero. As an exception, the turbidity was particularly high for the 50 mol% PDADMA PEC, even in the absence of salt. After seven days, the turbidity contour map was very different, Figure 2.5b. It is first interesting to note that most of the contour map indicates a very low level of turbidity, and the color scale for turbidity decreases from 5.2 to 1.3 a.u for PECs aged seven days vs. those freshly prepared. Instead, it is indicative of the formation white solid precipitate, falling to the bottom of the cuvette and leaving behind a transparent, polymer-deficient phase, Figure 2.2b. At higher salt concentrations, this drop in turbidity is

commensurate with the dissolution of PECs, Figure 2.2c. On the other hand, only at low NaCl concentrations and nonstoichiometric PDADMA/PSS ratios did turbidity remain, consistent with the stable complexes shown in Figure 2.2a.

From Figure 2.5, it is possible to discern the colloidally stable/unstable PEC boundary as the condition at which turbidity does or does not change over the course seven days. However, it should be noted that turbidity alone is not sufficient to demarcate between complexes that dissolve at high salt concentrations and those that are colloidally unstable at intermediate salt concentrations. The general shape of the stable/unstable PEC boundary bottoms out 50 mol% PDADMA and 0.2 M NaCl. At 50 mol% PDADMA and intermediate NaCl concentrations, PEC precipitation was observed. On the other hand, for 20 mol% PDADMA, the salt concentration for PEC precipitation was much higher at 1.5 M. The boundary appears mostly symmetric with only slight skewing.

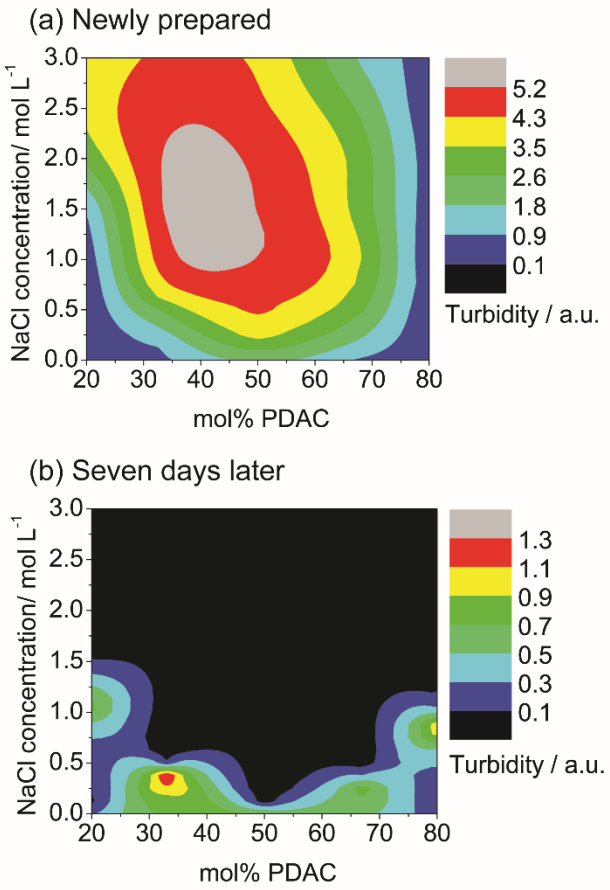

Figure 2.5. Turbidity of PEC mixtures: (a) newly prepared PECs and (b) aged seven days without disturbance. Turbidity was measured using UV-Vis-NIR spectroscopy and calculated as described in the Materials and Methods section. Reprinted with permission.[60] Copyright (2015) The Royal Society of Chemistry.

To further capture the evolution of turbidity with respect to time, the turbidity of newly formed complexes of each type (unstable, stable, and dissolving) were monitored over the course of 25 h, Figure 2.6. For the dissolving PEC (50 mol% PDADMA, 3 M NaCl) the turbidity was initially high at the beginning, but decreased slowly with time.

This turbidity change is consistent with the initial formation of a complex and its gradual dissolution into solvated polyelectrolyte chains. The unstable PEC (50 mol% PDADMA, 0.5 M NaCl) exhibited similar behaviour, except that the loss of turbidity arises from the precipitation of PECs. The stable PECs (20 mol% PDADMA, 0.5 M NaCl) exhibited no change in turbidity, consistent with visual observation.

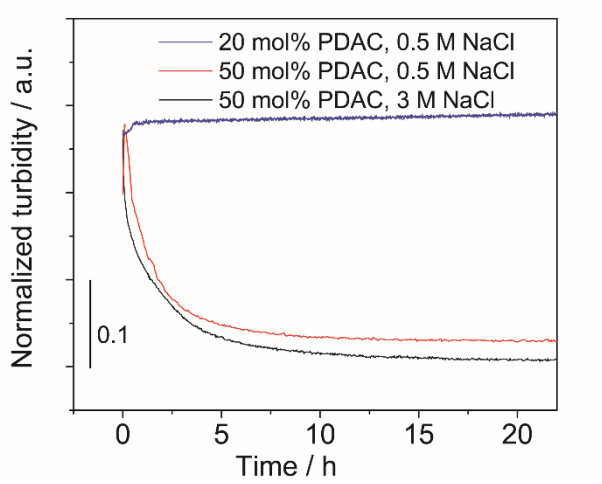

Figure 2.6. Turbidity of newly prepared stable, unstable, and dissolving PECs (20 mol% PDADMA and 0.5 M NaCl, 50 mol% PDADMA and 0.5 M NaCl, and 50 mol% PDADMA and 3 M NaCl, respectively). Each curve was shifted vertically on the y-axis to have the same initial turbidity. Reprinted with permission.[60] Copyright (2015) The Royal Society of Chemistry.

2.3.3 Hydrodynamic size and zeta potential measurements

To probe the origin of PEC stability, dynamic light scattering was employed to measure the temporal dependence of the PECs' hydrodynamic diameters, Figure 2.7. We have found that a nine-minute observation window is sufficient for identifying stable vs. unstable PECs even though large-scale precipitation tends to occur over the course of days. Because dissolution of complexes at high salt concentrations occurs over the course of hours, this approach is not reliable in distinguishing between unstable PECs and dissolving PECs. Over a longer time scale, unstable PECs aggregated together such that their size and dispersity became so large that DLS was no longer reliable. However for stable PECs, the hydrodynamic size remained constant over the course of 25 hours, Figure 2.8. We have denoted the data for which the polydispersity is greater than 0.7 by the shading in Figure 2.7. The shaded data loosely coincides with unstable and dissolving PECs, although there are some unstable PECs for which the polydispersity was below the 0.7 cutoff.

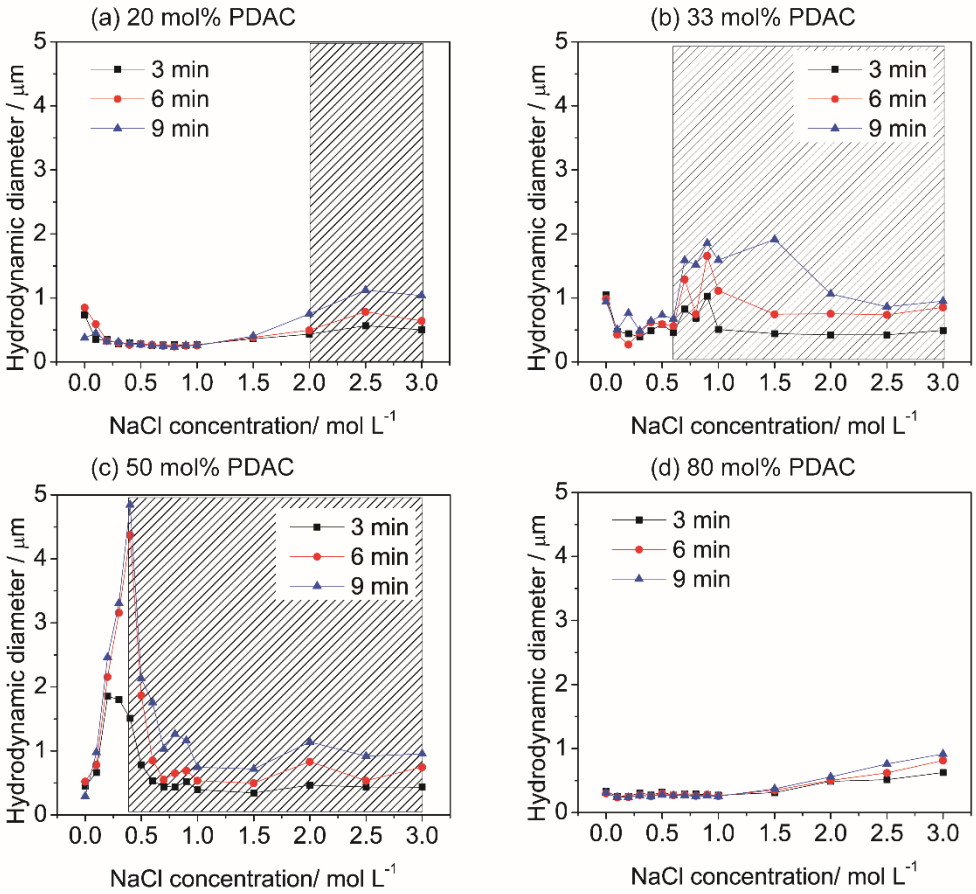

Figure 2.7. Hydrodynamic diameters of PECs with varying compositions measured using DLS. The shaded region denotes data in which the polydispersity was > 0.7, so the exact hydrodynamic diameter is uncertain. Reprinted with permission.[60] Copyright (2015) The Royal Society of Chemistry.

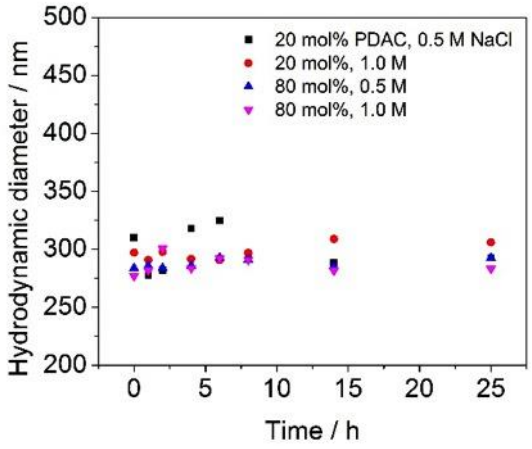

Figure 2.8. Time-lapsed hydrodynamic diameter of stable PECs.

For highly nonstoichiometric PECs (20 and 80 mol% PDADMA), the boundary between stable and unstable is quite clear, Figure 2.7a and Figure 2.7b. Below 1.5 M NaCl, PEC hydrodynamic size (230 nm to 320 nm) remained constant over the course of nine minutes, consistent with stable PECs. Above a NaCl concentration of 1.5 M, the hydrodynamic diameter steadily increased with time, consistent with unstable PECs. Therefore, the critical salt concentration for colloidal stability at these highly nonstoichiometric conditions can be assigned to 1.5 M NaCl. These results match well with the boundaries defined by UV-Vis-NIR turbidity measurements presented earlier.

For a stoichiometric composition (50 mol% PDADMA, Figure 2.7c), PEC hydrodynamic diameter increased regardless of NaCl concentration, suggestive of instability. PEC size was particularly large, on the order of microns, when NaCl concentrations were between 0.2 mol/L to 0.5 mol/L. These results mirror the very turbid

region, for which larger particles are more effective light scatters, depicted in Figure 2.5a for freshly prepared complexes.

Zeta potential is another convenient means to probe the origin of PEC stability. It has been posited by Li and coworkers that zeta potentials above |30 mV| yield stable colloidal suspensions and that those below are marginal or unstable.[126, 127] Figure 2.9 shows average zeta potentials of three separate measurements for PEC mixtures as a function of ionic strength and mixing ratio. It is acknowledged that experimental error is introduced when highly aggregating systems are examined by zeta potential. Therefore, to reduce this effect, we examined only freshly prepared PECs. For PECs prepared from 50 mol% PDADMA and above, the zeta potentials were positive. In contrast, the zeta potentials were negative for PECs prepared from 33 mol% PDADMA and below. As the ionic strength increased, the zeta potentials approached zero. At a given NaCl concentration, the absolute zeta potential of the stoichiometric PEC was lowest. When PSS was in excess, the zeta potential was larger in magnitude as compared to the case when PDADMA is in excess. This is due to the hydrophilicity differences between PDADMA and PSS, which is consistent with previous work where the more hydrophilic excess polyelectrolyte showed lower zeta potentials.[128] It is also curious that a stoichiometric complex should exhibit a positive zeta potential, whereas a value of zero might be expected; this result is possibly attributed to differences in PDADMA and PSS hydrophilicity as well. Applying the criteria put forth by Li and coworkers, the zeta potential of |30 mV| occurred at a NaCl concentration of about 1.5 mol/L for 20 mol% PDADMA, for example.

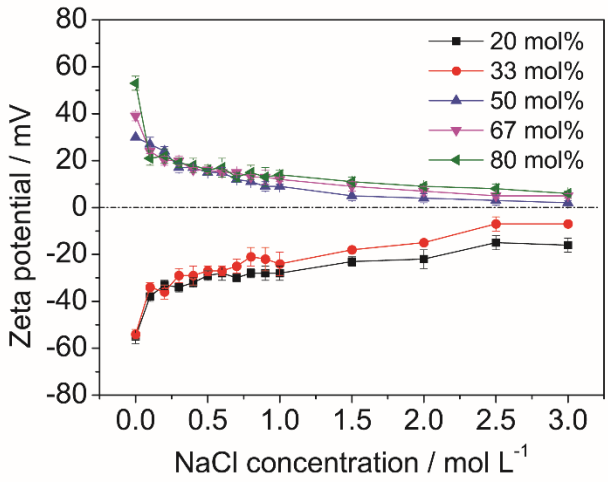

Figure 2.9. Zeta potential of newly prepared PDADMA/PSS PECs. The composition is given in mol% PDADMA. Reprinted with permission.[60] Copyright (2015) The Royal Society of Chemistry.

2.3.4 Molecular simulations of PECs

All-atom molecular dynamics simulations were performed to characterize the structure of the PECs with the aim of using the structural insight gained to connect the experimentally observed behavior with its molecular origins. Figure 2.10 shows examples for the final structures of PECs simulated at varying molar ratios without any additional salt. The Na^+ and Cl^- ions shown are counterions arising from the original polyelectrolyte prior to complexation. The 1 ns simulational relaxation performed on the PECs was sufficient for ion distribution equilibration but not for major structural reorganization of the complex. This means that the individual simulations represent kinetically trapped configurations – even though the data presented throughout is an average of different

initial configurations, the electrostatic barriers obtained in this fashion are estimates and their magnitudes rely directly on the PEC dimensions (choice of simulation system size). Furthermore, no evaluation of the difference in steric barriers between excess PDADMA and PSS was considered here as the charging was assumed to dictate behaviors. We emphasize that the simulational charge distributions reflect only qualitatively the stability of the complexes. While the polymer ratios match, the size of the complexes in experiments and in the simulations differs significantly because of different polymer lengths. As a result, the simulated complexes represent in small form the resulting charge distribution from that particular mixing ratio. In these simulations, the polyelectrolyte component in excess wraps around the minority component to form the complex. This results in the excess component dictating the outward characteristics of the PEC. It is noted that the excess component may remain partially soluble in the aqueous phase.

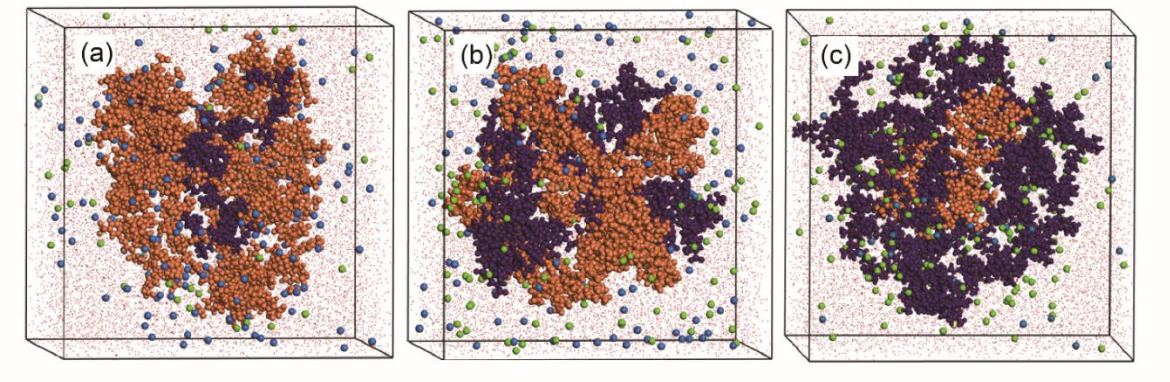

Figure 2.10. Representative snapshots of PDADMA/PSS complexes with (a) 17, (b) 50, and (c) 83 mol% PDADMA (5 PSS_{40}-1 $PDADMA_{40}$, 3 PSS_{40}-3 $PDADMA_{40}$, and 1PSS_{40}-5 $PDADMA_{40}$ systems, see Materials and Methods for details). PSS is highlighted in orange, PDADMA in dark blue, Na^+ ions in purple, and Cl^- in green. Reprinted with permission.[60] Copyright (2015) The Royal Society of Chemistry.

The temporal stability of PECs is dictated by the barriers in their free energy landscape needed to deter aggregation. For charged molecular aggregates, these barriers typically arise dominantly from charge repulsion although polymeric components have significant steric barriers as well. To get insight towards the barrier, we calculated the effective charge distribution for the PECs formed at 17, 50 and 83 mol% PDADMA in the presence of no added salt, 1 M, and 2 M excess NaCl (Figure 2.11). First, the data show that all PECs are effectively neutral near their core but that the PECs formed in excess of one component have significant effective charging at distances corresponding to their surface (at distances between 2.5 nm-4.5 nm from the center of mass of the simulated PECs). This charging was stronger for excess PSS than for excess PDADMA because as

the more hydrophilic of the two, PDADMA packs more loosely on the PEC surface in the simulations. As a consequence, in the experiments, a molar ratio corresponding to excess PSS results in a higher zeta potential value than the reverse excess PDADMA case. These results support the experimentally observed asymmetry in the temporal stability and PEC size distribution. Specifically, the excess charge from PDADMA is distributed over a larger space than with a corresponding amount of excess PSS. For the stoichiometric composition, some local charging at the PEC surface was observed in the simulations but was neutral overall.

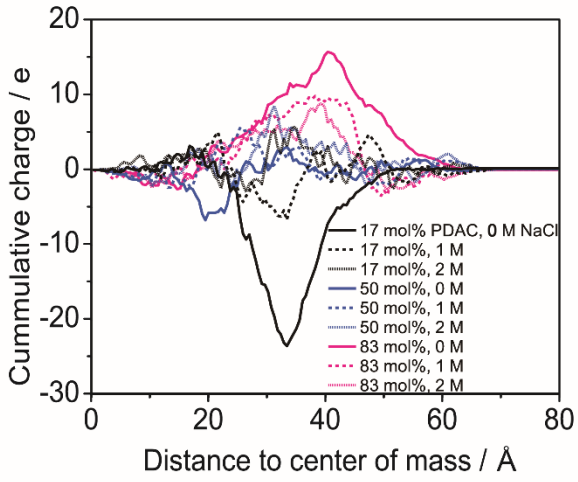

Figure 2.11. Effective charge distribution calculated for PDADMA/PSS complexes of varying composition (17, 50, and 83 mol% PDADMA) and salt concentration (0, 1, and 2 M added NaCl). Each data curve measures the cumulative charge resulting from the presence of PSS, PDADMA, and any ions in the solution as a function of distance from the center of mass of the PEC. Reprinted with permission.[60] Copyright (2015) The Royal Society of Chemistry.

The effect of NaCl was particularly pronounced in the snapshots and the cumulative charge distribution. As NaCl concentration increased from 1 M and 2 M, the effective charge at distances between 2.5 nm-4.5 nm became screened for the nonstoichiometric compositions. A concentration of 2 M NaCl resulted in a relatively flat charge distribution in the simulational PECs. Specifically, in the presence of excess salt, screening resulted dominantly from ions condensing to the outer PEC surface and partially from ions entering the PEC itself. For the case of no added salt, the solvated counterions entered the complex for nonstoichiometric compositions (contributing to charge neutralization in the core), whereas counterions tended to remain outside the complex for stoichiometric composition (with the core being compensated intrinsically by the polyelectrolytes themselves).

2.4. Discussion

The process of complexation is governed by a two-step mechanism: formation of primary PEC particles, followed by growth of secondary PECs from the aggregation of the primary particles.[26, 53] The appearance of white string-like precipitates in our unstable PDADMA/PSS complex is consistent with the formation of secondary PEC aggregates. On the other hand, stable PDADMA/PSS complexes appear to consist of mostly primary particles, as evidenced by the lack of change in hydrodynamic diameter with time. We will first begin our discussion of stability by addressing the effects of salt and composition, which appear to strongly control the time-dependent behavior of PECs.

Without added salt, all PECs exhibited stable behavior. The mixtures remained turbid over seven days, and the hydrodynamic diameter did not change appreciably. The

hydrodynamic diameters were in the range of 230 to 320 nm and the zeta potentials were greater than |30 mV| for all compositions. It is noted that some compositions exhibited a second population of larger particles, which we believe are secondary particles. However, the lack of change in the diameter and turbidity with time suggests that further particle aggregation and growth was arrested. Given the high absolute zeta potential and the charge density profiles from simulations, it is likely that aggregation and growth of secondary particles is arrested by electrostatic interactions and self-repulsion of PECs.

In the presence of added NaCl, screening occurs, which is characterized by a drop in absolute zeta potential and instability of PECs. Simulations support this idea, and also shed light on the location of small counterions. As salt concentration increases, there is a marked shift of counterions condensed at the PEC surface to counterions present throughout the PEC. These results, in the broader context, support observations of "saloplastics" by the Schlenoff group, who have also observed the influence of salt.[29, 77, 104-108] At even higher salt concentrations (< 2.5 M NaCl), the screening effect is strong and electrostatic interactions, which hold the polyelectrolyte chains together, are reduced.[102] This is readily observed by the behaviour in Figure 2.2c, where a complex is initially formed, but then gradually dissolves.

We next turn to the effect of composition on stability, hydrodynamic diameter, and zeta potential. Inspection of Figure 2.5 shows that PECs formed at stoichiometric compositions were initially very turbid; after seven days, the solution became transparent as much of the PEC has precipitated or dissolved, depending on salt concentration. This result is explained by the zeta potential of the stoichiometric composition, which is

generally lower in absolute value as compared to the highly nonstoichiometric cases. Simulations support this idea, in which the charge distribution of stoichiometric complexes shows only a small amount of cumulative charge regardless of salt concentration. Experimentally, the stoichiometric complex formed at 0.2 M NaCl (zeta potential of +23.6 mV) lies at the transition from being colloidally stable to unstable. The weak charging on stoichiometric PECs is hence the primary reason that they are more susceptible to aggregation and eventual precipitation as compared to the nonstoichiometric case. It is possible that the weak charging on the PECs is associated with the penetration of unassociated salt into the complex.

For the case of nonstoichiometric compositions (20 and 80 mol% PDADMA), the behavior is markedly different. Much higher salt concentrations (1.5 M NaCl) were required to render the PECs unstable. For example, the hydrodynamic diameter remained around 230 nm to 320 nm for nonstoichiometric PECs at salt concentrations below 1.5 M NaCl; in comparison, stoichiometric complexes were generally much larger as they were comprised of growing secondary PECs. These results are consistent with zeta potential measurements, in which the absolute zeta potential is highest for the most nonstoichiometric compositions. Simulations also support that nonstoichiometric PECs have a highly charged surface. Therefore, we conclude that the zeta potential of the PEC (which is affected by composition and salt concentration) is primarily responsible for the observed stability trends.

The composition dependence on turbidity is noteworthy. The contour map shown in Figure 2.5a is somewhat symmetric with slight skewing towards the left. One might

expect such a contour map to be symmetric, but the result here is otherwise. One potential reason for this result is that PSS is more hydrophobic than PDADMA, thus driving phase separation and increased turbidity at higher PSS compositions. Another possible reason is ascribed to differences in polymer structure or chain flexibility.[23] Else, the mismatch in the linear charge density between PDADMA and PSS might explain the slight skewing; PDADMA has one charge per four carbons on its backbone, whereas PSS has one charge per two carbons.

Considering simulation and experimental results, the skewing is most likely a result of differences in hydrophilicity between the two polymers. Considering two cases where the compositions are nonstoichiometric but PDADMA-PSS ratios are reversed (20 mol% PDADMA vs. 80 mol% PDADMA), the 20 mol% PDADMA complexes generally had higher absolute zeta potential as compared to the reverse case with 80 mol% PDADMA PECs. Our simulations have shown that PDADMA is more hydrophilic than PSS, and that when excess PDADMA is part of the PEC, the PDADMA shell is much more diffuse and PDADMA samples more of the solution space as opposed to the reverse case. This result possibly yields a lower apparent zeta potential for the case of excess PDADMA.

From these results, we propose a diagram the colloidally stable/unstable and colloidally unstable/solution boundaries, Figure 2.12. The lower orange curve demarcates the boundary between colloidally stable (region a) and unstable (region b) states; the upper brown striped curve separates the colloidally unstable and solution (region c) states). The a-b boundary was selected as the salt concentration at which a steady change in

hydrodynamic diameter with time emerges, Figure 2.7. We chose to assign the a-b boundary in this manner as the temporal evolution of hydrodynamic diameter matches well with the turbidity diagram shown in Figure 2.5. The b-c boundary was chosen from long-term visual inspection of PDADMA-PSS mixtures, since DLS and turbidity were unsuitable. The curve is not drawn to be sharp – rather there exists a transition zone where intermediate behaviour was sometimes observed.

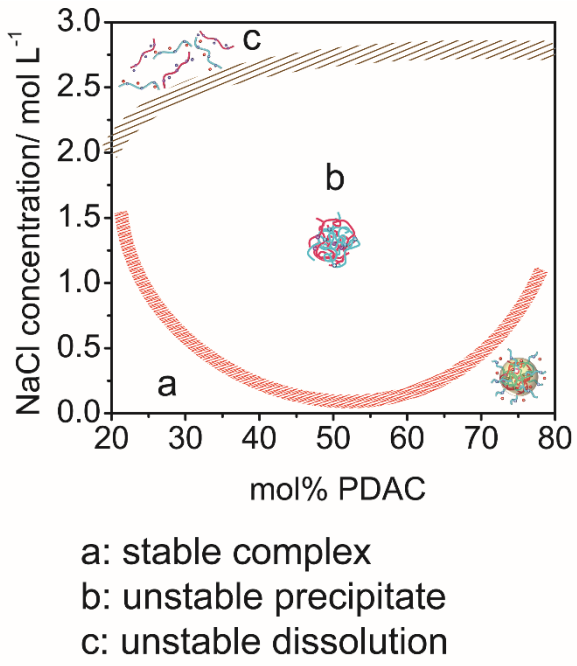

Figure 2.12. Diagram of PDADMA-PSS behaviour as a function of salt concentration and PDADMA content. Regions *a*, *b*, and *c* stand for PECs that are colloidally stable, unstable, or dissolving, respectively. The insets depict possible PEC configurations that lend themselves towards specific phase behavior. Reprinted with permission.[60] Copyright (2015) The Royal Society of Chemistry.

The origin of stability and instability arises from the mechanism of PEC formation. Let us consider the nonstoichiometric composition with no added salt as an example of the stable case. Upon initial mixing of the two polyelectrolytes, neutral small-size primary PEC particles are formed, and then excess polyelectrolyte surrounds the PEC particle nucleus. The formation of PECs with neutral cores and stabilization from the excess polyelectrolyte has previously been reported by Dautzenberg et al.[17] Our findings are in full agreement, where the initial state is typified by PEC particles of high absolute zeta potential (> 30 mV) and size of about 200-400 nm. The charge on the primary PECs is sufficiently large so as to illicit self-repulsion and long-term stability, rather than aggregation and precipitation.[26] However, as the ionic strength increases, small counterions screen and penetrate the PECs, the zeta potential decreases, and the PECs aggregate, resulting in larger secondary PECs and eventual precipitation.[129] At even higher concentrations, ion-pairing is screened and PECs, if initially formed, dissolve into soluble chains. This mechanism has also been reported computationally.[72] The drawings inside Figure 2.12 depict the observed states.

Our molecular simulations aid in pinpointing the origins of stability: PECs assembled at uneven molar ratios in low ionic strength possess a charge-charge repulsion which acts as a barrier against their aggregation when the PECs diffuse to distances corresponding to the peak in cumulative charge. Excess PSS results in enhanced effective charge, and therefore higher adsorption barrier, in comparison to PDADMA in the simulations. This is because PDADMA extends further to the aqueous phase due to its more hydrophilic nature; the position, form, and height of the PEC cumulative charge peak

depends naturally on the polyelectrolytes and on the size of the complex. Experimentally, this manifests as slight asymmetry in the temporal stability and aggregate size development between different excess PSS and excess PDADMA ratios (excess PDADMA results in temporally more stable PECs). At stoichiometric composition, the effective PEC charge, and the repulsion resulting from it is significantly smaller, and correspondingly, the stability is reduced. Excess salt results in screening of the charge peak and similar outcome. Hence, decreased temporal stability, and enhanced aggregation propensity is expected for stoichiometric compositions and/or high assembly solution ionic strength, as shown by the experimental data.

2.5. Conclusions

In this work, we outlined the conditions (ionic strength and polycation/polyanion composition) that form the boundary between colloidally stable and unstable polyelectrolyte complexes, as well as solutions. This was accomplished by monitoring PEC turbidity and hydrodynamic diameter as a function of time, and by comparing the zeta potential of PECs against experimental simulations. Stable PECs were typified by a constant turbidity and hydrodynamic diameter with respect to time, and were most commonly observed for conditions of no added salt and/or nonstoichiometric composition. Further, stable PECs exhibited a high absolute zeta potential and a cumulative charge focused at the PEC corona or shell. On the other hand, unstable PECs exhibit a gradual formation of a string-like precipitate and a steady increase in hydrodynamic diameter with time, and were most commonly observed at high ionic strength and/or stoichiometric composition. The absolute zeta potential of unstable PECs was low, and the cumulative

charge profile was near-flat, consistent with the formation of a neutral particle. It is the action of these neutral particles, aggregating into larger secondary particles, that leads to colloidal instability and the formation of precipitate. Aggregation, colloidal stability, and dissolution appear to be controlled by a complex interplay of screening by added salt within the PEC particle.

These results represent only an early step in understanding the temporal behavior of PECs, which tend to exist in a metastable or kinetically trapped state. Future work should focus upon other polyelectrolytes families (i.e., weak polycations and polyanions), pH conditions, and temperatures. Here, we investigated only strong polyelectrolytes, which are not very responsive to pH. Future studies with weak polyelectrolytes and pH with respect to time should provide a rich area of study. Varying temperature may also prove interesting, in which temperature provides a potential handle to move the stable/unstable boundary or to accelerate the rate of PEC aggregation.

CHAPTER III

THERMAL TRANSITION IN POLY(ALLYLAMINE HYDROCHLORIDE)-POLY(ACRYLIC ACID) COMPLEXES[2]

3.1. Introduction

Polyelectrolyte complexes (PECs), prepared *via* mixing oppositely charged polymer solutions together, have attracted increasing attention in recent years in terms of fundamental phase behavior.[18, 25, 27, 60, 130, 131] PECs can be processed into films[31, 132] and extrudable shapes,[77, 104] thus opening up a broad range of applications. Further, PEC structure is finely controlled by complexation conditions and parameters such as polymer charge density and molecular weight, ionic strength, and pH value.[57, 133] Once formed, PECs act as "smart" materials in which they respond to various external stimuli including ionic strength, pH, and temperature.[70, 77, 86] These stimuli-responsive behaviors are almost always observed in the hydrated state because dry PECs are somewhat glassy and intractable.[8] Of these external stimuli, temperature is particularly intriguing because the origin of temperature-effects on PECs is not immediately obvious as compared to ionic strength or pH-effects.

---

[2] Modified and reprinted with permission from American Chemical Society http://pubs.acs.org/doi/abs/10.1021%2Facs.macromol.6b00742 "Effect of Water on the Thermal Transition Observed in Poly (allylamine hydrochloride)–Poly (acrylic acid) Complexes" by Yanpu Zhang, Fei Li, Luis D. Valenzuela, Maria Sammalkorpi and Jodie L. Lutkenhaus, *Macromolecules*, 2016. 49(19), 7563–7570, Copyright 2016, American Chemical Society

For over a decade, it has been known that hydrated polyelectrolyte multilayers or layer-by-layer (LbL) films undergo a "glass-melt" transition with some assigning this temperature as the melting temperature T_m or the glass transition temperature T_g [81, 82, 134] This thermal transition has been further leveraged to release cargo from capsules and induce Rayleigh instabilities in microtubes.[44, 75, 135-137] General observations indicate hydrated polyelectrolyte multilayers soften and that polymer chains relax as they are heated through the transition.[76, 82, 134, 138] Most literature in this area focuses on hydrated polyelectrolyte multilayers, with recent work showing that hydrated PECs have a similar tendency.[77]

On the other hand dried polyelectrolyte multilayers and complexes have markedly different behavior comparing with hydrated ones, which suggests that water plays a critical role in the thermal transition. Shamoun et al. reported no distinctive thermal transition for dried extruded complexes of strong polyelectrolytes poly(diallyldimethylammonium chloride) (PDADMAC) and poly(sodium 4-styrenesulfonate) (PSS).[77] Huglin et al. found that dried PECs consisting of poly(4-vinylpyridinium chloride) and poly[sodium(2-acrylamido-2-methyl propane sulfonate)] possessed no discernable T_g due to the high density of ionic crosslinking.[85] Electrospun weak polyelectrolyte poly(allylamine hydrochloride)-poly(acrylic acid) (PAH-PAA) PEC fibers exhibited no T_g as well.[86] In our own work we have demonstrated that PAH/PAA multilayers also exhibit no T_g and instead undergo thermal crosslinking.[139, 140] These findings show that dried PECs generally do not possess a T_g because of extensive ion-pairing, which results in a highly physically crosslinked PEC network.

Remarkably in the presence of water, these same PEC systems exhibit the glass-melt thermal transition, T_{tr} or T_g. Shamoun *et al.* demonstrated that hydrated PDADMA-PSS complexes have a T_g that is dependent on ionic strength, but the effect of water composition on the T_g was not explored.[77] Separately, we have demonstrated that hydrated PDADMA/PSS multilayers also have a salt-dependent thermal transition.[34, 141] These results are consistent with the pioneering work of Michaels, who described that PECs were brittle when dry but "leathery or rubberlike " when hydrated.[8] These results suggest that water acts as a plasticizer, possibly lowering the PEC's or multilayer's thermal transition temperature from an unobservable value in the dry state to an observable value in the hydrated state. This is supported by observations of PDADMA-PSS complexes' dehydration under osmotic stress[15] and water-polyelectrolyte interactions in PDADMA/PSS multilayers.[142]

Our recent experimental and simulational findings on the PDADMA/PSS system suggest that the thermal transition is not a classical glass transition, but is rather initiated by rearrangement of water molecules around the polyanion.[78] It is thus hypothesized that as the hydrogen bonding lifetime between water-polyanion shortens, the polyelectrolyte chains relax, leading to the observed glass-transition-like behavior. Elsewhere, it has been discussed that the transition may arise from the breaking and reformation of polyelectrolyte-polyelectrolyte ion pairs (here called "intrinsic ion pairs") facilitated by salt-doping and water.[77] In both cases, water is considered a key factor, although its exact role remains unclear. Therefore, a thorough understanding of water's role in the transition,

whether it proceeds by the former, later, or both mechanisms is of fundamental importance, and motivates the present study.

There also remains a question as to whether PECs of weak polyelectrolytes undergo a transition by the same mechanism. The thermal properties of hydrated complexes containing weak polyelectrolytes are presently not well described, and such information could yield valuable insight into water's influence. An added complication rises from the pH of complexation altering the polyelectrolyte charge density and the resulting PEC structure.[37, 38] Earlier we investigated PAH/PAA multilayers and microtubes, in which a pH-dependent T_{tr} was observed using both quartz crystal microbalance with dissipation (QCM-D), modulated differential scanning calorimetry (MDSC), and microscopy.[35, 75] Motivated by these results, we hypothesized that hydrated complexes would show distinct thermal transitions and would be affected by the complexation pH value and hydration conditions.

Here, the thermophysical properties of dried and hydrated PAH−PAA complexes are investigated. This weak polyelectrolyte system is chosen because information regarding its thermal transition is sparse, and because the system provides a unique opportunity to explore pH and ionization effects not normally accessible in strong polyelectrolyte systems. In experiments, PAH-PAA complexes are prepared at varying complexation pH values. The degree of PAA ionization and the PEC composition are analyzed using Fourier-transform infrared (FTIR) and proton nuclear magnetic resonance (^{1}H-NMR) spectroscopy, respectively. The thermal behavior of PECs with varying hydration is studied using MDSC. The effect of water mixtures with 1-propanol, 1,2-

propanediol, 1,3-propanediol, and urea on the T_{tr} is also examined. A connection between the thermal transition and water-intrinsic ion pair interactions is made, and discussed in the broader context of a proposed two-step mechanism for the thermal transition.

3.2 Materials and methods

3.2.1 Materials

Poly(allylamine hydrochloride) (PAH, M_w = 120 000−200 000 g/mol, 40 wt% solution) was purchased from Polysciences, Inc. and poly(acrylic acid) (PAA, M_w = 100 000 g/mol, 35 wt% in H_2O) was obtained from Sigma-Aldrich. Both polyelectrolytes were used as received without any further treatment. Deuterium chloride 35% in D_2O solution used in proton nuclear magnetic resonance (^{1}H-NMR) was also purchased from Sigma-Aldrich. 2,2-dimethyl-2-silapentane-5-sulfonate (DSS) was kindly provided by the Texas A&M University NMR Facility. The water used in all experiments was Milli-Q water with resistivity 18.2 MΩ·cm.

3.2.2 Preparation of polyelectrolyte complexes

Individual solutions of PAH or PAA were prepared at concentrations of 100 mM with respect to their repeat unit. 1 M HCl or NaOH was used to adjust the solution pH to desired values. 50 mL of PAH and PAA at matching pH values were mixed, with PAH being added rapidly to PAA under constant stirring. The complex was dialyzed against water at matching pH for 4 days. The complex mixture was decanted after centrifugation at 8,500 rpm for 10 min. Then the complex was air-dried for ca. 12 h. This preliminary air-dried complex was finely ground into a powder, then placed in a vacuum oven at 303

K for another 7 days and stored in a desiccator until further characterizations. This yielded the “dried” PEC, although it is acknowledged that it is impossible to remove all bound water. A PEC prepared at pH *m* will be referred to as a “$(PAH{-}PAA)_m$ PEC.”

3.2.3 Modulated differential scanning calorimetry (MDSC)

MDSC (Q200, TA Instruments) was performed on PECs using a heat-cool method unless otherwise stated. The sample mass ranged between 5 and 10 mg, depending on sample availability. Dried samples were loaded into a Tzero aluminum pan (TA Instruments) and held at 313 K isothermally under nitrogen purge (50 mL/min) for 60 min prior to the scan to further remove any remaining water. The dried sample was heated up to 573 K from 313 K at a rate of 10 K/min followed by cooling at the same rate for two heat-cool cycles.

Tzero pans and hermetic lids were used for hydrated samples. Hydrated samples were prepared by weighing the dried complex in the Tzero pans and adding water at matching assembly pH using microliter syringe. The samples were then dried at room temperature until the desired hydration content (15.3, 17.4, 20, 21.9 or 24.2 wt %) was reached. This hydration value represents the known amount of water added to the dried PEC and not the precise water content in the PEC. The pans were subsequently sealed with Tzero hermetic lids and left at room temperature for 24 h for equilibration before measurements. Hydrated samples were ramped from 278 K to 388 K at a rate of 2 K/min with an amplitude of 1.272 K and a period of 60 s. Measurements were conducted under a nitrogen purge. All MDSC thermograms are shown in the “exotherm down” format, and all data reported here correspond to the second heating cycle unless otherwise noted. The

T_{tr}/T_g was taken as the inflection point of MDSC thermogram. Three different measurements were run for each data point and the standard deviation was taken as the error estimate.

3.2.4 Fourier transform infrared spectroscopy

The chemical structure of the complex was investigated by attenuated total reflectance Fourier transform infrared spectroscopy (ATR-FTIR, Thermo, Nicolet Nexus 6700) using a Quest^{TM} diamond single-bounce ATR attachment (Specac). For each sample, ca. 5 mg PEC powder was placed on the sample stage to cover the ATR crystal. Spectra were taken by averaging 64 scans over a range of 600 cm^{-1} up to 4000 cm^{-1}, at a resolution of 2 cm^{-1}. All samples were kept in a desiccator prior to FTIR spectroscopy.

3.2.5 Proton nuclear magnetic resonance spectroscopy

Proton nuclear magnetic resonance (^{1}H-NMR) spectroscopy (500 MHz proton frequency, Varian Inova 500 spectrometer) was employed to measure the composition of PAH−PAA complexes as follows: 10 mg of dried complex sample was dissolved in 0.7 mL deuterium chloride in an NMR tube. 20 μL of 2 mg/mL DSS was added into the NMR tube as a standard internal reference just prior to recording the spectra.

3.3 Results

PAH-PAA complexes at stoichiometric mixing conditions and at pH values varying from 1 to 11 were prepared, Figure 3.1. Complex precipitates easily formed between pH 3 and pH 9, whereas more extreme pH values yielded almost no precipitate. For this reason, we selected pH values of 3.5, 5.5, 7, and 9 for further investigation; these

values also match prior studies on PAH/PAA layer-by-layer assemblies,[35, 38] which allows for comparison with PECs. The complexes were then dialyzed, separated by centrifugation, and dried for further use.

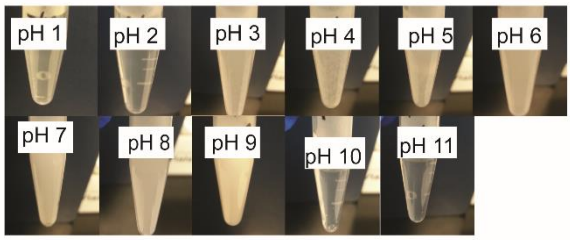

Figure 3.1. Digital images of PAH−PAA complexes from pH 1 to pH 11.

^{1}H-NMR spectra of PAA, PAH, and complexes (Figure 3.2) were used to calculate the composition of the complexes. The PAA mol% (by repeat unit) was 62%, 56%, 53% and 50% for complexes prepared from pH 3.5, 5.5, 7 and 9 solutions, respectively. As the pH of complexation increases, the amount of PAA in the complex decreases.

Figure 3.2 shows the ^{1}H NMR spectra of (a) pure PAA, (b) pure PAH, (c) - (f) PAH−PAA complexes prepared from pH 3.5, 5.5, 7, and 9, respectively. The standard internal reference DSS chemical shift was assigned 0 ppm.[57] The spectra of pure PAA (Figure 3.2a) shows four distinct resonances centered at δ = 2.48, 2.00, 1.83, 1.69 ppm. The resonance at 2.48 ppm is assigned to α hydrogen and the three resonances between 1.6 to 2.0 ppm are assigned to β hydrogen, which is assigned to the methylene resonances of triad distribution of the *rr*, *mr*, and *mm* sequences.[143] The spectral pattern here is consistent with previous reports with peaks shifting downfield due to lower pD value.[144]

For pure PAH (Figure 3.2b), the spectra shows three distinct resonances centered at δ = 3.14, 2.13, 1.60 ppm, which are assigned to H_c, H_d and H_e marked in Figure 3.2.[145]

The PAH−PAA complex NMR spectra, as shown in Figure 3.2c to f, show both PAH and PAA characterized chemical shifts peaks. Two notable peaks represent the H_c and H_a marked in Figure 3.2. The composition of the complex can be calculated using equation 3.1:

$$\text{PAA mol\%} = \frac{\text{PAA}}{(\text{PAH+PAA})} = \frac{A(H_a)}{(\frac{1}{2}A(H_c)+A(H_a))} \qquad 3.1$$

Based on the spectra and equation 3.1, the calculated PAA mol% were 62%, 56%, 53% and 50% for solutions of pH 3.5, 5.5,7 and 9, respectively.

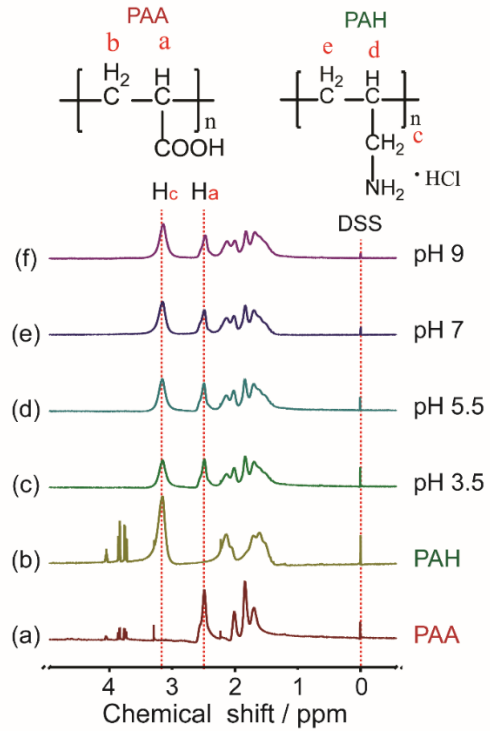

Figure 3.2. ^{1}H-NMR spectra for homopolymer PAA, PAH and PAH−PAA complexes prepared from pH 3.5, 5.5, 7 and 9 solutions.

Figure 3.3a shows ATR-FTIR spectra of the PAH−PAA complex precipitate powders. Two distinct absorption bands related to PAA carboxylic acid functional groups were observed at 1698 cm^{-1} (C=O stretching in −COOH) and at 1531 cm^{-1} (ionized carboxylate COO^- asymmetric stretching). The PAH asymmetric NH_3^+ stretching band was also present at 1620 cm^{-1}. Bands attributed to covalent amide crosslinking were not observed (1540 and 1670 cm^{-1} carbonyl stretching in CONH amide bending).[146] These results confirm that PAH and PAA are both present in the sample, that they have some degree of ionization, and that they are not covalently crosslinked.

The degree of ionization (α) of PAA within PAH−PAA complexes was quantified using FTIR spectroscopy.[38, 147] The degree of ionization α and pK_a of a weak polyelectrolyte can change strikingly from its pure solution state when assembled into multilayers or complexes.[86, 147] The extinction coefficients of the ionized and not ionized forms of carboxylic acid are the same.[148, 149] The absorbance (Abs) of −COOH and COO^- bands are related to α by the following expression:[147]

$$\alpha = \frac{\mathrm{Abs}(COO^-)}{\mathrm{Abs}(COO^-)+\mathrm{Abs}(COOH)} \times 100\% \qquad 3.2$$

From equation 3.2, the degrees of ionization of PAA within PECs of pH 3.5, 5.5, 7 and 9 were 74%, 92%, 93% and 95%, Figure 3.3b. As the complexation pH increases, α increases.

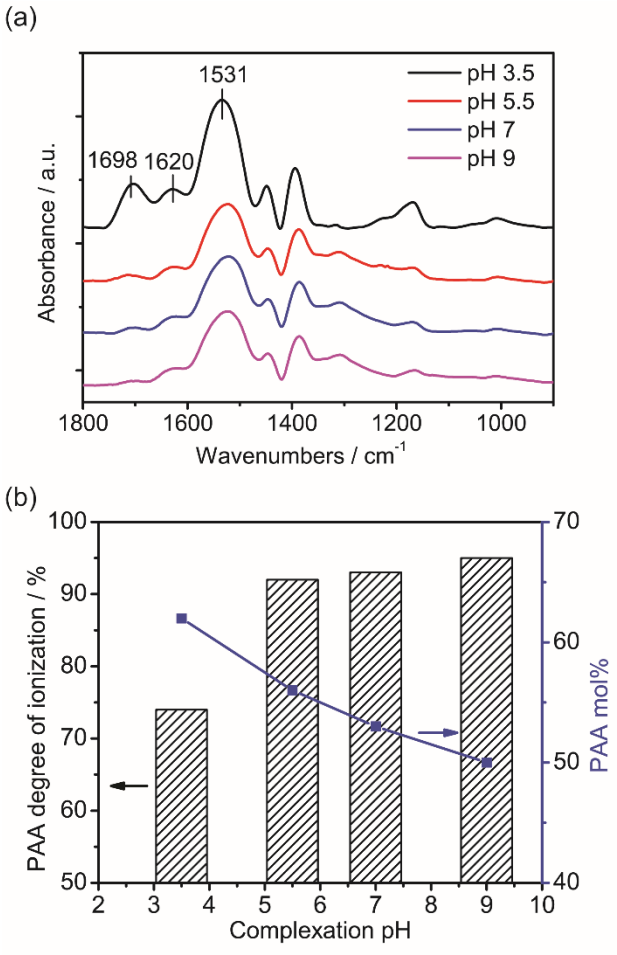

Figure 3.3. (a) FTIR spectra, (b) PAA degree of ionization and PAA mol% (by repeat unit) for PAH−PAA complexes prepared from pH 3.5, 5.5, 7 and 9 solutions. Initial mixing ratio was 1:1 PAH to PAA by repeat unit, and PECs were separated by dialysis and centrifugation. Reprinted with permission.[79] Copyright (2016) American Chemical Society.

To establish the general behavior of dried PAH-PAA PECs, conventional DSC was performed on $(PAH{-}PAA)_{3.5}$ complexes, Figure 3.4a and Figure 3.5a. From Figure 3.4a, in the 1st heating cycle, two endothermic peaks at 406 K and 516 K with a combined

heat of 277 J/g were observed. These peaks did not appear in the second heating cycle, indicating that the observed endothermic processes were irreversible. This result is similar to the thermal behavior of dried PAH/PAA LbL films. The low temperature peak was assigned to the loss of bound water, and the high temperature peak was assigned to amide cross-linking.[139] No glass-transition-like behavior was observed in the dried complex.

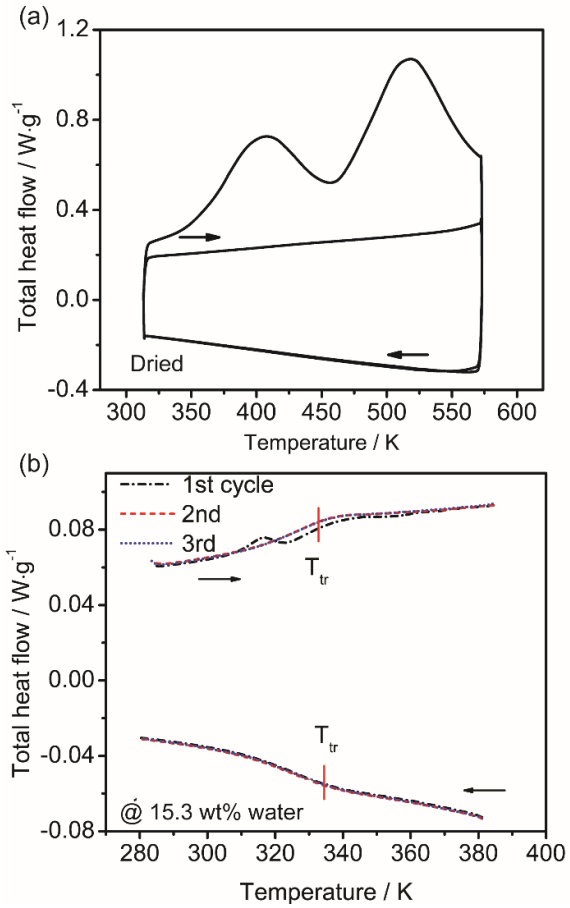

Figure 3.4. (a) Conventional DSC of dry $(PAH{-}PAA)_{3.5}$ complex at a scan rate of 10 K/ min; and (b) MDSC total heat flow of hydrated $(PAH{-}PAA)_{3.5}$ complex (15.3 wt% water) at a scan rate of 2 K/min with an amplitude of 1.272 K and a period of 60 s. All thermograms are shown in "exotherm down" format. Reprinted with permission.[79] Copyright (2016) American Chemical Society.

The thermal behavior of hydrated PAH−PAA complexes was next investigated using MDSC. MDSC is different from traditional DSC because it applies superimposed sinusoidal (modulated) and linear heating rates. This separates the total heat flow into reversing and non-reversing heat flows depending on the heat flow response. Heat capacity, melting and glass transition events are observed in the "reversing heat flow" curve, and the "nonreversing heat flow" is associated with kinetic processes such as crosslinking and aging.[150] The "total heat flow" is the sum of the reversing and nonreversing heat flow, resembling the response of conventional DSC. MDSC was required here because the transitions observed were generally weak.

The total heat flow from MDSC of hydrated $(PAH{-}PAA)_{3.5}$ complex (15.3 wt% water) is shown in Figure 3.4b. A sigmoidal transition appears in all successive scans, for which the inflection point is assigned as the thermal transition temperature T_{tr}. Both 2nd and 3rd scans overlap, indicating reversible behavior. Figure 3.5b shows the corresponding reversing and nonreversing heat flows for the second heating scan. The sigmoidal transition is captured in the reversing heat flow, accompanied by enthalpic relaxation in the nonreversing heat flow as described by a broad, weak peak. For comparison, the dried complex exhibited none of these features, Figure 3.5a. As controls, water, hydrated homopolymer PAA, and homopolymer PAH (15.3 wt% water) were also examined, Figure 3.6; neither exhibited remarkable thermal features, consistent with prior reports.[35] These results demonstrate that the thermal transition is only observable for hydrated PAH−PAA complexes.

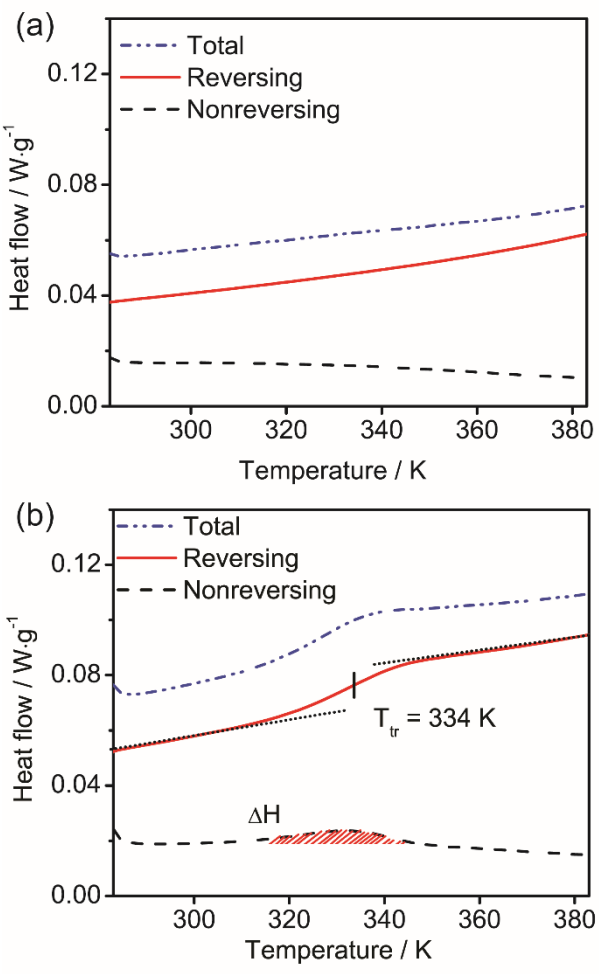

Figure 3.5. Modulated DSC heating scans of (a) dried and (b) 15.3% hydrated $(PAH{-}PAA)_{3.5}$. The 2nd heating scans are shown. The T_{tr} and ΔH (enthalpic relaxation, shaded area in b) are labeled.

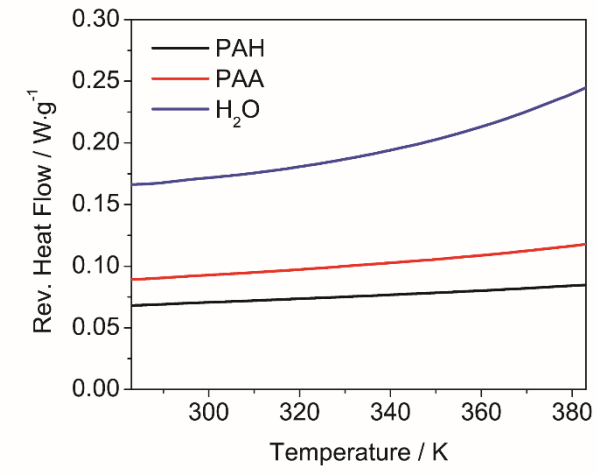

Figure 3.6. MDSC thermograms of 15.3% hydrated homopolymer PAH, PAA and water. The 2nd heating scans are shown.

The effects of varying complexation pH and water content on T_{tr} were further examined using MDSC. Figure 3.7a shows a collection of reversing heat flow curves taken from the second heating scan for (PAH−PAA)$_{3.5}$ complexes with various added water content, where the subscript denotes the complexation pH. As the added water content increased from 15.3 to 24.2 wt%, T_{tr} decreased from 334 K to 296 K. Figure 3.7b shows similar curves for the case of varying complexation pH values and constant added water content (15.3 wt%). As the complexation pH increased from pH 3.5 to 9, T_{tr} increased from 334 K to 363 K. Figure 3.7c summarizes the observed T_{tr} for a matrix of added water content and complexation pH. The general observation is that T_{tr} decreases with decreasing complexation pH and increasing hydration.

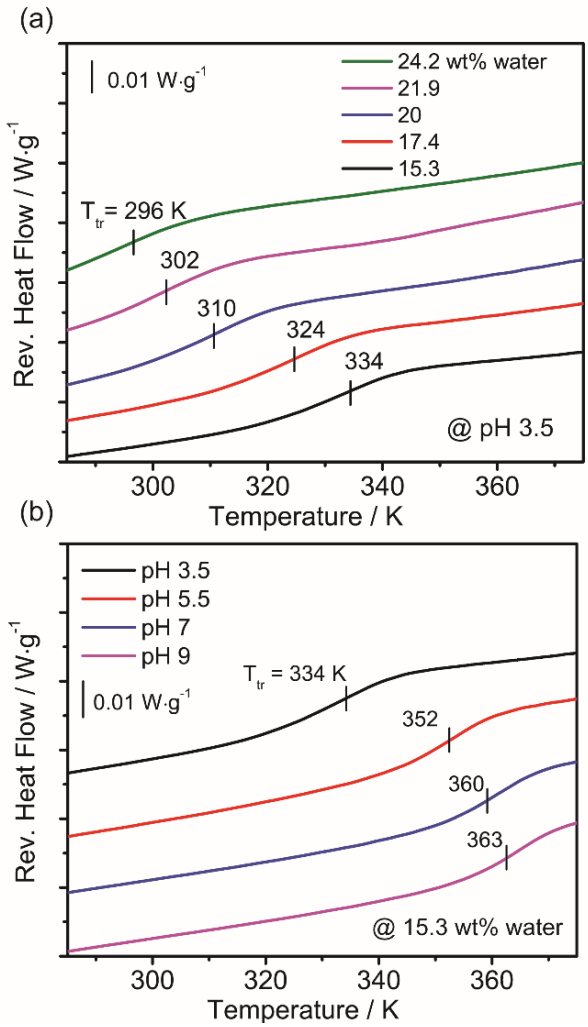

Figure 3.7. Reversing heat flows of (a) $(PAH{-}PAA)_{3.5}$ complexes of varying water content, and (b) varying complexation pH values and constant water content (15.3 wt% water). For (a) and (b), second heating scans are shown, and curves have been shifted along the y-axis for clarity. (c) T_{tr} for PAH-PAA complexes for varying complexation pH values and water content. Reprinted with permission.[79] Copyright (2016) American Chemical Society.

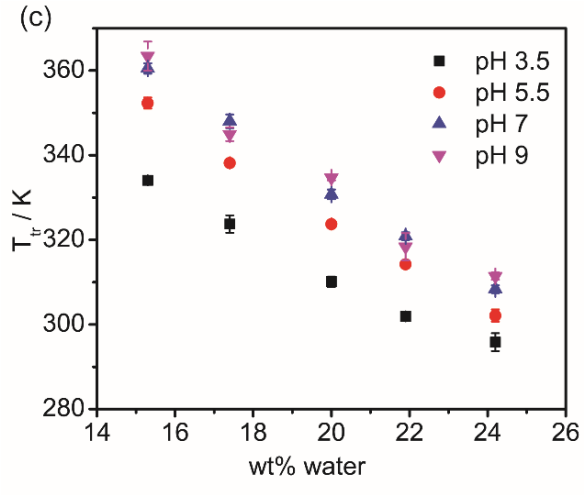

Figure 3.7. Continued.

Besides, T_{tr}, the enthalpic relaxation (ΔH), taken as the integrated area under the peak in the non-reversing heat flow, was examined as a function of complexation pH and added water content, Table 3.1. The value of ΔH ranged from 0.52 to 3.81 J/g which is considered very small as compared to enthalpies of melting (188 J/g for poly(ethylene oxide)[151]) but similar to enthalpies associated with a lower critical solution temperature (LCST) – type phase transitions (0.21 to 0.46 J/g for a *N*-isopropylacrylamide polymer hydrogel).[152] In general, ΔH decreased with increasing hydration, whereas no trend in complexation pH was observed.

Table 3.1 Enthalpy associated with T_{tr} of PAH−PAA complexes prepared from different pH solutions.

sample	wt% water	ΔH(J/g)
pH 3.5	15.3%	3.81
	17.4%	3.36
	20%	2.98
	21.9%	1.37
	24.2%	0.52
pH 5.5	15.3%	3.58
	17.4%	3.44
	20%	3.14
	21.9%	2.48
	24.2%	1.98
pH 7	15.3%	3.33
	17.4%	3.64
	20%	3.08
	21.9%	2.73
	24.2%	2.46

Table 3.1 Continued.

sample	wt% water	ΔH(J/g)
pH 9	15.3%	3.56
	17.4%	3.58
	20%	3.08
	21.9%	2.77
	24.2%	2.00

The trends in Figure 3.7c are curious in that each curve has the same general shape and appear to be shifted from one another to some extent. To explore the possibility of any unifying controlling parameters, we attempted to collapse the data in Figure 3.7c into a master curve by plotting T_{tr} against various permutations of degree of ionization, PAH−PAA composition, and water content. Only when T_{tr} was plotted against the number of water molecules divided by the number intrinsic ion pairs did the data successfully collapse into a single master curve, Figure 3.8a. Three assumptions were made to calculate the number of intrinsic ion pairs: (1) PAH degree of ionization was 100% from pH 3.5 to pH 9,[147] and (2) every PAH unit participated in intrinsic ion pairing. The former assumption is reasonable given that the pKa's of polyelectrolytes tend to shift by as much as 2-3 units upon complexation; PAH, normally having a pKa of about 8.5, would thus shift to 10.5 or 11.5. This shift was clearly observed here for PAA using FTIR, but due to overlapping peaks could not be clearly observed for PAH. (3) The number of water molecules was calculated as the total amount of water added to the PEC. A plot of

ln(water/intrinsic ion pair) *vs* $1/T_{tr}$ yielded a straight line in the form of ln(water/intrinsic ion pair) = 1267.7 $(1/T_{tr})$ - 3.18 (R^2 = 0.991), Figure 3.8b. This presents an Arrhenius-type or Boltzmann energy distribution-type relationship, yielding an energy of −10.5 kJ/mol from the fitted slope. The meaning of this relationship is not yet perfectly clear and deserves more attention. The successful collapse of T_{tr} into a single master curve without any adjustable parameters is remarkable considering this has not been previously demonstrated, and has strong implications on the role of water around intrinsic ion pairs for the thermal transition.

To further understand the role of water, we investigated PECs in the presence of water-solvent mixtures, specifically $(PAH{-}PAA)_{3.5}$ in the presence of 1-propanol and water. 1-propanol has a boiling point close to that of water, and mixtures of 1-propanol and water led to increased viscosity and decreased surface tension.[32] The T_g of water is 135 K[153] and that of 1-propanol is 96.2 K.[154] The relative permittivity of water is 80.36 at 293 K[155] and that of 1-propanol is 20.45 at 293 K.[156] Also, an individual water molecule can participate in hydrogen bonding at two sites, whereas 1-propanol can participate at one. Figure 3.9 shows T_{tr} for $(PAH{-}PAA)_{3.5}$ complexes in the presence of mixtures of varying water/1-propanol content and of varying added liquid content, where "liquid" stands for the combined water and 1-propanol mass. It is generally observed that T_{tr} increases with decreasing added liquid and with decreasing water content. For example, at a constant liquid content of 20 wt% (red bars, middle panel), T_{tr} increased from 310 K to 369 K as the water content in the liquid decreased from 100 wt% to 40 wt%. At high 1-

propanol content, T_{tr} exceeded observable limits, (labeled as N/A, bottom panel). This observation suggests that 1-propanol does not plasticize the complex.

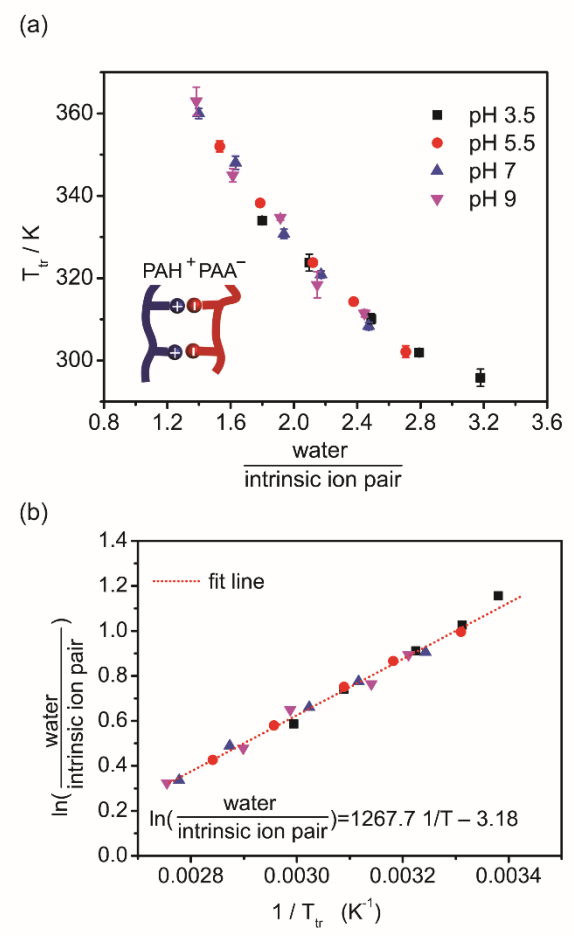

Figure 3.8. (a) T_{tr} *vs* number of water molecules per intrinsic ion pair in hydrated PAH−PAA PECs prepared at pH 3.5, 5.5, 7, and 9. The number of water molecules is taken as the total amount of water added to the complex. The number of intrinsic ion pairs is calculated from the PEC mass and PAH−PAA composition, assuming that all PAH units are ionized and participate in intrinsic ion pairing. (b) Linear fitting of ln(water / intrinsic ion pair) *vs* $1/T_{tr}$. The legend in (a) also applies to (b). Reprinted with permission.[79] Copyright (2016) American Chemical Society.

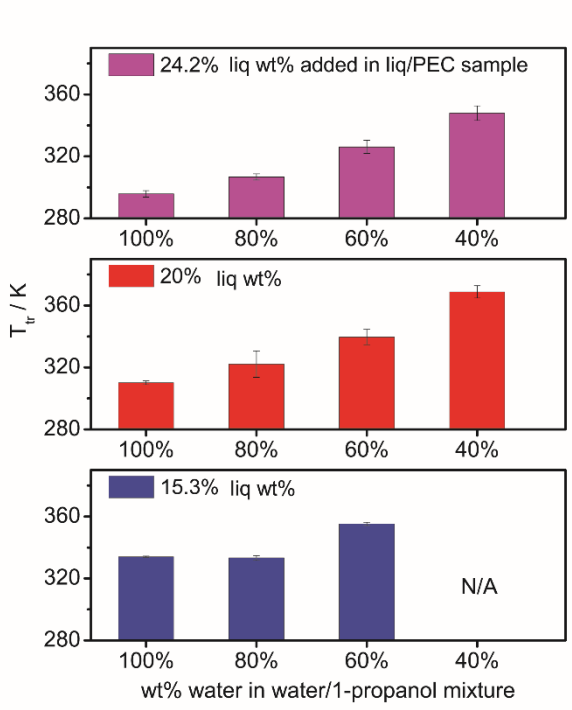

Figure 3.9. T_{tr} of $(PAH{-}PAA)_{3.5}$ complexes with varying water/1-propanol ratios and liquid to PEC ratio (where liquid denotes water and 1-propanol together). Reprinted with permission.[79] Copyright (2016) American Chemical Society.

To further investigate the role of hydrogen bonding in regard to the thermal transition, we measured T_{tr} in the presence of aqueous urea solution, Figure 3.10. Urea is known to compete with hydrogen bonding interactions and to slow water dynamics of water interacting with urea molecules.[157] The T_{tr} of $(PAH{-}PAA)_{3.5}$ at 20 wt% water was 310 K, whereas the T_{tr} for the PEC at equivalent aqueous urea solutions of 0.01 M, 0.1 M and 1 M were 310 K, 311 K and 322 K, respectively. As urea content increases, T_{tr} increases.

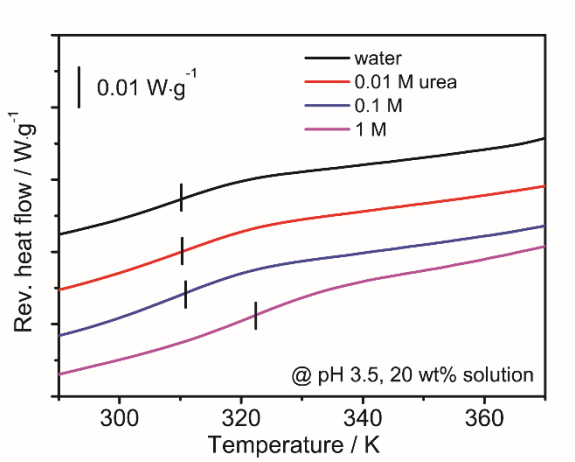

Figure 3.10. MDSC reversing heat flows of 20 wt% hydrated $(PAH{-}PAA)_{3.5}$ with water or with aqueous urea solution. 2nd heating scans were shown. Reprinted with permission.[79] Copyright (2016) American Chemical Society.

From the preceding, it is clear that increasing water content lowers T_{tr}. To further investigate the influence of water, we plot T_{tr} as a function of the water to PEC mass ratio in Figure 3.11 where data are aggregated from $(PAH{-}PAA)_{3.5}$ complexes in the presence of pure water or other liquid mixtures. Because the preparation pH was kept constant at 3.5, the extent of intrinsic ion pairing is expected to remain constant. The water/PEC data are shown as black squares, water/1-propanol/PEC as red circles, and urea as cyan diamonds. We also investigated 1,2- and 1,3-propanediol (blue and purple triangles, respectively). We also investigated 1,2- and 1,3-propanediol (blue and purple triangles, respectively). Remarkably, the different sets of data overlap and follow a general trend of T_{tr} decreasing with increasing water content. The fact that the data overlap regardless of

whether 1-propanol or propanediol is present suggests that neither strongly affect T_{tr} and that the added solvents may not be interacting strongly with intrinsic ion pairs.

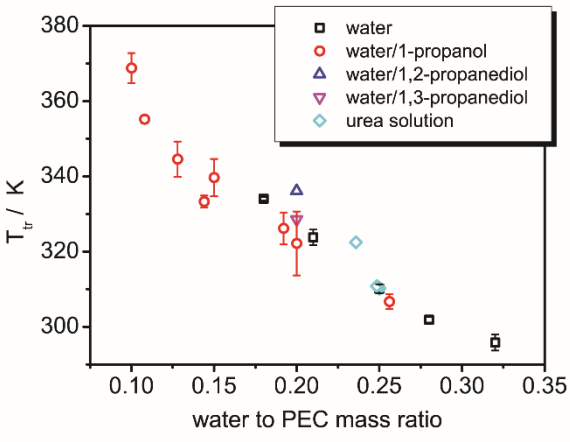

Figure 3.11. T_{tr} of $(PAH{-}PAA)_{3.5}$ complexes as a function of only water to PEC mass ratio for samples treated with water or other liquid mixtures. Reprinted with permission.[79] Copyright (2016) American Chemical Society.

3.4. Discussion

Complexes and LbL assemblies are often compared to one another because they are formed using the same interactions. In prior work,[35] we measured T_{tr} for PAH/PAA LbL assemblies as a function of assembly pH (and therefore composition). Table 3.2 compares these aspects for both LbL assemblies and complexes. At a given pH, LbL assemblies and complexes have strikingly different compositions. This is most likely because the complexes were dialyzed for 4 days against a matching pH buffer solution, which may give longer time for equilibration.[8] In contrast, LbL assemblies are generally recognized as non-equilibrium structures.[158] Whereas complexes demonstrate a steady

trend in T_{tr} with pH, LbL assemblies do not. Significantly, this comparison shows that T_{tr} depends on structure (composition) even if the assembly pH-values are identical.

Table 3.2 Properties of hydrated PAH/PAA LbL films and complexes (with 15.3 wt% water).

	wt% PAA, LbL[a]	$T_{tr,LbL}$ [a] (K)	wt% PAA, complexes	$T_{tr,complex}$ (K)
pH 3.5	51±3	335±1	67±1	334±0.4
pH 5.5	29±2	324±6	61±1	352±1
pH 7.0	43±1	N/A	58±3	360±1
pH 9.0	15±2	333±10	55±1	363±3

[a] Data are taken from Ref.[35]

Also, these results show that complexation pH influences polyelectrolyte degree of ionization in PAH−PAA complexes, Figure 3.3b. At pH 3.5, the degree of PAA ionization α in the complex was 74%, which is dramatically higher than that of spin-cast PAA (10%) and of PAA in an LbL assembly (45%) at equivalent conditions.[38, 86] This suggests that PAA within the PAH−PAA complex has a very low pK_a (well below that of 3.5), which is lower than that of homopolymer PAA (pK_a = 5.5-6.5) and perhaps nearer to

that of the LbL assembly (pK_a = 2.5-2.75).[86, 159] This is because complexation lowers the ionization barrier for PAA.[86]

Complexation pH also influences the composition of the PAH−PAA complex. Although these are formed from stoichiometric (by repeat unit) mixtures, the resulting dialyzed complexes have compositions ranging from 62 to 50 mol% PAA as complexation pH increases from 3.5 to 9. This is because of mismatched degree of ionizations between PAA and PAH. At pH 3.5, PAA is partially ionized and PAH is fully ionized; therefore, more PAA must participate in complexation so as to fully neutralize PAH. Not until pH 7 to 9 does a stoichiometric mixture approach the composition of a stoichiometric complex. Similar behavior could be expected for LbL films but the data of Table 3.2 shows that the film composition does not comply with a systematic trend. As already noted, this is very likely due to LbL films being out-of-equilibrium.

The results show that water strongly affects the transition, and appears to have a plasticizing effect by which T_{tr} decreases with increasing water content. Dried PAH−PAA complexes do not exhibit any evidence of a T_g or T_{tr} because extensive intrinsic ion pairing lowers the mobility of polymer chain segments and raises T_{tr} outside of reasonable observation. As water is added to the PAH-PAA complex, we first observe the appearance of a T_{tr} at 15.3 wt% water. As more water is added, T_{tr} decreases further until it lies below our observation range, Figure 3.7a. Notably, homopolymer controls samples hydrated with 15.3 wt% water yielded no thermal features, Figure 3.6. These results show that water is essential for the transition.

Water may exist in several forms within the PEC: as bulk water, water bound at extrinsic ion pairs, and water bound at intrinsic ion pairs. Given the fairly low hydration levels we explored, we expect the latter two to be of more significance. The collapse of all T_{tr} into a single master curve when plotted against the ratio of added water to intrinsic ion pairs suggests that water at this site is very important to the transition. To test the significance of the water/intrinsic ion pair ratio, we also plot T_{tr} for PAA, PAH, water/extrinsic PAA sites, and water/neutral PAA sites in Figure 3.12. PAA units will exist in three distinct states: (1) ionized and intrinsically compensated, (2) ionized and extrinsically compensated, and (3) neutral. PAH is expected to exist as fully ionized and intrinsically compensated over the range of pH values studies. Only in the case of PAH is a master curve reproduced, consistent with our assumptions.

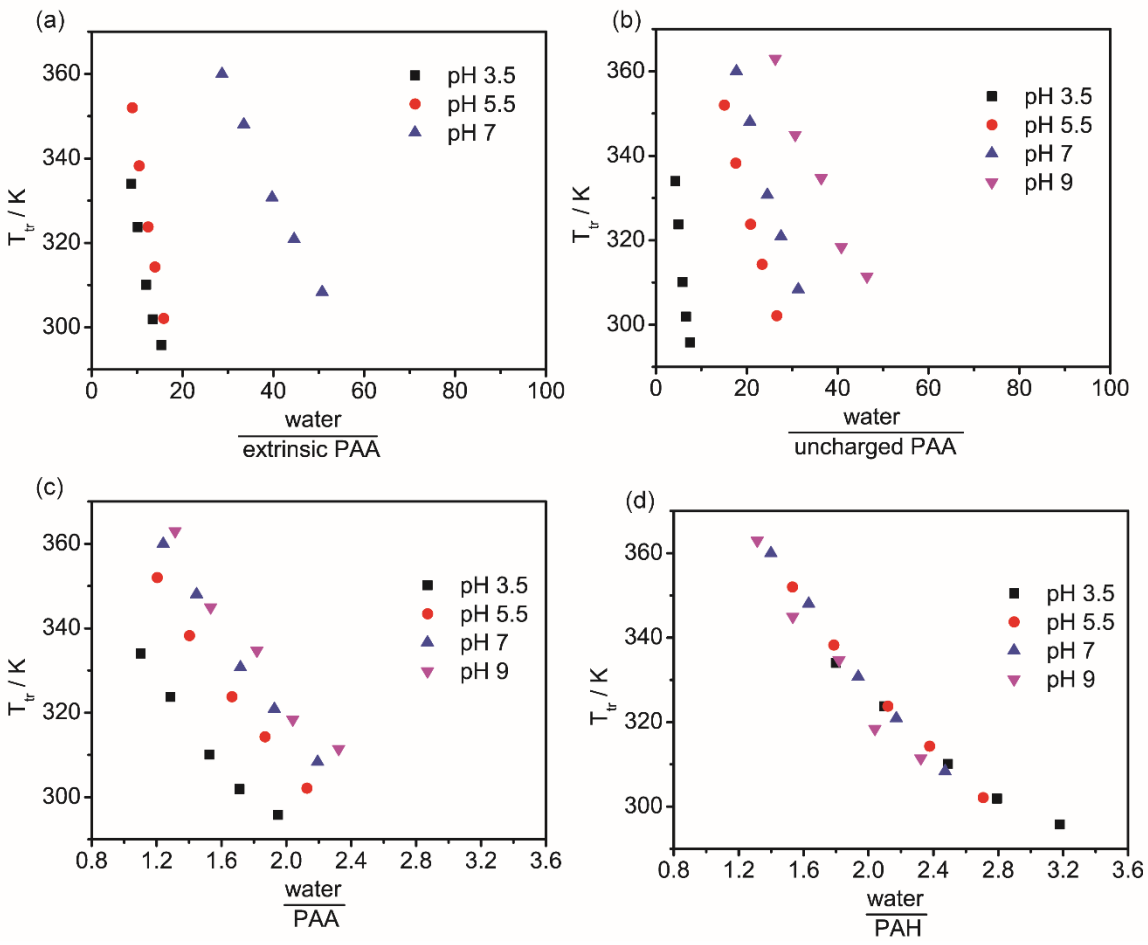

Figure 3.12. T_{tr} with number of water molecules per (a) extrinsic PAA, (b) uncharged PAA, (c) PAA, (d) PAH repeating unit.

Plotted another way, we show T_{tr} *vs.* composition and *vs.* PAA ionization at a constant hydration in Figure 3.13. T_{tr} generally increases with decreasing PAA composition and with increasing PAA ionization. In light of our findings, we attribute this trend to the general increase in the number of intrinsic PAH−PAA ion pairs within the complex and the corresponding decrease in the number of water molecules per intrinsic ion pair. Ion-pairs act as noncovalent cross-links and reduce chain mobility, thus

increasing T_{tr}. As the composition approaches stoichiometric values (towards pH 9), the number of intrinsic ion-pairs should increase, consistent with an increase in T_{tr} (Figure 3.7b and Figure 3.7c).

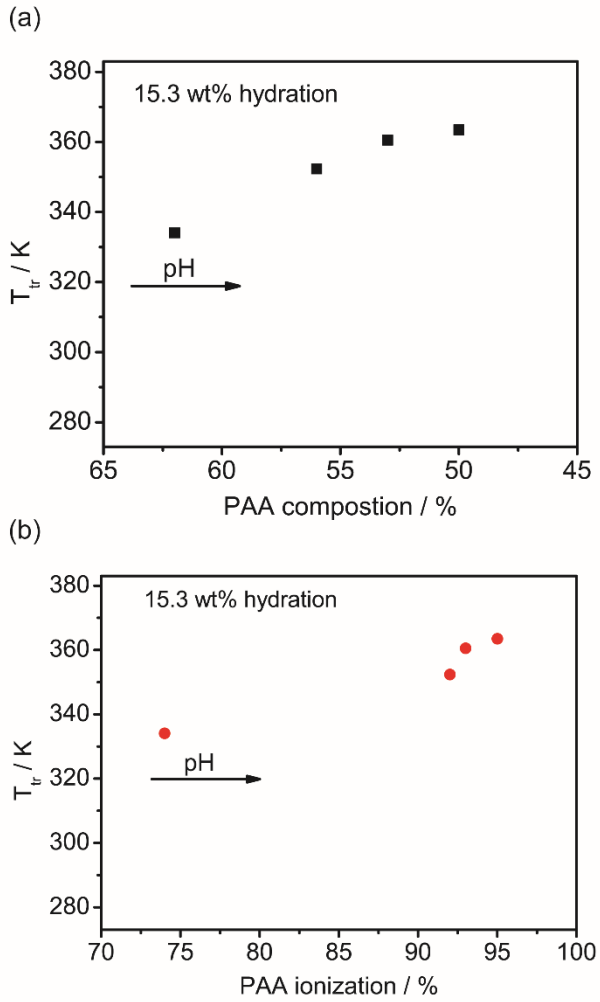

Figure 3.13. $(PAH\text{-}PAA)_{3.5}$ complex T_{tr} as a function of (a) PAA composition and (b) PAA ionization.

In light of our prior simulations[78] and the results presented here, water may play multiple roles in the thermal transition. Our prior simulations of PDADMA-PSS complexes indicate that the thermal transition is accompanied by a decrease in the number of water molecules surrounding the extrinsic PSS site and a change in the hydrogen bonding water-polyelectrolyte network. On the other hand, the work presented here points to the role of water at the intrinsic ion pair. It is possible that adding water to the PEC decreases PAH−PAA intrinsic attractions, meaning that the electrostatic interactions between PAH and PAA may be reduced. Consequently, the volume for chain relaxation increases with increasing hydration and water acts as a plasticizer, assisting with chain motion. Our past and current findings lead us to propose a two-step mechanism to describe the thermal transition observed in hydrated PECs: (1) water-polymer hydrogen bonding force decreases first as temperature increases and (2) this is followed by polymer chain relaxation facilitated by water at intrinsic ion pair sites.

This proposed mechanism is further supported by the results for water/solvent mixtures shown in Figure 3.11. The fact that these all water/solvent mixtures overlap for a graph of T_{tr} *vs* water/PEC mass indicates the transition is controlled by water alone and that the solvent is acting as a spectator. Possible reasons are that alcohol does not hydrate the polymer matrix and that less polyelectrolyte-water hydrogen bonds are formed as compared with pure water. The latter is supported by the fact that neither 1,2- or 1,3-propanediol caused significant deviations from the curve in Figure 3.11. With regard to urea, it was observed that increasing urea content increased T_{tr}. It may be interpreted as the ability of urea to disrupt hydrogen bonds,[157, 160] thus reducing the “apparent” water

content. However, no remarkable departure from the curve in Figure 3.11 was observed, so the results with urea may be interpreted similar to that of 1-propanol and the propanediols. Changes in the dielectric constant may also be considered, where the dielectric constant of 1-propanol is lower than that of water (20.45 *vs.* 80.36 at 293 K), such that the Debye screening length is reduced in 1-proponol. As a consequence, water hydrating polyelectrolyte-polyelectrolyte ion pairs can be expected to reduce the Coulombic interaction between the ion pairs significantly in comparison to propanol as the solvent. Complementary results regarding water content have been observed for organic solvent and osmotic agents for PECs and with LbL assemblies, where deswelling and stiffening occurs.[77, 142, 161, 162]

3.5. Conclusion

The glass-transition-like thermal transition in polyelectrolyte complexes containing weak polyelectrolytes PAH and PAA was probed experimentally as a function of water content and complexation pH. Dried PAH-PAA PECs did not bear an observable T_{tr} in contrast to hydrated PECs. As the hydration content increased over a narrow range, T_{tr} decreased by 10s of degrees. PECs prepared at lower pH values (pH 3.5) had a lower T_{tr} because of mismatching charge density, less ion pairs per unit volume, and higher PAA content. For PECs of $(PAH{-}PAA)_7$ and $(PAH{-}PAA)_9$, their composition and ionization were similar, which led to similar T_{tr} values. It was demonstrated that T_{tr} collapsed onto a single master curve when plotted against the ratio of water molecules to intrinsic ion pairs for all pH-values investigated. The master curve demonstrated linearity when plotting ln(water/intrinsic ion pair) *vs* ($1/T_{tr}$). These results lead us to propose that the glass-

transition-like thermal transition follows a two-step relaxation mechanism initiated with the reducing water-polymer interactions, followed by the relaxation of the polymer chains facilitated by water surrounding intrinsic ion pairs. Our future work will encompass molecular simulations to examine this proposal as well as further experimental investigation. In total, the implications of this study extend beyond dried PECs and are important to a range of areas related to water dynamics and influence on the polyelectrolyte systems including complexes and multilayers.

CHAPTER IV

THERMAL TRANSITION IN POLY(DIALLYLDIMETHYLAMMONIUM CHLORIDE)−POLY(SODIUM 4-STYRENESULFONATE) COMPLEXES

4.1 Introduction

Polyelectrolyte complexes (PECs) are prepared from the association of oppositely charged polymers by mixing their aqueous solutions together, leading to the formation of solid-like complexes or liquid-like coacervates.[67, 131, 163] The formation and properties of PECs are influenced by both the chemistry of the starting materials and the external conditions, especially the pH and ionic strength.[59, 60, 64, 164, 165] PECs have been actively involved in many application areas such as self-healing materials,[30] controlled drug release,[166] bone remodeling,[46] and membrane separations.[167] Numerous investigations have been conducted on the mechanism of PEC formation[59, 168, 169] and various physicochemical aspects including conductivity, mechanical properties, and thermal properties.[30, 77, 170] A particularly interesting physical phenomenon for PECs is the glass or thermal transition (T_g or T_{tr}), as it defines their processability and their applications as thermally responsive materials.[171, 172]

Glass-transition-like thermal events have been identified and extensively studied in hydrated PECs and their counterparts, polyelectrolyte multilayers (PEMs). Köhler et al. first reported that poly(diallyldimethylammonium chloride)/poly(sodium 4-styrenesulfonate) (PDADMA/PSS) capsules changed in size upon heating in aqueous solution, for which a glass-melt transition was detected using calorimetry.[82] Vidyasagar et al. observed a distinct T_g in exponentially growing PEMs, as shown by the increase in

softness using quartz crystal microbalance with dissipation (QCM-D) monitoring.[34] Thermal transition events in PEMs have been widely displayed as a step change in microstructure size, heat capacity, mass, modulus, or impedance.[34, 81, 82, 141]

In all of these cases, the complexes or multilayers required some critical amount of hydration so as to observe a glass transition. However, the effect of water on the glass transition for PECs or PEMs, and the reasoning behind this, is not well understood. Earlier, it was reported that dried PECs were brittle, having no detectable T_g.[8, 85, 86] However upon immersion in salt water, PECs became soft enough for processing.[77] The strong correlation between PEC/PEM physical properties and water has been noticed elsewhere. For example, PEMs were annealed with water and interlayer diffusion increased.[39] Nolte et al. observed plasticization of PEMs by water accompanied by substantial changes in modulus and thickness.[173] Gu et al. discovered that sticky hydrated PEMs contracted and dehydrated when in contact with organic solvent.[161, 174] Peterson and coworkers observed humidity history-dependent mechanical moduli for PECs.[89] These effects are generally attributed to water plasticization and a lowering of the T_g, but the underlying mechanism needs further explanation.[15, 77] This is because PECs possess mixed ion pairing character, and the location of water molecules and their states have not been fully quantified. A recent FTIR investigation suggests that fully hydrated PEMs contained a mixture of water populations.[175]

The PEC or PEM structure is considered a physical network, with polycation-polyanion pairs (intrinsic ion pairs) acting as physical cross-links. Salt doping disrupts the intrinsic ion pairs and converts them into polyion−counterion pairs (extrinsic ion pairs),

which increases polymer mobility.[105, 176] Salt doping of the PEC may be described according to the following equation 4.1:

$$\mathrm{Pol^+Pol^- + Na^+ + Cl^-} \rightleftharpoons \mathrm{Pol^+Cl^- + Pol^-Na^+} \qquad 4.1$$

Further, the molar ratio of salt to polymer repeat unit (assuming that the PEC has stoichiometric composition) is defined as the salt doping level,[11] shown in the equation:

$$y = \frac{\mathrm{NaCl}}{\mathrm{Pol^+Pol^-}} = \frac{\mathrm{Cl^-}}{\mathrm{Pol^+}} = \frac{\mathrm{Na^+}}{\mathrm{Pol^-}} \qquad 4.2$$

This leads to the formulation of an association constant K_a defined as in equation:

$$K_a = \frac{(1-y)a^2}{y^2} \rightarrow \frac{a^2}{y^2} \; (as\; y \rightarrow 0) \qquad 4.3$$

where a is the activity of the salt in the polyelectrolyte solution. The question is, then, how water and doping are interrelated to the glass transition.

Recently, we experimentally examined the thermal behavior of poly(allylamine hydrochloride)−poly(acrylic acid) (PAH−PAA) complexes as a function of pH (i.e., charge density or intrinsic ion pairing density) and water content. Glass transition-like behavior was observed and the T_g was labeled as a generic thermal transition (T_{tr}) since its mechanism was unclear. For the first time, a master curve was shown to link T_g (or T_{tr}) to the molar ratio of water to intrinsic ion pairs, indicating the key role of water surrounding intrinsic ion pair sites.[79] This relationship had the general linearized form of ln(water/intrinsic ion pair) = m(1/T)-b, where m and b are the slope and intercept. Our complementary simulation work for a different PEC system suggested that the thermally induced events observed were initiated by the changing dynamics of water molecules instead of a traditional glass transition event.[78] It was proposed that the shortening of the

hydrogen bond lifetime at water–polyelectrolyte hydrogen binding sites facilitated polymer chain relaxation. Prior to us, interchain hydrogen bond reorganization has also been reported to alter the physical properties of strong polyelectrolyte brushes.[177] In sum these recent findings suggest that the T_g, the doping level, and the water content are inextricably linked. However, as that was only one study, there remained uncertainty as to whether this simple equation could be linked to other PEC systems and whether the equation had robust physical significance.

This question is mirrored to the concept of time-temperature-salt or time-humidity superpositioning, as described by others for PECs and PEMs.[77, 170, 178-180] To this end, the relationship of salt with the thermal and mechanical properties of PECs has been examined.[77] The addition of salt has been shown to facilitate extrusion of PECs[104] and increase polymer chain diffusion of PEMs.[39] Many studies have identified the T_g using dynamic mechanical or rheological measurements. Shamoun et al. observed that T_g decreased with increasing salt doping level and decreasing frequency, deducing a time/temperature/salt superposition.[77] The T_g in PEMs exhibited a similar trend in that T_g decreased as NaCl concentration increased.[34] The T_g of PEMs when exposed to divalent salt solution was also examined.[84] Tekaat et al. have shown time-pH superpositioning in PAA/PDADMAC complex coacervates.[178] Perry et al. explored the dynamic mechanical response of PDADMA/PSS/KBr system in both coacervate and precipitate states and identified a salt-driven liquid-to-solid transition using a frequency-invariant analysis strategy of time-salt superposition data.[179] These studies in general show that salt influences chain relaxation in that salt generally increases the mobility of the

polyelectrolyte chains and decreases the observed T_g. Other than shear modulus, Cramer et al. established a time-humidity-superposition principle in ion-conducting PECs using frequency-dependent conductivity measurements.[180] The absorbed water facilitated ion motion both in long-range transport and short-range scales in a similar way.

Here, the role of salt and water on the thermal transition in PDADMA−PSS complexes was investigated. PDADMAC and PSS, highly charged synthetic polyelectrolytes, form the preferred model pair of PECs.[34, 64, 141, 142] This is distinctly different from our prior work which examined pH-temperature relationships in weak polyelectrolyte complexes of PAH−PAA. By examining the PDADMA−PSS system, we show the universality the relationship among the T_g, hydration, and ion pairing, which deepens its physical interpretation, indicating that the thermal transition is a glass transition. PDADMA−PSS complexes were prepared from NaCl solution with concentrations ranging from 0 to 1.5 M. The PEC compositions and salt doping levels were analyzed using neutron activation analysis (NAA) and nuclear magnetic resonance (NMR) spectroscopy. The T_g was detected using modulated DSC. MD simulations performed on the corresponding PEC model separate the intrinsic and extrinsic ion pairs and study the hydrogen bonding between water and PSS repeat units as a function of temperature. The findings draw a quantitative connection between the T_g and the molar ratio of water to intrinsic ion pairs in PECs, which allows for the interpretation of the water plasticization role.

4.2. Materials and methods

4.2.1 Materials

Poly(diallyldimethylammonium chloride) (PDADMAC, 20 wt % in water, Sigma Aldrich, M_w = 200 000−350 000 g/mol) and poly(sodium 4-styrenesulfonate) (PSS, Scientific Polymer Products, M_w = 500 000 g/mol) were used as received. Polyelectrolyte solutions were prepared using deionized water with 18.2 MΩ·cm resistivity. Sodium chloride (EMD Chemicals Inc.) was added to the polyelectrolyte solution to adjust the ionic strength.

4.2.2 Preparation of polyelectrolyte complexes

The homopolymer solutions of PDADMAC and PSS were prepared at 50 mM concentration with respect to their repeat unit. The concentration of the salt in the polyelectrolyte solution was adjusted to 0, 0.1, 0.5, 1.0 and 1.5 M by adding NaCl. The polyelectrolyte complexes (PECs) were prepared by mixing stoichiometric amounts of PDADMAC and PSS solutions under stirring. The precipitate PECs were centrifuged at 10000 rpm for 10 min, pressed at 6000 psi pressure using Carver Press, and quickly rinsed with copious water. After being dried in a convection oven at 343 K overnight, the PECs were ground into fine powders. The powders were intensively dried in vacuum at 423 K for 6 h and sealed in a container until further characterization.

4.2.3 Neutron activation analysis

Neutron activation analysis (NAA) is a highly sensitive and well developed nuclear technique for multi-elemental quantification purposes. It has been shown to be an

accurate detection method of counterions or metal elements in polymeric materials. [181-184] The basic theory is described briefly as follows. The various isotopes of elements in the sample capture neutrons when exposed to a steady and uniform flux of thermal neutrons for a period of time, forming compound nuclei at excited states. The activated nuclei instantaneously de-excite into a more stable configuration, radioisotopes in most of the cases, by rapid emission of gamma rays (photons). The subsequent delayed gamma radiation generated by the radioisotopes can be utilized for detection and identification of the elements.[185] NAA detection of Na, Cl, and S elements were used for calculating the composition of the PECs. While the amount of sulfur atoms S is a telltale sign of PSS fraction in the system, two assumptions were made to calculate the PDADMA mol%: (1) The dried PEC powder samples were assumed to be electroneutral, and (2) all Na^+ and Cl^- ions were assumed to be associated with the charged groups of the polyelectrolyte chains. This means, the Na^+ and Cl^- ions are assumed to form extrinsic ion pairs with the polyelectrolyte and not NaCl crystals in the PECs. Notably, the sample here is solid powder instead of aqueous suspension.

Transfer of the PEC powder, weighing from 20 to 40 mg, into irradiation containers was carried out in a nitrogen glovebox to avoid moisture absorption. The samples were irradiated in a 1 MW TRIGA reactor for 30 s at a neutron flux of 9.1×10^{12} n/(cm^2·s) and cooled for intervals of 270 s and up to 1 to 3 h prior. The subsequent gamma-ray photons were counted using a high-purity Ge (HPGe) gamma-ray detector. The Na, Cl and S mass fractions were quantified using multiple gamma-ray emissions from the decay of ^{24}Na, ^{38}Cl, and ^{37}S, respectively. All of the uncertainties are recorded at the 2 s.

The compositions of the PECs were estimated based on an assumption that the dried PEC powder was macroscopically electroneutral.[186] The NAA measured S atom content was used for determining the PSS content in moles. The number of negatively charged groups or ions was equal to the number of positively charged ones: $PSS^- + Cl^- = PDADMA^+ + Na^+$.

4.2.4 Proton nuclear magnetic resonance spectroscopy

Proton nuclear magnetic resonance spectroscopy (^{1}H NMR) (500 MHz proton frequency, Varian Inova 500 spectrometer) was employed to measure the composition of the PECs. 30 mg dried PEC sample was dissolved in 0.7 mL 2.5 M KBr in D_2O in an NMR tube. ^{1}H NMR was additionally used to examine the PEC composition. The NMR spectra of PDADMAC, PSS, and PEC were used to calculate the composition of the PECs. The D_2O peak was chosen as the reference at 4.79 ppm.[187] The PEC composition is calculated by comparing the integration of NMR peak areas of the 4 aromatic hydrogens of PSS (between 5.5 and 9 ppm) and the 16 aliphatic hydrogens of PDADMAC and 3 of PSS (between 0 and 4.6 ppm).[104] In line with the NAA analysis, the PSS mol % (by repeat unit) was found to be ca. 43 to 46 % in various samples and again the compositions showed no clear trend based on the starting solution salt concentration.

4.2.5 Modulated differential scanning calorimetry

Modulated DSC (Q200, TA Instruments) was performed on PECs in both dried and hydrated states. Dried PEC powder was loaded in a Tzero pan and covered with Tzero lid. Hydrated samples were prepared by adding water into the PEC powder using a

microliter syringe dropwise until required mass was reached. The pan was subsequently sealed with a Tzero hermetic lid and rested for at least 24 h. The water content was varied from 16 to 32 wt % at intervals of 2 wt %. Modulated DSC was performed on samples in a heat-cool-heat-cool cycle. The samples were ramped from 278 K to 413 K at a rate of 2 $K \cdot min^{-1}$ with amplitude of 1.272 K for a period of 60 s. Nitrogen was used as a purge gas at 50 $mL \cdot min^{-1}$. The T_g was taken as the inflection point of the second heating cycle.

4.2.6 Molecular dynamics simulations

All-atom molecular dynamics (MD) simulations of assemblies consisting of more than 40 $PDADMA_{20}$ and PSS_{20} molecules, where the subscript 20 refers to the number of repeat unit in each chain, were performed using the Gromacs 5.1.3 package[188, 189] and the OPLS-aa force field.[190, 191] Sodium and chloride ion parameters were from Refs.[192, 193] and PSS partial charges from Ref.[194]. Water was modelled by the explicit TIP4P water model.[195] Electrostatics were described by the PME method.[196] Temperature control was by the V-rescale thermostat[197] and pressure control at reference pressure 1 bar by the Parrinello-Rahman barostat[198] with coupling constants 0.1 ps and 2 ps, respectively. Van der Waals interactions employed a 1.0 nm cut-off.

Throughout the simulations, all the bonds in the polyelectrolytes and water molecules were controlled by the LINCS [199] and SETTLE [200] algorithms, respectively. A 2 fs (initially 0.5 fs) time step within the leap-frog integration scheme was applied and the trajectories were written every 1000 steps. The polyelectrolytes were coupled to the heat bath as one thermostatting group while water and the ions were coupled to the heat bath as another group.

The chemical structures of polyelectrolytes and sample chain fragment conformations are presented in Figure 4.1. The initial configurations were generated using PACKMOL[201], with polyelectrolyte chain conformations extracted from dilute solution. The detailed steps of obtaining polyelectrolytes assemblies with relatively uniform structure and water distribution are presented in the Table 4.1. The generated initial configurations were simulated for 100 ns in an elevated 370 K temperature after which the temperature was brought down to 290 K in 10 ns time as the relaxation before the production run. System compositions reflect the compositions determined experimentally using neutron activation analysis as closely as reasonably feasible. The ions wt % and PSS to PDADMA ratio (based on repeat unit molar ratio) in each simulation are gathered in the Table 4.2 and the detailed simulation compositions in the Table 4.3.

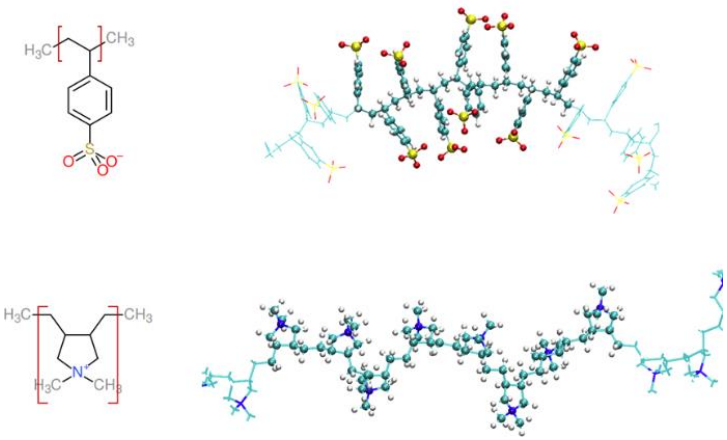

Figure 4.1. The chemical structures of the examined polyelectrolytes and snapshots of the structures from molecular dynamics simulations. PSS^- is at the top panel and $PDADMA^+$ at the bottom.

Table 4.1 Molecular dynamics simulation protocol

No	Ensemble	Duration [ns]	t step [fs]	T [K]	Simulation box	Comments
1	NVT	1	0.5	290	20x20x20 nm	Initial hydration of the PEs with position restraints applied on the PE chains (prevents PE-PE bonding without water shell)
2	NPT	0.5	0.5	290	Isotropic pressure coupling	Initial box size relaxation (short time step because of significant compression of the box to reach approximately 1 bar pressure)
3	NPT	50	2	370		Equilibration in elevated temperature
4	NPT	50	2	370	Anisotropic pressure coupling (off-diagonal compressi-bilities set to zero to keep box rectangular)	Continuation of the equilibration in elevated temperature with a more flexible simulation box
5	NPT	10	2	Linear cooling from 370 to 290 K during the first 6 ns. Then 290 K.		Relaxation
6	NPT	225	2	Stepwise temperature, 290 to 360 K with 5 K increase steps. 15 ns each step.		Production run

Table 4.2 Composition of the PECs in the simulations and experiments. The experimental PEC composition is based on the neutron activation analysis as discussed in detail in the Results section.

	0M		0.5M		1.5M	
	Experiments	Simulations	Experiments	Simulations	Experiments	Simulations
Na^+ [wt%]	0.012	0.00	0.382	0.350	1.56	1.54
Cl^- [wt%]	0.91	1.04	2.54	2.69	3.35	3.37
PSS to PDADMA ratio	0.922	0.913	0.833	0.826	0.922	0.913

Table 4.3 Composition of the simulated systems. The NaCl concentration refers to the experimental assembly process.

Molecule type		0M NaCl	0.5M NaCl	1.5M NaCl
		Number of molecules		
PSS_{20}		21	19	21
$PDADMA_{20}$		23	23	23
Na^+		0	20	95
Cl^-		40	100	135
Water	22 wt%	2138	2064	2225
	26 wt%	2664	2571	2772
	30 wt%	3250	3137	3382

Modelled assembly compositions correspond to 0, 0.5, and 1.5 M NaCl preparation solutions. For each NaCl concentration, hydrations of 22, 26, and 30 wt % water were studied. Simulation compositions reflect the NAA determined compositions.

The initial configurations were generated using PACKMOL.[201] In the production run, the temperature was increased from 290 K to 360 K in 5 K steps of 15 ns each for a total simulation duration of 215 ns. The first 1 ns of each temperature step was disregarded in the analysis. The ion pairing classification was conducted at the beginning of the production run at 290 K. The ion pairing did not change significantly during the temperature ramping which implied that the simulation time scale is insufficient to capture polyelectrolyte chain motion. A PSS monomer is defined as extrinsically compensated if a Na^+ ion is within a cut-off separation of 0.45 nm from the PSS S atom and intrinsically compensated otherwise. For hydrogen bond analysis, a 0.35 nm cut-off distance and 30º angle was used. The hydration shell around a PSS charged group was determined using a cut-off defined by the minimum after the first peak of the respective RDF, shown in Figure 4.2. The presented results correspond to the average of three different initial configurations, unless otherwise stated. The employed timescale is too short to capture polymer chain relaxation and diffusion but water and ion dynamics are captured. All simulations employ periodic boundary conditions. Visualizations were done by the VMD software.[202]

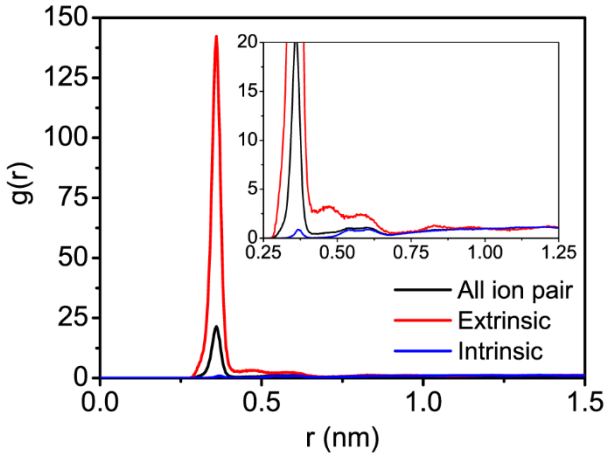

Figure 4.2. Radial distribution function calculated from the molecular dynamics simulations between the S atom in PSS group and Na^+ ion in PECs with 22 wt % water and prepared from 0.5M NaCl.

4.3. Results

Figure 4.3 shows the compositions of PECs prepared and isolated from stoichiometric mixtures of PDADMA and PSS in the presence of various salt concentrations. From elements detection of NAA, the PDADMA and PSS compositions were calculated, Figure 4.3a. NMR results in Figure 4.4 are fully consistent with the NAA results (Figure 4.3a), which validates the later detection technique. For PECs at all salt concentrations, PDADMA was in excess at 52 to 55 mol%. This non-stoichiometric composition has also been observed elsewhere using scintillation counting.[68]

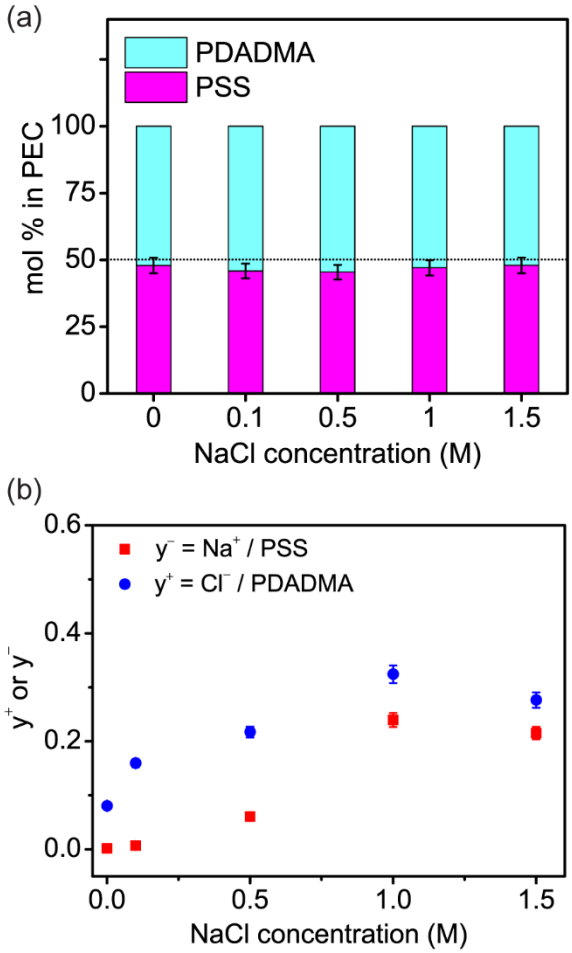

Figure 4.3. (a) PEC composition based on PDADMA and PSS repeat units for PECs prepared at varying NaCl concentrations measured. (b) Doping levels, for which y– and y+ and are the molar ratios of Na+ to PSS and Cl– to PDADMA, respectively. The error bars represent the uncertainties (95% confidence level).

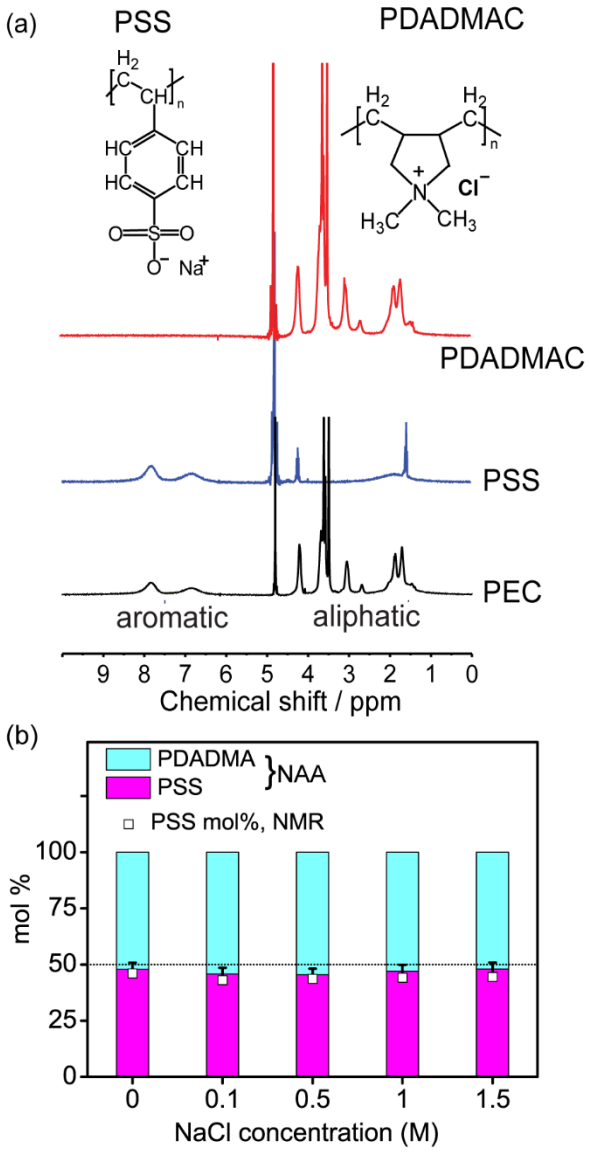

Figure 4.4. (a) ^{1}H NMR spectra for homopolymer PDADMAC, PSS, and PDADMA−PSS complexes in 2.5 M KBr in D_2O, (b) PEC composition based on PDADMA and PSS repeat units for PECs prepared at varying NaCl concentrations measured using NAA or NMR.

Due to the observed nonstoichiometry of the PECs, the salt doping level y in Equation 4.2, was divided into cationic and anionic doping level contributions:

$$y^+ = \frac{\mathrm{Cl}^-}{\mathrm{PDADMA}}; \quad y^- = \frac{\mathrm{Na}^+}{\mathrm{PSS}} \qquad 4.4$$

NAA allowed for the estimation of these doping levels y^+ and y^- (Figure 4.3b). If all Na^+ and Cl^- ions are assumed to participate in extrinsic ion pairing, then y may be considered equivalent to the fraction of extrinsic polyelectrolyte repeat units. The doping level y^+ and y^- generally increased with increasing complexation salt concentration up to 1 M. A complexation concentration of 1.5 M NaCl resulted in a decreased doping level, but this meaning of this particular result is circumspect on account of the extreme softness of the material and the tendency of the PEC to lose salt during the isolation procedure. In all PECs, y^+ was greater than y^-, which can be explained by the excess PDADMA in the PECs. Elsewhere, doping level has been estimated using scintillation counting,[68] inductively coupled plasma mass spectrometry (ICP-MS),[203] thermal gravimetric analysis,[104] and conductivity.[77] The trend observed here using NAA most closely mimics that observed using ICP-MS and conductivity, Figure 4.5.[77, 203]

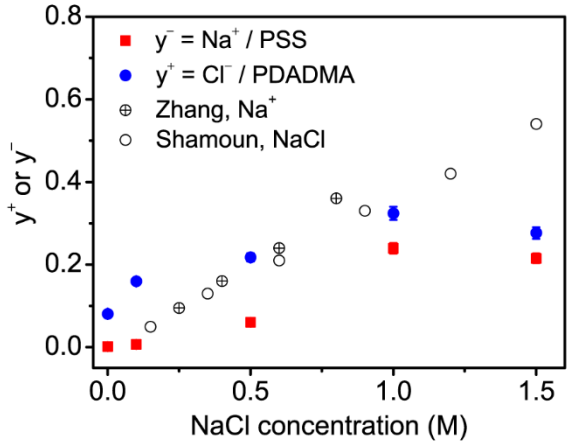

Figure 4.5. Comparison of current work and previous work on salt doping level of PDADMAC−PSS complexes. Ratio of Na^+ to PSS^- (red ■) or Cl^- to $PDADMA^+$ (blue ●) as a function of solution NaCl concentration, measured by neutron activation analysis. Work from Zhang et al.,[203] detection of Na^+ (⊕) using ICP-MS, and Shamoun et al.,[77] detection of NaCl (○) using solution conductivity.

Adsorbed water influences polyelectrolyte dynamics,[204] which significantly impacts PEC thermal properties. To explore this further, the effect of hydration on the PEC's T_g was examined using modulated DSC, Figure 4.6a. The inflection point of the sigmoidal reversing heat flow response was assigned as T_g. An enthalpic relaxation peak in the nonreversing heat flow curve was also present, Figure 4.7a. For a fixed complexation salt concentration of 0.5 M, T_g decreased from 387 K to 300 K as water content increased from 16 to 32 wt %. For comparison, a dried PEC exhibited no remarkable thermal features, Figure 4.7b. From Figure 4.6b, it shows the response for PECs of varying complexation NaCl concentrations at a fixed hydration level of 24 wt %.

T_g decreased from 345 K to 325 K as the NaCl concentration increased from 0 to 1.5 M. As shown here, the effects of salt doping on the T_g are much less as compared to the effect of hydration. The effects of hydration and salt on the T_g are summarized in Figure 4.6c for a range of water content and complexation salt concentrations. This emphasizes the general trend that T_g decreases with increasing water content and complexation NaCl concentration. These results confirm the plasticizing effect of water,[15, 79, 89] and also the effects of salt doping, which breaks intrinsic ion pairs and lowers the T_g.[77, 80]

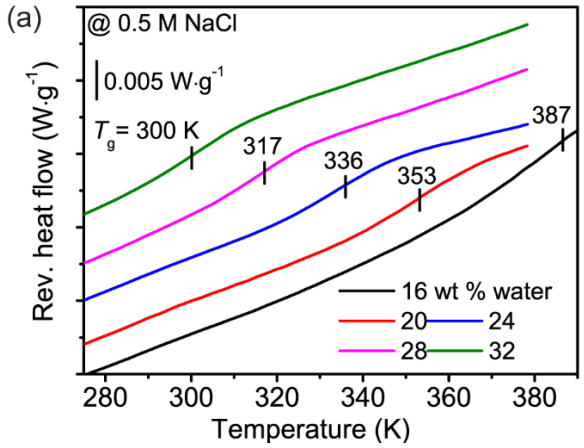

Figure 4.6. Reversing heat flow curves for PDADMA−PSS PECs of (a) varying water content and fixed 0.5 M NaCl complexation concentration, and (b) varying NaCl complexation concentration and fixed water content of 24 wt %. (c) T_g values for PDADMA−PSS complexes of varying complexation NaCl concentration and hydration. For (a) and (b), second heating scans are shown with "exotherm down", the curves have been shifted vertically for clarity, and the scale bar represents 0.005 W/g. Heating at 2 K/min, amplitude of 1.272 K for a period of 60 s. The error bars in panel (c) represent the standard error of 3 samples.

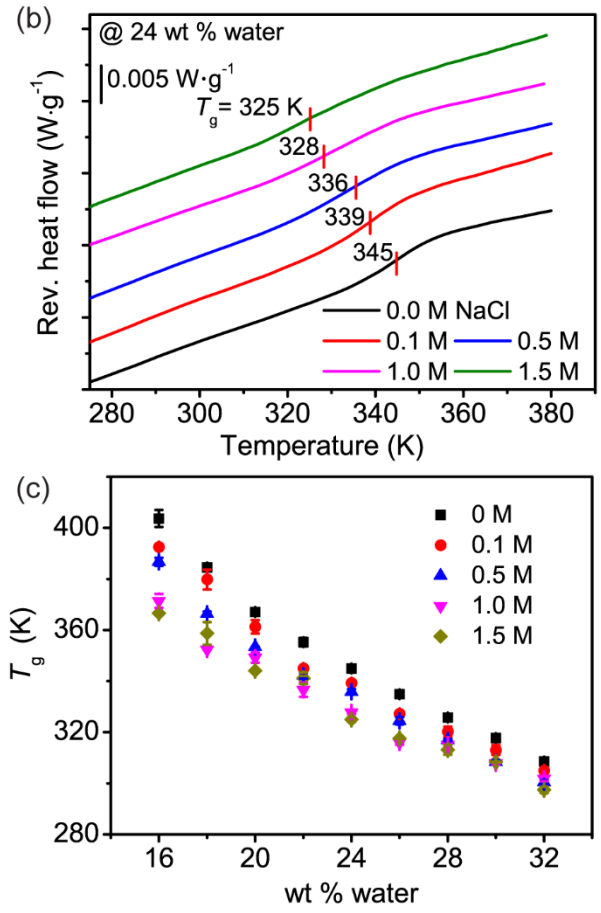

Figure 4.6. Continued.

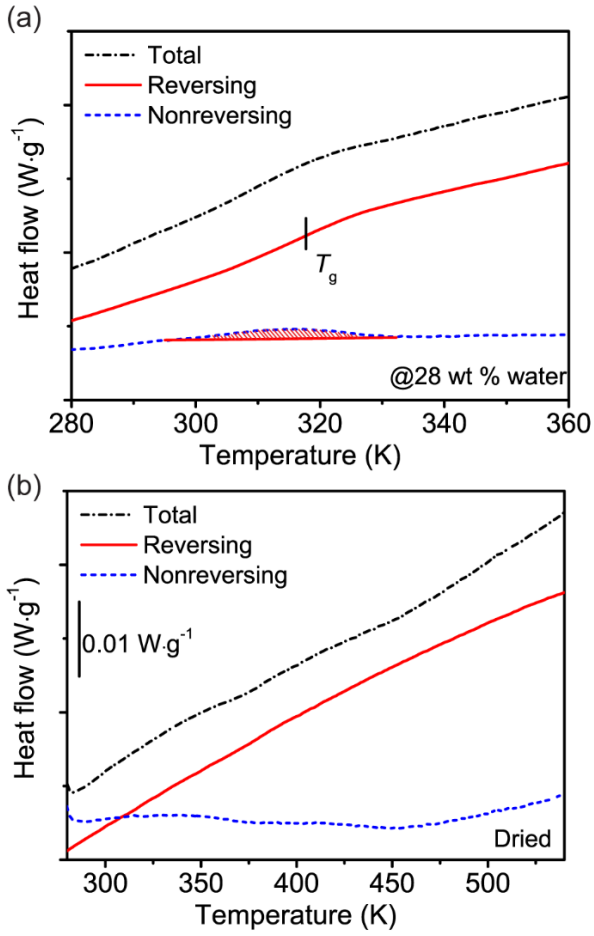

Figure 4.7. Modulated DSC thermograms of (a) 28 wt % and (b) dried PDADMA−PSS complexes isolated from 0.5 M NaCl. Second heating scans were shown here with "exotherm down" format. Heating at 2 K·min^{-1} with 60 s period and 1.272 K amplitude. Curves have been shifted along y-axis for clarity.

A unifying parameter, the molar ratio of water molecules to intrinsic ion pairs, has been suggested to control T_g or (T_{tr}) in PAH−PAA complexes.[79] To examine this idea for the PDADMA−PSS system, the amount of intrinsic ion pairs was obtained from the results in Figure 4.3. The amount of water was taken as that added to the dried PECs. Simulations

shown later address the water distribution and discuss the possible states of water – whether water molecules bind at intrinsic or extrinsic ions pairs. T_g values from Figure 4.6c for PDADMA−PSS complexes were plotted against the ratio of water molecules per intrinsic ion pairs $\frac{n_{H_2O}}{n_{\text{intrinsic ion pair}}}$, Figure 4.8a. This ratio can also be expressed in terms of a doping level y+ and y–, depending on which species is a minority. Here, with PSS being the minority, its doping level is an indicator of the intrinsic ion pair density, so the molar ratio of water to intrinsic ion pairs becomes $\frac{n_{H_2O}}{n_{PSS}(1-y^-)}$. Remarkably, the T_g values all collapsed into a single master curve for all hydration levels and salt concentrations examined. Figure 4.8b shows the linearization of this master curve in the form of ln(water/intrinsic ion pair) = $1.30\times(1000/T_g) - 1.98$ ($R^2 = 0.984$). This plot provides an energy of −10.8 kJ/mol, which is close in value to the van't Hoff enthalpy ΔH associated with the disruption of one O−H···O unit (10.5 kJ/mol).[205] The enthalpy is also similar to values obtained from the proton conductivity of polymer membranes and Nafion nanofibers.[206, 207] This possibly suggests a link between the glass transition and hydrogen bond distribution in PECs. The successful collapse and linearization of T_g values for PDADMA–PSS complexes is notably similar to that observed in PAH–PAA complexes, shown in Figure 4.8b for comparison. The slopes and energies for both types of complexes are similar, which further suggests the generalized role of water in the relaxation.

These results show generalized behavior between two very different types of PECs (strong vs weak), yet there still remains the question of if this behavior is similar for charged assemblies made by a completely different path. To examine this, we performed

the same analysis for PDADMA–PSS PEMs made using the layer-by-layer assembly technique. Whereas PECs are made here by the rapid mixing of polycation and polyanion solutions, PEMs are made by the alternate and sequential adsorption of polycations and polyanions from solution to a surface. PEMs can possess stratified or mixed structure,[208, 209] and the assembly conditions here were selected so as to give a more mixed structure within the layers. PDADMA–PSS PEMs were exposed to various salt concentrations and water contents, and their T_g's were measured. Elemental analysis was performed as before to obtain the doping level and intrinisic/extrinisic ion pair content.[210] The results, plotted in Figure 4.9, show the nearly perfect overlay of PEM and PEC behavior. Despite being formed by very different methods, the manner in which water controls the T_g appears to be essentially the same.

Therefore, this master curve identifies a unifying parameter, namely the molar ratio of water to intrinsic ion pairs, that controls the T_g in the charged assemblies and reflects the roles of both the water and ionization in PECs. The T_g for PECs is concluded to follow the general relationship:

$$\frac{1}{T_g} \sim \ln\left(\frac{n_{H_2O}}{n_{intrinsic\ ion\ pair}}\right) \qquad 4.5$$

The y-intercepts for the linear fits shown in Figure 4.8b are different, however, although the meaning is not immediately clear. The difference may be attributed to the charged group size (e.g., PDADMA repeat units are larger than PAH repeat units), linear charge density, and/or the water distribution around the charged groups between these two PEC systems. However, the two lines did not overlay well after plotting ln(water/intrinsic

ion pair/backbone carbon number) vs 1/ T_g, implying that linear charge density cannot fully explain the underlying thermal behavior of PECs. It may be more instructive to consider the ion pair size and the behavior of water in PDADMA−PSS and PAH−PAA PECs. The PDADMA−PSS ion pair is physically larger than the PAH−PAA ion pair, such that the PDADMA−PSS ion pair may accommodate more water molecules in the surrounding hydration layer, perhaps resulting in the different y-intercept. Additionally, water distribution may be affected by all PDADMA and PSS repeat units being charged, whereas for the weak polyelectrolytes PAH and PAA, the charged repeat units hydrate more strongly.

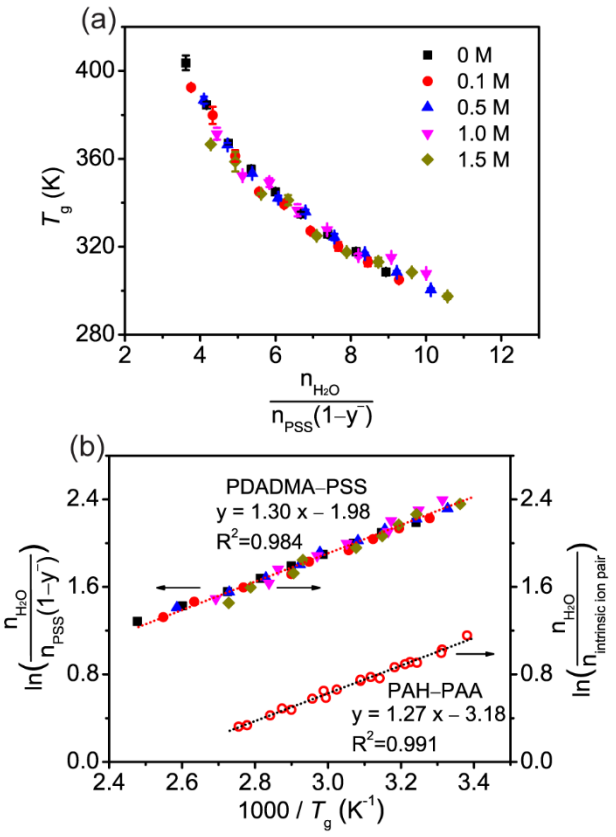

Figure 4.8. (a) T_g as a function of the molar ratio of water molecules per intrinsic ion pair in hydrated PDADMA−PSS complexes prepared from solutions of different NaCl concentrations. (b) Linear fitting of ln(water/intrinsic ion pair) vs 1000/ T_g (dotted lines). The legend in (a) also applies to (b). PAH−PAA data are from the authors' previous work.[79] The left y-axis applies to PDADMA−PSS and the right y-axis applies to both PDADMA−PSS and PAH−PAA.

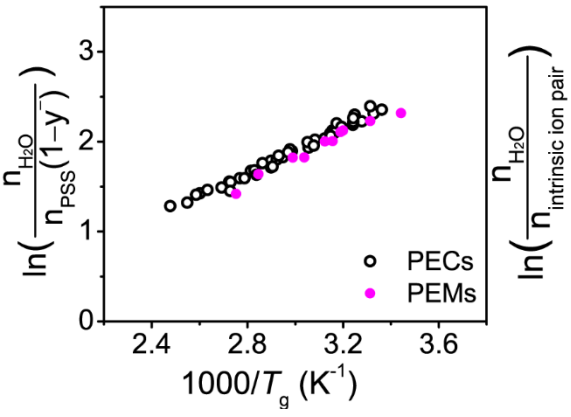

Figure 4.9. $\ln(n_{H_2O}/n_{\text{intrinsic ion pair}})$ vs $1000/T_g$ for PDADMA−PSS polyelectrolyte complexes (PECs, black circles) and polyelectrolyte multilayers (PEMs, pink circles).

To further investigate the water distribution as well as the underlying molecular interactions that give rise to the observed plasticization effect, molecular dynamics (MD) calculations were performed regarding the intermolecular hydrogen bonds. Figure 4.10 displays a simulated PEC structure corresponding to 1.5 M NaCl concentration and 30 wt % water, as well as the visualization of extrinsic and intrinsic ion pairs (upper left and right panels, respectively). In Figure 4.10, the magnification of an extrinsic pair site shows a Na^+ counterion surrounded by multiple charged PSS groups, demonstrating a three-dimensional packing configuration. In these simulations, it was found that compensation at a specific polyelectrolyte site could result in both intrinsic and extrinsic character due to this three-dimensional character. Because of this, a PSS repeat unit was defined as "extrinsically compensated" if a Na^+ ion was within a cut-off separation of 0.45 nm from the PSS S atom and "intrinsically compensated" otherwise. Figure 4.10 also shows a uniform water distribution in the PEC, hydrating both intrinsic and extrinsic ion pairs. It

also exhibits intrinsic ion pairing as the dominating intermolecular interaction. Figure 4.11 compares the mole fraction of intrinsically compensated PSS groups calculated from simulations and experiments; the generally good agreement between the experimental and simulation approaches supports the validity of the quantitative calculation in Figure 4.8. The simulation produces a relatively realistic configuration as 3D packing. The experimental results were obtained from simpler 2D configuration.[11] At 0 and 0.5 M NaCl complexation conditions, the results obtained from simulations matches the experimental results. At higher salt concentration of 1.5 M, counterions are insufficiently solvated, i.e. at high salt doping and low hydration, and the simulation values exceed experimental ones.

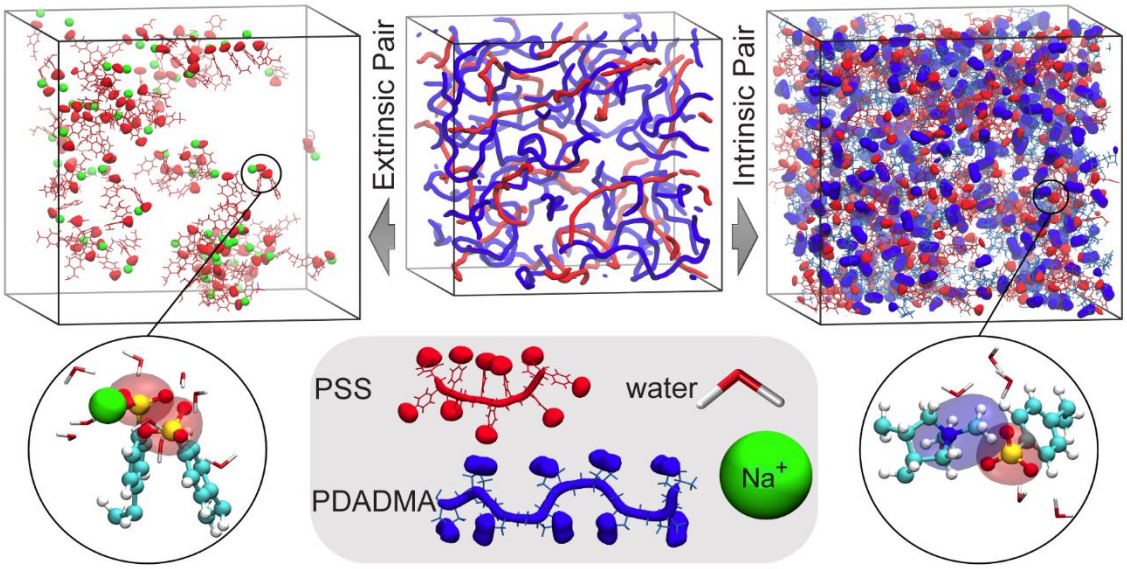

Figure 4.10. Representative snapshots of a hydrated PDADMA−PSS complex corresponding to 1.5 M NaCl concentration and 30 wt % water and its intrinsic (right) and extrinsic (left) ion pairs.

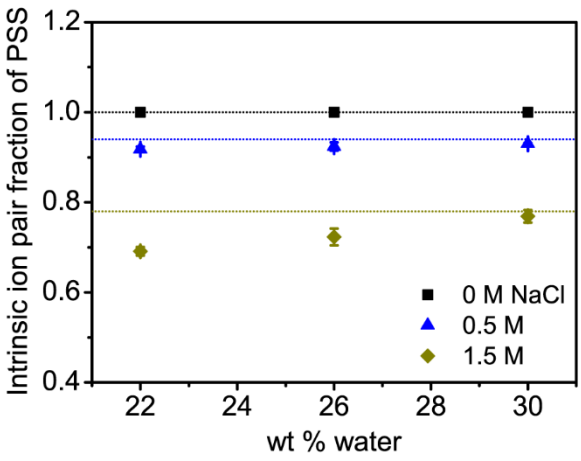

Figure 4.11. (Solid data points) Calculated intrinsic ion pair fraction of PSS groups from simulation work; (dashed lines) experimental values from ion pairing model of PECs.

To understand the molecular origins of the observed thermal transition, the distribution and location of water molecules in the PECs were further investigated. The analysis focused on the PSS group because our recent work on PDADMA/PSS assemblies has shown indications that the observed thermal transition behavior is linked with shortening of the hydrogen bond life time between PSS and water.[78] The data in Figure 4.12a and Figure 4.12b show that the total number of water−sulfonate hydrogen bonds decreases with increasing temperature and that the decrease results dominantly from water at the intrinsic ion pairs. For extrinsically compensated ion pairs, the number of hydrogen bonds with water was relatively insensitive to temperature, Figure 4.12c. Likely, this results from the Na^+ ion in the extrinsic ion pairs pinning nearby water molecules. The system contained much more intrinsically charge compensated ion pairs, see Figure 4.10, so it is rational that the decrease in the total water-sulfonate hydrogen bonds tracks closely

with that of the intrinsic ion pairs.[78] As water content increased, the error bar size decreased, which was a manifestation of the faster dynamics due to water plasticization.

In prior simulation work, a clear transition in the lifetime, and consequently the number of hydrogen bonds between PSS sulfonate groups and water was observed and interpreted to be associated with the thermal transition or T_g. [78] The data shown in Figure 4.12a and Figure 4.12b corresponds to a much larger simulation system so the transition here was relatively weak. In a single simulation, the transition is much more apparent, showing a visible kink for the intrinsically compensated PSS groups, Figure 4.12d. The plot in Figure 4.12c and Figure 4.12e present the insensitivity of hydrogen bonds between water and extrinsically compensated PSS.

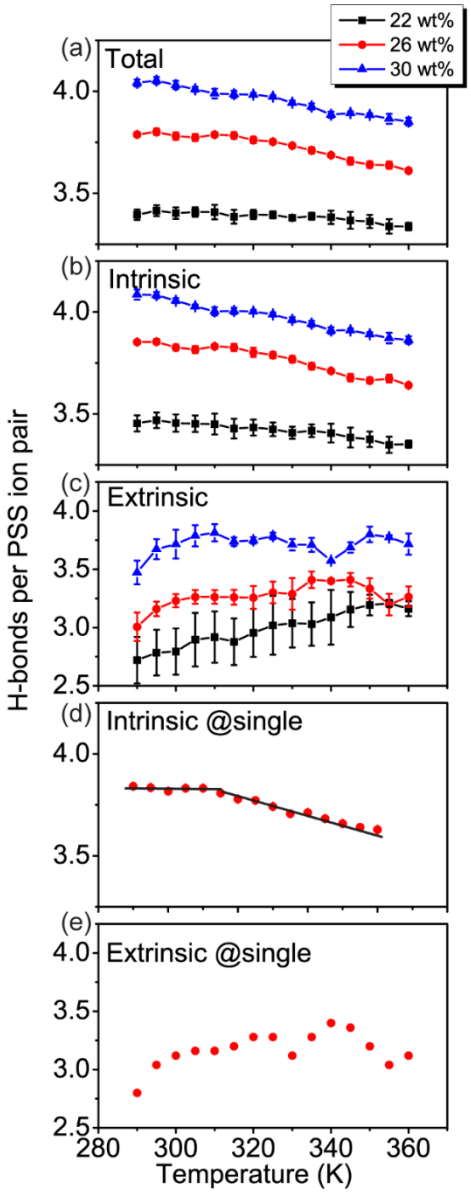

Figure 4.12. PSS−water hydrogen bond analysis for simulations of PECs of different water content prepared to correspond to complexation solution of 0.5 M NaCl. (a) Total, (b) intrinsically, (c) extrinsically, (d) single set of intrinsically, (e) single set of extrinsically compensated ion pairing of PSS. Figs (a-c) Correspond to the average of three simulations, and (d) and (e) correspond to a single simulation.

Figure 4.13 presents the number of water molecules of the hydration shell of PSS intrinsically and extrinsically compensated. At 0 M NaCl condition, all PSS monomers form intrinsic ion pairs since there are no Na^+ ions in the simulated PECs. PECs prepared from 0.5 and 1.5 M presents both intrinsic and extrinsic ion pairs. The number of water molecules in the hydration shell rises with increasing water wt % for all investigated systems. When comparing number of water in intrinsic and extrinsic ion pairs, the differences were below 13%, although water was not evenly distributed between intrinsic and extrinsic ion pairs. No clear trend on the number of water as the function of the specific salt doping level was observed. The calculated magnitude matched the value from experimental section calculation, from 3.6 to 11.0 water per ion pair. The 0.5 nm shell used in the simulations based approximately corresponds to the first hydration shell, and thus could underestimate the number of molecules associated with the site. The PSS hydration shell size (in water molecules) depended on hydration, salt concentration, and whether the PSS sulfonate group was intrinsically of extrinsically compensated.

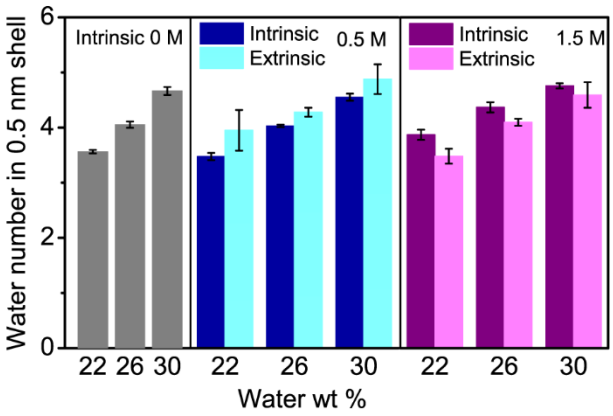

Figure 4.13. Number of water molecules in the first hydration shell of PSS in hydrated PECs prepared from complexation solutions of varying NaCl concentration.

4.4. Discussion

The current work targets the plasticization effects of water and salt on the thermal characteristics of PDADMA–PSS complexes via modulated DSC and molecular modelling. PECs and PEMs are known to be plasticized via heat, salt, and water.[34, 77, 104] Here, we emphasize the effects of water and salt on the T_g of PDADMA–PSS complexes quantitatively.

The results show that salt plasticizes the PEC in that the T_g decreases with increasing salt content (Figure 4.6b). Doping has an intense local effect on screening between intrinsic ion pairing, which decreases physical cross-linking and increases polymer mobility.[11, 41, 51, 211] This saloplastic effect has been validated in the literature; for example, the T_g of PECs and PEMs decreased with increasing solution salt concentration.[34, 77] The increase of polymer chain relaxation was also evidenced from the reduction of

elastic modulus of PEMs[51] and the enhanced self-healing ability of PECs with increasing NaCl content.[30] At a significantly high saline aqueous environment, PECs dissolved due to limited intrinsic ion pairing.[59, 72, 102, 123, 212] Zhang et al. have reported the anti-plasticization effect of salt,[80] which was not observed in the current work since the prepared PECs possessed a low salt doping level and high water content.

Also noted, the association constant K_a or salt doping constant K_{dop} has been utilized to evaluate the strength of the salt doping and ion pairing.[68] To compare our results to others, here the Equation 4.3 is revised as:

$$K_a = \frac{a_{\mathrm{NaCl}}^2}{y^+ y^-} \qquad 4.6$$

where y^+ and y^- were obtained from NAA. The NaCl activity in solution a_{NaCl} was converted from NaCl concentration using an activity coefficient. Here, we estimate that K_a was 11.6 ± 1.9, which is larger than the previously reported value of 3.3.[105] This discrepancy may arise from differences in the PEC isolation process.

As for water, we observed that an increasing water content led to a decrease of the T_g, see Figure 4.6a. Dried PECs are brittle and show no distinct thermal transition due to the strong ionic cross-links.[34, 85, 86, 139] Hydrated PECs, on the other hand, are processable and experience polymer chain relaxation. Water contributes to the PEC plasticization via (1) enhancing free volume which facilitates polymer chain motion,[15, 80, 213-215] (2) lubricating the polymer chains by decreasing the internal resistance of polymer sliding motions,[15, 204] and (3) reducing polyelectrolyte intrinsic ion pairing. Whereas the first two effects are associated with traditional plasticization,[213, 215] the last effect in polyelectrolyte

complexes and assemblies makes water a nontraditional plasticizer, analogous to salt. Zhang et al. observed the direct contact number of intrinsic ion pair decreased as water content increased.[80]

The MD simulation scrutinizes the origin of molecular interactions connected with the transition, which follows the trend obtained in the DSC measurement. With the addition of water, the number of H-bonds between water and PSS increases (Figure 4.12a) in view of the fact that water hydrates the charged groups by clustering around both intrinsic and extrinsic ion pairs. Water experiences faster rotation and vibration movements upon heating, as indicated by the shortening of H-bond life time and increase of molecular diffusion coefficient.[78, 80] Increasing temperature induces significant changes in H-bonds formed between intrinsically compensated PSS but not the extrinsically compensated PSS, indicating that water around the intrinsic ion pairs reflects the transition response, Figure 4.12.

One unifying parameter, namely the molar ratio of water to intrinsic ion pairs, is identified to control the T_g in the PECs as shown in the master curve of Figure 4.8, reflecting both the water and salt roles in PECs. Surprisingly, this parameter holds true in both PDADMA–PSS complexes, PAH–PAA complexes, and PDADMA–PSS multilayers. Additionally, the activation energies obtained from the master curves in PDADMA–PSS complexes (10.8 kJ·mol^{-1}) and PAH–PAA complexes (10.5 kJ·mol^{-1})[79] were quite close to the value of perturbation of one hydrogen bond (10.5 $\pm$ 2.5 kJ·mol^{-1}).[205] This finding leads to the proposal that water plasticization is possibly linked with perturbation of H-bonds formed between water and intrinsically compensated polyelectrolytes. The

water/intrinsic ion pair ratio is in the range of 3.6 up to 11.0, matching well with previously literature (8 to 13 in PDADMA/PSS multilayers[142] and 10 in hydrated PECs).[68]

Our results provide insights in terms of (1) the mechanism of water plasticization, and (2) the domination of water at the intrinsic ion pair for the glass transition. Current work complements our investigations on thermal properties of polyelectrolyte assemblies. Experimentally, we have studied PDADMA/PSS and PAH/PAA assemblies in multilayer films,[34, 35] microtubes,[75] and complexes.[79] The thermal transition has been coupled to changes in DSC heat flow,[79] film viscoelasticity,[34, 35] film resistance,[141] and microtube size.[75] From simulation studies, T_g was linked with changes in volume, water diffusion coefficient, and H-bond life time.[78, 80] These findings furthermore connect with broad research work regarding the water and salt annealing effects, as well as time-salt-temperature superpositioning, in polyelectrolyte theory and application.

4.5. Conclusion

The influence of salt doping and water on the glass transition of PDADMA−PSS complexes was investigated using modulated DSC and molecular dynamic (MD) simulations. T_g was reduced with increasing salt doping level, as more intrinsic ion pair crosslinks were converted to extrinsic pairs. The decrease of T_g with increasing water content indicated the plasticizing effect of water. A universal parameter, the molar ratio of water to intrinsic ion pair, was found to control the T_g in both PDADMA−PSS and PAH−PAA complexes. The linear fitting of the $1/T_g$ and $\ln(\frac{n_{H_2O}}{n_{\text{intrinsic ion pair}}})$ showed an activation energy close to the energy accompanying hydrogen bond restructuring in both

types of PECs. MD simulations of PDADMA−PSS directly observed the intrinsic and extrinsic ion pairs separately. By monitoring the number of H-bonds with changing temperature, T_g was connected to the decrease of H-bonds between water−PSS in intrinsically compensated pairs. In sum, these findings imply the underlying mechanism: water plasticizes the PECs by reducing intrinsic ion pairing attractions and water surrounding the intrinsic ion pair is a crucial parameter in controlling the T_g of polyelectrolyte complexes and assemblies. Our future work focus on polymer segmental chain mobility using dynamic mechanical analysis to further investigate the thermal properties of PECs under controlled relative humidity.

CHAPTER V

SUMMARY AND FUTURE WORK

5.1. Summary

In conclusion, this dissertation investigated the phase behavior and thermal properties of polyelectrolyte complexes (PECs). The influence of mixing ratio and ionic strength on the colloidal stabilities of PDADMA–PSS complexes was investigated. Thermal properties of hydrated PECs were studied in both PAH–PAA and PDADMA–PSS complexes. NMR, FTIR and NAA were used to determine the composition and the number of intrinsic/extrinsic ion pairs in PECs. Modulated DSC was used to measure the glass transition temperature T_g of PECs.

The influence of mixing ratio of oppositely charged polymers and ionic strength on the colloidal stabilities of PDADMA–PSS complexes in aqueous media were studied in Chapter II. UV-Vis-NIR measured the turbidity of PECs, implying the formation and phase separation of PEC particles. DLS was used to measure the hydrodynamic size and the zeta potential of PECs, which indicated the structure and surface charge of PECs. Stable PECs showed constant turbidity and hydrodynamic size with respect to time. Unstable PECs exhibited a gradual formation of precipitate and an increase of hydrodynamic size. For nonstoichiometric PECs, the critical salt concentration of PECs changed from colloidally stable to unstable state was 1.5 M NaCl. For stoichiometric PECs, on the other hand, the critical salt concentration was between 0.2 and 0.5 M NaCl. As the salt concentration increased, salt screening effect became stronger, which decreased the absolute value of zeta potential of the primary PEC particles and made them aggregate.

Based on the results, a phase diagram containing both the salt concentration and the mixing ratio were plotted, which could be used as a guidance for preparation of different types of PECs.

Thermal properties of PECs, especially T_g, were investigated in Chapter III. Weak PAH–PAA complexes were prepared at different pH. The composition and the degree of ionization of polyelectrolyte were measured using NMR and FTIR, respectively. The results allowed the quantification of the number of intrinsic ion pair within PECs. There were more PAA than PAH due to the mismatch of degrees of ionization, and the degree of ionization of PAA was lower than PAH. As the solution pH increased, the degree of ionization of PAA increased. PECs were scanned using modulated DSC to determine the T_g. The T_g of dry PECs was not detectable. For hydrated PECs, the results showed that T_g decreased with increasing water content (15 to 24 wt%) or decreasing pH (from 3.5 to 9). T_g collapsed on a master curve when plotted against the ratio of water to intrinsic ion pair $\frac{n_{\text{water}}}{n_{\text{intrinsic ion pair}}}$, for all samples prepared at different pH values. When water-organic solvent mixture was added to PECs, the T_g only depended on the water content. These findings suggested that water is a nontraditional plasticizer to PECs and T_g is controlled by the number of water at intrinsic ion pair.

The thermal properties of PECs consisting of strong polyelectrolytes, PDADMA–PSS, were studied in Chapter IV. Strong polyelectrolytes are insensitive to solution pH. However, the added salt could change the composition and internal structures of PECs because of the salt screening effect. PDADMA–PSS complexes were assembled from solutions of different salt concentrations. The composition and the ion pairing types were

estimating using NAA. As the salt concentration increased from 0 to 1.5 M, the salt doping level generally increased, and the number of intrinsic ion pair decreased. T_g of hydrated PECs were determined using modulated DSC. The results showed that T_g decreased with increasing salt doping level or increasing water content. MD simulation showed that the number of hydrogen bond between water-intrinsic PSS decreased as the temperature increased. Both salt and water plasticized the PECs but the mechanisms were different. Salt doping broke the intrinsic ion pairing, which increased the chain mobility of polyelectroltyes. Water decreased the electrostatic attractions between polycation and polyanion and formed hydrogen bonds with polyelectrolytes. As temperature increased, the connections between water and PSS decreased, which contributed to the segmental mobility of PECs. T_g was controlled by the ratio of water to intrinsic ion pair in a linear relationship $1/T_g \sim \ln(\frac{n_{H_2O}}{n_{\text{intrinsic ion pair}}})$. This relationship was observed in both PAH–PAA and PDADMA–PSS complexes, indicating that this quantitative correlation was applicable to both strong (salt-sensitive) and weak (pH-sensitive) PECs.

5.2. Future work

Polyelectrolyte multilayers (PEMs) has been utilized in ion transport and selectivity applications. PEM coating can function as an effective barrier to enhance the monovalent/divalent electrodialysis selectivity of Nafion cation-exchange membrane.[216] Mobile cations and anions, monovalent or multivalent ions, compensating the charged groups on polyelectrolyte chains, impact the structures and behaviors of PECs. The physicochemical properties of PEMs are influenced by the counterions in exposed

solutions and temperatures. Many prior studies have focused on the effects of monovalent salt on the PECs.[11, 60] The effect of divalent salt on PEMs and polyelectrolyte brushes has also been studied,[24, 217, 218] which have shown that the PEMs shrank due to crosslinking between polyelectrolytes and divalent ions. Multivalent salts alter the structure of the polyelectrolyte brushes reversibly by modifying the multivalent salt concentration.

Electrochemical impedance spectroscopy (EIS) is a versatile technique to provide sensitive and in situ characterization of PEMs modified on conductive surfaces.[141, 219, 220] EIS provides implication regarding the film structure and the interactions between the PEMs and the small ions in the supporting electrolyte, by monitor the redox couple reaction. Sung et al. determined the thermal transition temperature of PDADMA/PSS in NaCl electrolyte.[141] The thermal transition behavior associated with the structural rearrangement of film, resulting in decrease of film resistance and charge transfer resistance. Elsewhere, Silva et al. has studied the strong influence of the supporting electrolytes and temperature on PSS/PAH film in a temperature range from 15 to 45 ^{o}C.[220] However, rare work has been reported about the effect of divalent ions on the thermal properties of PECs using EIS.

In this future work, the effect of divalent counterions on the thermal properties of PDADMA/PSS multilayers will be investigated using EIS. The studied divalent salts are $MgCl_2$, $CaCl_2$ and Na_2SO_4. In addition, the effect of ionic strength will also be explored besides electrolyte type. The impedance of PDADMA–PSS in contact with divalent salts will be recorded at different temperatures. From the impedance results, a transition

temperature T_g of PEMs will be estimated, which can be further compared to the T_g of PEMs in contact with monovalent salt NaCl.

REFERENCES

1. Ouyang, L.; Malaisamy, R.; Bruening, M. L. Multilayer polyelectrolyte films as nanofiltration membranes for separating monovalent and divalent cations. *Journal of Membrane Science* **2008,** 310, (1), 76-84.

2. Yang, Q.; Wang, S.; Fan, P.; Wang, L.; Di, Y.; Lin, K.; Xiao, F.-S. pH-Responsive Carrier System Based on Carboxylic Acid Modified Mesoporous Silica and Polyelectrolyte for Drug Delivery. *Chemistry of Materials* **2005,** 17, (24), 5999-6003.

3. Smitha, B.; Sridhar, S.; Khan, A. A. Polyelectrolyte Complexes of Chitosan and Poly(acrylic acid) As Proton Exchange Membranes for Fuel Cells. *Macromolecules* **2004,** 37, (6), 2233-2239.

4. Wang, D.; Gong, X.; Heeger, P. S.; Rininsland, F.; Bazan, G. C.; Heeger, A. J. Biosensors from conjugated polyelectrolyte complexes. *Proceedings of the National Academy of Sciences* **2002,** 99, (1), 49-53.

5. Dobrynin, A. V.; Rubinstein, M. Theory of polyelectrolytes in solutions and at surfaces. *Progress in Polymer Science* **2005,** 30, (11), 1049-1118.

6. Pergushov, D. V.; Muller, A. H. E.; Schacher, F. H. Micellar interpolyelectrolyte complexes. *Chemical Society Reviews* **2012,** 41, (21), 6888-6901.

7. Priftis, D.; Tirrell, M. Phase behaviour and complex coacervation of aqueous polypeptide solutions. *Soft Matter* **2012,** 8, (36), 9396-9405.

8. Michaels, A. S. POLYELECTROLYTE COMPLEXES. *Industrial & Engineering Chemistry* **1965,** 57, (10), 32-40.

9. Philipp, B.; Dautzenberg, H.; Linow, K.-J.; Kötz, J.; Dawydoff, W. Polyelectrolyte complexes — recent developments and open problems. *Progress in Polymer Science* **1989,** 14, (1), 91-172.

10. Zezin, A. B.; Kabanov, V. A. A new class of complex water-soluble polyelectrolytes. *Russian Chemical Reviews* **1982,** 51, (9), 833-855.

11. Fu, J.; Schlenoff, J. B. Driving Forces for Oppositely Charged Polyion Association in Aqueous Solutions: Enthalpic, Entropic, but Not Electrostatic. *Journal of the American Chemical Society* **2016,** 138, (3), 980-990.

12. Fares, H. M.; Schlenoff, J. B. Diffusion of Sites versus Polymers in Polyelectrolyte Complexes and Multilayers. *Journal of the American Chemical Society* **2017**.

13. Bucur, C. B.; Sui, Z.; Schlenoff, J. B. Ideal mixing in polyelectrolyte complexes and multilayers: entropy driven assembly. *Journal of the American Chemical Society* **2006,** 128, (42), 13690-13691.

14. Ankerfors, C.; Ondaral, S.; Wågberg, L.; Ödberg, L. Using jet mixing to prepare polyelectrolyte complexes: Complex properties and their interaction with silicon oxide surfaces. *Journal of Colloid and Interface Science* **2010,** 351, (1), 88-95.

15. Hariri, H. H.; Lehaf, A. M.; Schlenoff, J. B. Mechanical properties of osmotically stressed polyelectrolyte complexes and multilayers: Water as a plasticizer. *Macromolecules* **2012,** 45, (23), 9364-9372.

16. Tsuchida, E.; Osada, Y.; Sanada, K. Interaction of poly(styrene sulfonate) with polycations carrying charges in the chain backbone. *Journal of Polymer Science Part A-1: Polymer Chemistry* **1972,** 10, (11), 3397-3404.

17. Dautzenberg, H.; Jaeger, W. Effect of charge density on the formation and salt stability of polyelectrolyte complexes. *Macromolecular Chemistry and Physics* **2002,** 203, (14), 2095-2102.

18. Michaels, A. S.; Miekka, R. G. Polycation-polyanion complexes: Preparation and properties of poly-(vinylbenzyltrimethylammonium) poly-(styrenesulfonate). *The Journal of Physical Chemistry* **1961,** 65, (10), 1765-1773.

19. Donati, I.; Feresini, M.; Travan, A.; Marsich, E.; Lapasin, R.; Paoletti, S. Polysaccharide-Based Polyanion–Polycation–Polyanion Ternary Systems. A Preliminary Analysis of Interpolyelectrolyte Interactions in Dilute Solutions. *Biomacromolecules* **2011,** 12, (11), 4044-4056.

20. Birch, N. P.; Schiffman, J. D. Characterization of Self-Assembled Polyelectrolyte Complex Nanoparticles Formed from Chitosan and Pectin. *Langmuir* **2014,** 30, (12), 3441-3447.

21. Lim, S.; Moon, D.; Kim, H. J.; Seo, J. H.; Kang, I. S.; Cha, H. J. Interfacial Tension of Complex Coacervated Mussel Adhesive Protein According to the Hofmeister Series. *Langmuir* **2014,** 30, (4), 1108-1115.

22. Márquez-Beltrán, C.; Castañeda, L.; Enciso-Aguilar, M.; Paredes-Quijada, G.; Acuña-Campa, H.; Maldonado-Arce, A.; Argillier, J.-F. Structure and mechanism formation of polyelectrolyte complex obtained from PSS/PAH system: effect of molar

mixing ratio, base–acid conditions, and ionic strength. *Colloid and Polymer Science* **2013,** 291, (3), 683-690.

23. Sato, H.; Nakajima, A. Formation of a Polyelectrolyte Complex from Carboxymethyl Cellulose and Poly(ethylenimine). *Polym J* **1975,** 7, (2), 241-247.

24. Wen, H.; Zhou, J.; Pan, W.; Li, Z.; Liang, D. Assembly and Reassembly of Polyelectrolyte Complex Formed by Poly(ethylene glycol)-block-poly(glutamate sodium) and S5R4 Peptide. *Macromolecules* **2016,** 49, (12), 4627-4633.

25. Chollakup, R.; Smitthipong, W.; Eisenbach, C. D.; Tirrell, M. Phase Behavior and Coacervation of Aqueous Poly(acrylic acid)−Poly(allylamine) Solutions. *Macromolecules* **2010,** 43, (5), 2518-2528.

26. Starchenko, V.; Müller, M.; Lebovka, N. Sizing of PDADMAC/PSS Complex Aggregates by Polyelectrolyte and Salt Concentration and PSS Molecular Weight. *The Journal of Physical Chemistry B* **2012,** 116, (51), 14961-14967.

27. Perry, S. L.; Leon, L.; Hoffmann, K. Q.; Kade, M. J.; Priftis, D.; Black, K. A.; Wong, D.; Klein, R. A.; Pierce, C. F.; Margossian, K. O.; Whitmer, J. K.; Qin, J.; de Pablo, J. J.; Tirrell, M. Chirality-selected phase behaviour in ionic polypeptide complexes. *Nature Communications* **2015,** 6, 6052.

28. Petzold, G.; Schwarz, S., Polyelectrolyte complexes in flocculation applications. In *Polyelectrolyte complexes in the dispersed and solid state II*, Springer: 2013; pp 25-65.

29. Porcel, C. H.; Schlenoff, J. B. Compact polyelectrolyte complexes:“saloplastic” candidates for biomaterials. *Biomacromolecules* **2009,** 10, (11), 2968-2975.

30. Zhang, H.; Wang, C.; Zhu, G.; Zacharia, N. S. Self-Healing of Bulk Polyelectrolyte Complex Material as a Function of pH and Salt. *ACS Applied Materials & Interfaces* **2016,** 8, (39), 26258-26265.

31. Kelly, K. D.; Schlenoff, J. B. Spin-Coated Polyelectrolyte Coacervate Films. *ACS Applied Materials & Interfaces* **2015,** 7, (25), 13980-13986.

32. Wang, Q.; Schlenoff, J. B. Single- and Multicompartment Hollow Polyelectrolyte Complex Microcapsules by One-Step Spraying. *Advanced Materials* **2015,** 27, (12), 2077-2082.

33. Decher, G. Fuzzy Nanoassemblies: Toward Layered Polymeric Multicomposites. *Science* **1997,** 277, (5330), 1232-1237.

34. Vidyasagar, A.; Sung, C.; Gamble, R.; Lutkenhaus, J. L. Thermal Transitions in Dry and Hydrated Layer-by-Layer Assemblies Exhibiting Linear and Exponential Growth. *ACS Nano* **2012,** 6, (7), 6174-6184.

35. Vidyasagar, A.; Sung, C.; Losensky, K.; Lutkenhaus, J. L. pH-Dependent Thermal Transitions in Hydrated Layer-by-Layer Assemblies Containing Weak Polyelectrolytes. *Macromolecules* **2012,** 45, (22), 9169-9176.

36. Li, Y.; Wang, X.; Sun, J. Layer-by-layer assembly for rapid fabrication of thick polymeric films. *Chemical Society Reviews* **2012,** 41, (18), 5998-6009.

37. Shiratori, S. S.; Rubner, M. F. pH-Dependent Thickness Behavior of Sequentially Adsorbed Layers of Weak Polyelectrolytes. *Macromolecules* **2000,** 33, (11), 4213-4219.

38. Bieker, P.; Schönhoff, M. Linear and Exponential Growth Regimes of Multilayers of Weak Polyelectrolytes in Dependence on pH. *Macromolecules* **2010,** 43, (11), 5052-5059.

39. Krebs, T.; Tan, H. L.; Andersson, G.; Morgner, H.; Van Patten, P. G. Increased layer interdiffusion in polyelectrolyte films upon annealing in water and aqueous salt solutions. *Physical Chemistry Chemical Physics* **2006,** 8, (46), 5462-5468.

40. Ghostine, R. A.; Jisr, R. M.; Lehaf, A.; Schlenoff, J. B. Roughness and Salt Annealing in a Polyelectrolyte Multilayer. *Langmuir* **2013,** 29, (37), 11742-11750.

41. Selin, V.; Ankner, J. F.; Sukhishvili, S. A. Diffusional Response of Layer-by-Layer Assembled Polyelectrolyte Chains to Salt Annealing. *Macromolecules* **2015,** 48, (12), 3983-3990.

42. Gilbert, J. B.; Rubner, M. F.; Cohen, R. E. Depth-profiling X-ray photoelectron spectroscopy (XPS) analysis of interlayer diffusion in polyelectrolyte multilayers. *Proceedings of the National Academy of Sciences* **2013,** 110, (17), 6651-6656.

43. Krasemann, L.; Tieke, B. Selective Ion Transport across Self-Assembled Alternating Multilayers of Cationic and Anionic Polyelectrolytes. *Langmuir* **2000,** 16, (2), 287-290.

44. Zhou, J.; Pishko, M. V.; Lutkenhaus, J. L. Thermoresponsive layer-by-layer assemblies for nanoparticle-based drug delivery. *Langmuir* **2014,** 30, (20), 5903-10.

45. Priolo, M. A.; Gamboa, D.; Holder, K. M.; Grunlan, J. C. Super gas barrier of transparent polymer− clay multilayer ultrathin films. *Nano Letters* **2010,** 10, (12), 4970-4974.

46. Shah, N. J.; Hyder, M. N.; Quadir, M. A.; Dorval Courchesne, N.-M.; Seeherman, H. J.; Nevins, M.; Spector, M.; Hammond, P. T. Adaptive growth factor delivery from a polyelectrolyte coating promotes synergistic bone tissue repair and reconstruction. *Proceedings of the National Academy of Sciences* **2014,** 111, (35), 12847-12852.

47. Ghostine, R. A.; Markarian, M. Z.; Schlenoff, J. B. Asymmetric Growth in Polyelectrolyte Multilayers. *Journal of the American Chemical Society* **2013,** 135, (20), 7636-7646.

48. Izumrudov, V.; Kharlampieva, E.; Sukhishvili, S. A. Salt-induced multilayer growth: correlation with phase separation in solution. *Macromolecules* **2004,** 37, (22), 8400-8406.

49. Laugel, N.; Betscha, C.; Winterhalter, M.; Voegel, J.-C.; Schaaf, P.; Ball, V. Relationship between the growth regime of polyelectrolyte multilayers and the polyanion/polycation complexation enthalpy. *The Journal of Physical Chemistry B* **2006,** 110, (39), 19443-19449.

50. Salehi, A.; Desai, P. S.; Li, J.; Steele, C. A.; Larson, R. G. Relationship between Polyelectrolyte Bulk Complexation and Kinetics of Their Layer-by-Layer Assembly. *Macromolecules* **2015,** 48, (2), 400–409.

51. Jaber, J. A.; Schlenoff, J. B. Mechanical Properties of Reversibly Cross-Linked Ultrathin Polyelectrolyte Complexes. *Journal of the American Chemical Society* **2006,** 128, (9), 2940-2947.

52. Dautzenberg, H. Polyelectrolyte complex formation in highly aggregating systems: methodical aspects and general tendencies. *SURFACTANT SCIENCE SERIES* **2001**, 743-792.

53. Starchenko, V.; Müller, M.; Lebovka, N. Growth of polyelectrolyte complex nanoparticles: Computer simulations and experiments. *The Journal of Physical Chemistry C* **2008,** 112, (24), 8863-8869.

54. Priftis, D.; Laugel, N.; Tirrell, M. Thermodynamic characterization of polypeptide complex coacervation. *Langmuir* **2012,** 28, (45), 15947-15957.

55. Zhao, M.; Eghtesadi, S. A.; Dawadi, M. B.; Wang, C.; Huang, S.; Seymore, A. E.; Vogt, B. D.; Modarelli, D. A.; Liu, T.; Zacharia, N. S. Partitioning of Small Molecules in Hydrogen-Bonding Complex Coacervates of Poly (acrylic acid) and Poly (ethylene glycol) or Pluronic Block Copolymer. *Macromolecules* **2017,** 50, (10), 3818-3830.

56. Zhao, M.; Zacharia, N. S. Sequestration of Methylene Blue into Polyelectrolyte Complex Coacervates. *Macromolecular Rapid Communications* **2016,** 37, (15), 1249-1255.

57. Chollakup, R.; Beck, J. B.; Dirnberger, K.; Tirrell, M.; Eisenbach, C. D. Polyelectrolyte Molecular Weight and Salt Effects on the Phase Behavior and Coacervation of Aqueous Solutions of Poly(acrylic acid) Sodium Salt and Poly(allylamine) Hydrochloride. *Macromolecules* **2013,** 46, (6), 2376-2390.

58. Priftis, D.; Xia, X.; Margossian, K. O.; Perry, S. L.; Leon, L.; Qin, J.; de Pablo, J. J.; Tirrell, M. Ternary, Tunable Polyelectrolyte Complex Fluids Driven by Complex Coacervation. *Macromolecules* **2014,** 47, (9), 3076-3085.

59. Perry, S. L.; Li, Y.; Priftis, D.; Leon, L.; Tirrell, M. The effect of salt on the complex coacervation of vinyl polyelectrolytes. *Polymers* **2014,** 6, (6), 1756-1772.

60. Zhang, Y.; Yildirim, E.; Antila, H. S.; Valenzuela, L. D.; Sammalkorpi, M.; Lutkenhaus, J. L. The influence of ionic strength and mixing ratio on the colloidal stability of PDAC/PSS polyelectrolyte complexes. *Soft Matter* **2015,** 11, (37), 7392-7401.

61. Dautzenberg, H.; Rother, G. Response of Polyelectrolyte Complexes to Subsequent Addition of Sodium Chloride: Time‐Dependent Static Light Scattering Studies. *Macromolecular Chemistry and Physics* **2004,** 205, (1), 114-121.

62. Veis, A. Phase separation in polyelectrolyte systems. III. Effect of Aggregation and Molecular Weight Heterogeneity. *The Journal of Physical Chemistry* **1963,** 67, (10), 1960-1964.

63. Karibyants, N.; Dautzenberg, H. Preferential binding with regard to chain length and chemical structure in the reactions of formation of quasi-soluble polyelectrolyte complexes. *Langmuir* **1998,** 14, (16), 4427-4434.

64. Dautzenberg, H. Polyelectrolyte complex formation in highly aggregating systems. 1. Effect of salt: polyelectrolyte complex formation in the presence of NaCl. *Macromolecules* **1997,** 30, (25), 7810-7815.

65. Karibyants, N.; Dautzenberg, H.; Coelfen, H. Characterization of PSS/PDADMAC-co-AA polyelectrolyte complexes and their stoichiometry using analytical ultracentrifugation. *Macromolecules* **1997,** 30, (25), 7803-7809.

66. Priftis, D.; Farina, R.; Tirrell, M. Interfacial Energy of Polypeptide Complex Coacervates Measured via Capillary Adhesion†. *Langmuir* **2012,** 28, (23), 8721-8729.

67. Cohen Stuart, M. A.; Besseling, N. A. M.; Fokkink, R. G. Formation of micelles with complex coacervate cores. *Langmuir* **1998,** 14, (24), 6846-6849.

68. Fu, J.; Fares, H. M.; Schlenoff, J. B. Ion-Pairing Strength in Polyelectrolyte Complexes. *Macromolecules* **2017,** 50, (3), 1066-1074.

69. Huang, S.; Zhao, M.; Dawadi, M. B.; Cai, Y.; Lapitsky, Y.; Modarelli, D. A.; Zacharia, N. S. Effect of small molecules on the phase behavior and coacervation of aqueous solutions of poly(diallyldimethylammonium chloride) and poly(sodium 4-styrene sulfonate). *Journal of Colloid and Interface Science* **2018,** 518, 216-224.

70. Dautzenberg, H.; Karibyants, N. Polyelectrolyte complex formation in highly aggregating systems. Effect of salt: response to subsequent addition of NaCl. *Macromolecular Chemistry and Physics* **1999,** 200, (1), 118-125.

71. Požar, J.; Kovačević, D. Complexation between polyallylammonium cations and polystyrenesulfonate anions: the effect of ionic strength and the electrolyte type. *Soft Matter* **2014,** 10, (34), 6530-6545.

72. Antila, H. S.; Sammalkorpi, M. Polyelectrolyte Decomplexation via Addition of Salt: Charge Correlation Driven Zipper. *The Journal of Physical Chemistry B* **2014,** 118, (11), 3226-3234.

73. Yin, M.; Gu, B.; Zhao, Q.; Qian, J.; Zhang, A.; An, Q.; He, S. Highly sensitive and fast responsive fiber-optic modal interferometric pH sensor based on polyelectrolyte complex and polyelectrolyte self-assembled nanocoating. *Analytical and Bioanalytical Chemistry* **2011,** 399, (10), 3623-3631.

74. Suarez-Martinez, P. C.; Robinson, J.; An, H.; Nahas, R. C.; Cinoman, D.; Lutkenhaus, J. L. Spray-On Polymer–Clay Multilayers as a Superior Anticorrosion Metal Pretreatment. *Macromolecular Materials and Engineering* **2017,** 302, (6), 1600552-n/a.

75. Sung, C.; Vidyasagar, A.; Hearn, K.; Lutkenhaus, J. L. Temperature-triggered shape-transformations in layer-by-layer microtubes. *Journal of Materials Chemistry B* **2014,** 2, (15), 2088-2092.

76. Mueller, R.; Köhler, K.; Weinkamer, R.; Sukhorukov, G.; Fery, A. Melting of PDADMAC/PSS Capsules Investigated with AFM Force Spectroscopy. *Macromolecules* **2005,** 38, (23), 9766-9771.

77. Shamoun, R. F.; Hariri, H. H.; Ghostine, R. A.; Schlenoff, J. B. Thermal Transformations in Extruded Saloplastic Polyelectrolyte Complexes. *Macromolecules* **2012,** 45, (24), 9759-9767.

78. Yildirim, E.; Zhang, Y.; Lutkenhaus, J. L.; Sammalkorpi, M. Thermal Transitions in Polyelectrolyte Assemblies Occur via a Dehydration Mechanism. *ACS Macro Letters* **2015,** 4, (9), 1017-1021.

79. Zhang, Y.; Li, F.; Valenzuela, L. D.; Sammalkorpi, M.; Lutkenhaus, J. L. Effect of Water on the Thermal Transition Observed in Poly (allylamine hydrochloride)–Poly (acrylic acid) Complexes. *Macromolecules* **2016,** 49, (19), 7563-7570.

80. Zhang, R.; Zhang, Y.; Antila, H. S.; Lutkenhaus, J. L.; Sammalkorpi, M. Role of Salt and Water in the Plasticization of PDAC/PSS Polyelectrolyte Assemblies. *The Journal of Physical Chemistry B* **2017,** 121, (1), 322-333.

81. Köhler, K.; Shchukin, D. G.; Möhwald, H.; Sukhorukov, G. B. Thermal Behavior of Polyelectrolyte Multilayer Microcapsules. 1. The Effect of Odd and Even Layer Number. *The Journal of Physical Chemistry B* **2005,** 109, (39), 18250-18259.

82. Köhler, K.; Möhwald, H.; Sukhorukov, G. B. Thermal Behavior of Polyelectrolyte Multilayer Microcapsules: 2. Insight into Molecular Mechanisms for the PDADMAC/PSS System. *The Journal of Physical Chemistry B* **2006,** 110, (47), 24002-24010.

83. Zerball, M.; Laschewsky, A.; Köhler, R.; von Klitzing, R. The Effect of Temperature Treatment on the Structure of Polyelectrolyte Multilayers. *Polymers* **2016,** 8, (4), 120.

84. Reid, D. K.; Summers, A.; O'Neal, J.; Kavarthapu, A. V.; Lutkenhaus, J. L. Swelling and Thermal Transitions of Polyelectrolyte Multilayers in the Presence of Divalent Ions. *Macromolecules* **2016,** 49, (16), 5921-5930.

85. Huglin, M. B.; Webster, L.; Robb, I. D. Complex formation between poly(4-vinylpyridinium chloride) and poly[sodium(2-acrylamido-2-methyl propane sulfonate)] in dilute aqueous solution. *Polymer* **1996,** 37, (7), 1211-1215.

86. Boas, M.; Gradys, A.; Vasilyev, G.; Burman, M.; Zussman, E. Electrospinning polyelectrolyte complexes: pH-responsive fibers. *Soft Matter* **2015,** 11, (9), 1739-47.

87. Zhao, Q.; Qian, J.; An, Q.; Yang, Q.; Gui, Z. Synthesis and characterization of solution-processable polyelectrolyte complexes and their homogeneous membranes. *ACS Applied Materials & Interfaces* **2008,** 1, (1), 90-96.

88. Imre, Á. W.; Schönhoff, M.; Cramer, C. A conductivity study and calorimetric analysis of dried poly(sodium 4-styrene sulfonate)/poly(diallyldimethylammonium chloride) polyelectrolyte complexes. *The Journal of Chemical Physics* **2008,** 128, (13), 134905.

89. Lyu, X.; Clark, B.; Peterson, A. M. Thermal transitions in and structures of dried polyelectrolytes and polyelectrolyte complexes. *Journal of Polymer Science Part B: Polymer Physics* **2017,** 55, (8), 684-691.

90. Batys, P.; Luukkonen, S.; Sammalkorpi, M. Ability of the Poisson–Boltzmann equation to capture molecular dynamics predicted ion distribution around polyelectrolytes. *Physical Chemistry Chemical Physics* **2017,** 19, (36), 24583-24593.

91. Zhao, Q.; Lee, D. W.; Ahn, B. K.; Seo, S.; Kaufman, Y.; Israelachvili, J. N.; Waite, J. H. Underwater contact adhesion and microarchitecture in polyelectrolyte complexes actuated by solvent exchange. *Nature Materials* **2016,** 15, (4), 407-412.

92. Zhao, J.; Swartz, L. A.; Lin, W.-f.; Schlenoff, P. S.; Frommer, J.; Schlenoff, J. B.; Liu, G.-y. Three-Dimensional Nanoprinting via Scanning Probe Lithography-Delivered Layer-by-Layer Deposition. *ACS Nano* **2016,** 10, (6), 5656-5662.

93. Zhu, F.; Cheng, L.; Yin, J.; Wu, Z. L.; Qian, J.; Fu, J.; Zheng, Q. 3D Printing of Ultratough Polyion Complex Hydrogels. *ACS Applied Materials & Interfaces* **2016,** 8, (45), 31304-31310.

94. Zhu, Y.; Ahmad, M.; Yang, L.; Misovich, M.; Yaroshchuk, A.; Bruening, M. L. Adsorption of polyelectrolyte multilayers imparts high monovalent/divalent cation selectivity to aliphatic polyamide cation-exchange membranes. *Journal of Membrane Science* **2017,** 537, 177-185.

95. Li, Y.; Lokitz, B. S.; McCormick, C. L. Thermally responsive vesicles and their structural "locking" through polyelectrolyte complex formation. *Angewandte Chemie International Edition* **2006,** 45, (35), 5792-5795.

96. Wang, X.-S.; An, Q.-F.; Zhao, F.-Y.; Zhao, Q.; Lee, K.-R.; Qian, J.-W.; Gao, C.-J. Preparation and separation characteristics of polyelectrolyte complex membranes containing sulfated carboxymethyl cellulose for water–ethanol mixtures at low pH. *Cellulose* **2014,** 21, (5), 3597-3611.

97. Lin, Z.; Chang, J.; Zhang, J.; Jiang, C.; Wu, J.; Zhu, C. A work-function tunable polyelectrolyte complex (PEI: PSS) as a cathode interfacial layer for inverted organic solar cells. *Journal of Materials Chemistry A* **2014,** 2, (21), 7788-7794.

98. JeongáOh, Y.; HwanáCho, I.; YoungáPark, S. Bio-inspired catechol chemistry: a new way to develop a re-moldable and injectable coacervate hydrogel. *Chemical Communications* **2012,** 48, (97), 11895-11897.

99. Tsuchida, E.; Osada, Y.; Abe, K. Formation of polyion complexes between polycarboxylic acids and polycations carrying charges in the chain backbone. *Die Makromolekulare Chemie* **1974,** 175, (2), 583-592.

100. Kabanov, V. A.; Zezin, A. B. SOLUBLE INTERPOLYMERIC COMPLEXES AS A NEW CLASS OF SYNTHETIC POLY-ELECTROLYTES. *Pure and Applied Chemistry* **1984,** 56, (3), 343-354.

101. Lebovka, N., Aggregation of Charged Colloidal Particles. In *Polyelectrolyte Complexes in the Dispersed and Solid State I*, Müller, M., Ed. Springer Berlin Heidelberg: 2014; Vol. 255, pp 57-96.

102. Wang, Q.; Schlenoff, J. B. The Polyelectrolyte Complex/Coacervate Continuum. *Macromolecules* **2014,** 47, (9), 3108-3116.

103. Sukhishvili, S. A.; Kharlampieva, E.; Izumrudov, V. Where Polyelectrolyte Multilayers and Polyelectrolyte Complexes Meet. *Macromolecules* **2006,** 39, (26), 8873-8881.

104. Shamoun, R. F.; Reisch, A.; Schlenoff, J. B. Extruded saloplastic polyelectrolyte complexes. *Advanced Functional Materials* **2012,** 22, (9), 1923-1931.

105. Ghostine, R. A.; Shamoun, R. F.; Schlenoff, J. B. Doping and Diffusion in an Extruded Saloplastic Polyelectrolyte Complex. *Macromolecules* **2013,** 46, (10), 4089-4094.

106. Tirado, P.; Reisch, A.; Roger, E.; Boulmedais, F.; Jierry, L.; Lavalle, P.; Voegel, J. C.; Schaaf, P.; Schlenoff, J. B.; Frisch, B. Catalytic Saloplastics: Alkaline Phosphatase

Immobilized and Stabilized in Compacted Polyelectrolyte Complexes. *Advanced Functional Materials* **2013,** 23, (38), 4785-4792.

107. Reisch, A.; Roger, E.; Phoeung, T.; Antheaume, C.; Orthlieb, C.; Boulmedais, F.; Lavalle, P.; Schlenoff, J. B.; Frisch, B.; Schaaf, P. On the Benefits of Rubbing Salt in the Cut: Self‐Healing of Saloplastic PAA/PAH Compact Polyelectrolyte Complexes. *Advanced Materials* **2014,** 26, (16), 2547-2551.

108. Hariri, H. H.; Schlenoff, J. B. Saloplastic Macroporous Polyelectrolyte Complexes: Cartilage Mimics. *Macromolecules* **2010,** 43, (20), 8656-8663.

109. Böhme, U.; Scheler, U. Hydrodynamic Size and Charge of Polyelectrolyte Complexes†. *The Journal of Physical Chemistry B* **2007,** 111, (29), 8348-8350.

110. Ouyang, W.; Müller, M. Monomodal polyelectrolyte complex nanoparticles of PDADMAC/poly (styrenesulfonate): Preparation and protein interaction. *Macromolecular bioscience* **2006,** 6, (11), 929-941.

111. Sun, H. COMPASS: an ab initio force-field optimized for condensed-phase applications overview with details on alkane and benzene compounds. *The Journal of Physical Chemistry B* **1998,** 102, (38), 7338-7364.

112. *Material Studio Modeling Environment*; Accelrys Software Inc.: San Diego, Calif, USA, 2011.

113. Spyriouni, T.; Vergelati, C. A molecular modeling study of binary blend compatibility of polyamide 6 and poly (vinyl acetate) with different degrees of hydrolysis: an atomistic and mesoscopic approach. *Macromolecules* **2001,** 34, (15), 5306-5316.

114. Sun, H.; Rigby, D. Polysiloxanes: ab initio force field and structural, conformational and thermophysical properties. *Spectrochimica Acta Part A: Molecular and Biomolecular Spectroscopy* **1997,** 53, (8), 1301-1323.

115. Andersen, H. C. Molecular dynamics simulations at constant pressure and/or temperature. *The Journal of Chemical Physics* **1980,** 72, (4), 2384.

116. Leimkuhler, B.; Noorizadeh, E.; Theil, F. A gentle stochastic thermostat for molecular dynamics. *Journal of Statistical Physics* **2009,** 135, (2), 261-277.

117. Samoletov, A. A.; Dettmann, C. P.; Chaplain, M. A. Thermostats for "slow" configurational modes. *Journal of Statistical Physics* **2007,** 128, (6), 1321-1336.

118. Hünenberger, P. H., Thermostat algorithms for molecular dynamics simulations. In *Advanced Computer Simulation*, Dr. Holm, C.; Prof. Dr. Kremer, K., Eds. Springer Berlin Heidelberg: 2005; Vol. 173, pp 105-149.

119. Leimkuhler, B.; Noorizadeh, E.; Penrose, O. Comparing the efficiencies of stochastic isothermal molecular dynamics methods. *Journal of Statistical Physics* **2011,** 143, (5), 921-942.

120. Shuichi, N. Constant temperature molecular dynamics methods. *Progress of Theoretical Physics Supplement* **1991,** 103, 1-46.

121. Ewald, P. Evaluation of optical and electrostatic lattice potentials. *Ann. Phys* **1921,** 64, (253), ll.

122. Karasawa, N.; Goddard III, W. A. Acceleration of convergence for lattice sums. *The Journal of Physical Chemistry* **1989,** 93, (21), 7320-7327.

123. Antila, H. S.; Harkonen, M.; Sammalkorpi, M. Chemistry specificity of DNA-polycation complex salt response: a simulation study of DNA, polylysine and polyethyleneimine. *Physical Chemistry Chemical Physics* **2015,** 17, (7), 5279-5289.

124. Theodorou, D. N.; Suter, U. W. Detailed molecular structure of a vinyl polymer glass. *Macromolecules* **1985,** 18, (7), 1467-1478.

125. Chen, J.; Heitmann, J. A.; Hubbe, M. A. Dependency of polyelectrolyte complex stoichiometry on the order of addition. 1. Effect of salt concentration during streaming current titrations with strong poly-acid and poly-base. *Colloids and Surfaces A: Physicochemical and Engineering Aspects* **2003,** 223, (1), 215-230.

126. Li, D.; Muller, M. B.; Gilje, S.; Kaner, R. B.; Wallace, G. G. Processable aqueous dispersions of graphene nanosheets. *Nat Nano* **2008,** 3, (2), 101-105.

127. Müller, R. H.; Hildebrand, G.; Nitzsche, R.; Paulke, B.-R. Zetapotential und Partikelladung in der Laborpraxis. *PAPERBACK APV* **1996,** 37.

128. Zintchenko, A.; Dautzenberg, H.; Tauer, K.; Khrenov, V. Polyelectrolyte Complex Formation with Double Hydrophilic Block Polyelectrolytes: Effects of the Amount and Length of the Neutral Block. *Langmuir* **2002,** 18, (4), 1386-1393.

129. Sæther, H. V.; Holme, H. K.; Maurstad, G.; Smidsrød, O.; Stokke, B. T. Polyelectrolyte complex formation using alginate and chitosan. *Carbohydrate Polymers* **2008,** 74, (4), 813-821.

130. Dautzenberg, H.; Schuldt, U. T. E.; Grasnick, G.; Karle, P.; MÜLler, P.; LÖHr, M.; Pelegrin, M.; Piechaczyk, M.; Rombs, K. V.; GÜNzburg, W. H.; Salmons, B.; Saller, R. M. Development of Cellulose Sulfate-based Polyelectrolyte Complex

Microcapsules for Medical Applications. *Annals of the New York Academy of Sciences* **1999,** 875, (1), 46-63.

131. van der Gucht, J.; Spruijt, E.; Lemmers, M.; Cohen Stuart, M. A. Polyelectrolyte complexes: Bulk phases and colloidal systems. *Journal of Colloid and Interface Science* **2011,** 361, (2), 407-422.

132. Nam, S. Y.; Lee, Y. M. Pervaporation and properties of chitosan-poly (acrylic acid) complex membranes. *Journal of Membrane Science* **1997,** 135, (2), 161-171.

133. Buchhammer, H.-M.; Mende, M.; Oelmann, M. Formation of mono-sized polyelectrolyte complex dispersions: effects of polymer structure, concentration and mixing conditions. *Colloids and Surfaces A: Physicochemical and Engineering Aspects* **2003,** 218, (1), 151-159.

134. Fortier-McGill, B.; Reven, L. 2H NMR Studies of Polymer Multilayer Capsules, Films, and Complexes. *Macromolecules* **2009,** 42, (1), 247-254.

135. Ibarz, G.; Dähne, L.; Donath, E.; Möhwald, H. Controlled Permeability of Polyelectrolyte Capsules via Defined Annealing. *Chemistry of Materials* **2002,** 14, (10), 4059-4062.

136. Köhler, K.; Shchukin, D. G.; Sukhorukov, G. B.; Möhwald, H. Drastic Morphological Modification of Polyelectrolyte Microcapsules Induced by High Temperature. *Macromolecules* **2004,** 37, (25), 9546-9550.

137. Chen, D.; Chen, J.-T.; Glogowski, E.; Emrick, T.; Russell, T. P. Thin Film Instabilities in Blends under Cylindrical Confinement. *Macromolecular Rapid Communications* **2009,** 30, (4-5), 377-383.

138. Mueller, R.; Daehne, L.; Fery, A. Hollow Polyelectrolyte Multilayer Tubes: Mechanical Properties and Shape Changes. *The Journal of Physical Chemistry B* **2007,** 111, (29), 8547-8553.

139. Shao, L.; Lutkenhaus, J. L. Thermochemical properties of free-standing electrostatic layer-by-layer assemblies containing poly(allylamine hydrochloride) and poly(acrylic acid). *Soft Matter* **2010,** 6, (14), 3363-3369.

140. Jang, W.-S.; Jensen, A. T.; Lutkenhaus, J. L. Confinement Effects on Cross-Linking within Electrostatic Layer-by-Layer Assemblies Containing Poly(allylamine hydrochloride) and Poly(acrylic acid). *Macromolecules* **2010,** 43, (22), 9473-9479.

141. Sung, C.; Hearn, K.; Lutkenhaus, J. Thermal transitions in hydrated layer-by-layer assemblies observed using electrochemical impedance spectroscopy. *Soft Matter* **2014,** 10, (34), 6467-6476.

142. Schlenoff, J. B.; Rmaile, A. H.; Bucur, C. B. Hydration Contributions to Association in Polyelectrolyte Multilayers and Complexes: Visualizing Hydrophobicity. *Journal of the American Chemical Society* **2008,** 130, (41), 13589-13597.

143. Chang, C.; Muccio, D. D.; St. Pierre, T. Determination of the tacticity and analysis of the pH titration of poly(acrylic acid) by proton and carbon-13 NMR. *Macromolecules* **1985,** 18, (11), 2154-2157.

144. Garces, F. O.; Sivadasan, K.; Somasundaran, P.; Turro, N. J. Interpolymer complexation of poly(acrylic acid) and polyacrylamide: structural and dynamic studies by solution- and solid-state NMR. *Macromolecules* **1994,** 27, (1), 272-278.

145. Wang, Z.; Mohwald, H.; Gao, C. Nanotubes protruding from poly (allylamine hydrochloride)-graft-pyrene microcapsules. *ACS Nano* **2011,** 5, (5), 3930-3936.

146. Harris, J. J.; DeRose, P. M.; Bruening, M. L. Synthesis of passivating, nylon-like coatings through cross-linking of ultrathin polyelectrolyte films. *Journal of the American Chemical Society* **1999,** 121, (9), 1978-1979.

147. Choi, J.; Rubner, M. F. Influence of the degree of ionization on weak polyelectrolyte multilayer assembly. *Macromolecules* **2005,** 38, (1), 116-124.

148. Xie, A. F.; Granick, S. Local Electrostatics within a Polyelectrolyte Multilayer with Embedded Weak Polyelectrolyte. *Macromolecules* **2002,** 35, (5), 1805-1813.

149. Sukhishvili, S. A.; Granick, S. Layered, Erasable Polymer Multilayers Formed by Hydrogen-Bonded Sequential Self-Assembly. *Macromolecules* **2002,** 35, (1), 301-310.

150. Thomas, L. C. Modulated DSC Technology (MSDC-2006). *TA Instruments, Inc (www. tainstruments. com), New Castle, DE* **2006**.

151. Sung, C.; Vidyasagar, A.; Hearn, K.; Lutkenhaus, J. L. Effect of Thickness on the Thermal Properties of Hydrogen-Bonded LbL Assemblies. *Langmuir* **2012,** 28, (21), 8100-8109.

152. Hu, C.-H.; Zhang, X.-Z.; Zhang, L.; Xu, X.-D.; Zhuo, R.-X. Temperature- and pH-sensitive hydrogels to immobilize heparin-modified PEI/DNA complexes for sustained gene delivery. *Journal of Materials Chemistry* **2009,** 19, (47), 8982-8989.

153. Hancock, B. C.; Zografi, G. The Relationship Between the Glass Transition Temperature and the Water Content of Amorphous Pharmaceutical Solids. *Pharmaceutical Research* 11, (4), 471-477.

154. Takahara, S.; Yamamuro, O.; Suga, H. Heat capacities and glass transitions of 1-propanol and 3-methylpentane under pressure. New evidence for the entropy theory. *Journal of non-crystalline solids* **1994,** 171, (3), 259-270.

155. Collie, C. H.; Hasted, J. B.; Ritson, D. M. The Dielectric Properties of Water and Heavy Water. *Proceedings of the Physical Society* **1948,** 60, (2), 145.

156. Rana, V. A.; Vyas, A. D.; Mehrotra, S. C. Dielectric relaxation study of mixtures of 1-propanol with aniline, 2-chloroaniline and 3-chloroaniline at different temperatures using time domain reflectometry. *Journal of Molecular Liquids* **2003,** 102, (1–3), 379-391.

157. Ilmain, F.; Tanaka, T.; Kokufuta, E. Volume transition in a gel driven by hydrogen bonding. *Nature* **1991,** 349, (6308), 400-401.

158. Kim, B.-S.; Lebedeva, O. V.; Koynov, K.; Gong, H.; Glasser, G.; Lieberwith, I.; Vinogradova, O. I. Effect of organic solvent on the permeability and stiffness of polyelectrolyte multilayer microcapsules. *Macromolecules* **2005,** 38, (12), 5214-5222.

159. Zacharia, N. S.; DeLongchamp, D. M.; Modestino, M.; Hammond, P. T. Controlling Diffusion and Exchange in Layer-by-Layer Assemblies. *Macromolecules* **2007,** 40, (5), 1598-1603.

160. Aoki, T.; Kawashima, M.; Katono, H.; Sanui, K.; Ogata, N.; Okano, T.; Sakurai, Y. Temperature-Responsive Interpenetrating Polymer Networks Constructed with

Poly(acrylic acid) and Poly(N,N-dimethylacrylamide). *Macromolecules* **1994,** 27, (4), 947-952.

161. Gu, Y.; Zacharia, N. S. Self-Healing Actuating Adhesive Based on Polyelectrolyte Multilayers. *Advanced Functional Materials* **2015,** 25, (24), 3785-3792.

162. Gu, Y.; Ma, Y.; Vogt, B. D.; Zacharia, N. S. Contraction of weak polyelectrolyte multilayers in response to organic solvents. *Soft Matter* **2016,** 12, (6), 1859-1867.

163. Liu, X.; Haddou, M.; Grillo, I.; Mana, Z.; Chapel, J. P.; Schatz, C. Early stage kinetics of polyelectrolyte complex coacervation monitored through stopped-flow light scattering. *Soft Matter* **2016,** 12, (44), 9030-9038.

164. Perry, S. L.; Sing, C. E. PRISM-Based Theory of Complex Coacervation: Excluded Volume versus Chain Correlation. *Macromolecules* **2015,** 48, (14), 5040-5053.

165. Qin, J.; de Pablo, J. J. Criticality and Connectivity in Macromolecular Charge Complexation. *Macromolecules* **2016,** 49, (22), 8789-8800.

166. Blocher, W. C.; Perry, S. L. Complex coacervate-based materials for biomedicine. *Wiley Interdisciplinary Reviews: Nanomedicine and Nanobiotechnology* **2016,** 9, (4).

167. Wang, X.-S.; Ji, Y.-L.; Zheng, P.-Y.; An, Q.-F.; Zhao, Q.; Lee, K.-R.; Qian, J.-W.; Gao, C.-J. Engineering novel polyelectrolyte complex membranes with improved mechanical properties and separation performance. *Journal of Materials Chemistry A* **2015,** 3, (14), 7296-7303.

168. Kremer, T.; Kovačević, D.; Salopek, J.; Požar, J. Conditions Leading to Polyelectrolyte Complex Overcharging in Solution: Complexation of Poly(acrylate) Anion with Poly(allylammonium) Cation. *Macromolecules* **2016,** 49, (22), 8672-8685.

169. Laaser, J. E.; Lohmann, E.; Jiang, Y.; Reineke, T. M.; Lodge, T. P. Architecture-Dependent Stabilization of Polyelectrolyte Complexes between Polyanions and Cationic Triblock Terpolymer Micelles. *Macromolecules* **2016,** 49, (17), 6644-6654.

170. Imre, Á. W.; Schönhoff, M.; Cramer, C. Unconventional Scaling of Electrical Conductivity Spectra for PSS-PDADMAC Polyelectrolyte Complexes. *Physical Review Letters* **2009,** 102, (25), 255901.

171. Cohen Stuart, M. A.; Huck, W. T. S.; Genzer, J.; Muller, M.; Ober, C.; Stamm, M.; Sukhorukov, G. B.; Szleifer, I.; Tsukruk, V. V.; Urban, M.; Winnik, F.; Zauscher, S.; Luzinov, I.; Minko, S. Emerging applications of stimuli-responsive polymer materials. *Nature Materials* **2010,** 9, (2), 101-113.

172. Jaber, J. A.; Schlenoff, J. B. Polyelectrolyte Multilayers with Reversible Thermal Responsivity. *Macromolecules* **2005,** 38, (4), 1300-1306.

173. Nolte, A. J.; Treat, N. D.; Cohen, R. E.; Rubner, M. F. Effect of Relative Humidity on the Young's Modulus of Polyelectrolyte Multilayer Films and Related Nonionic Polymers. *Macromolecules* **2008,** 41, (15), 5793-5798.

174. Gu, Y.; Weinheimer, E. K.; Ji, X.; Wiener, C. G.; Zacharia, N. S. Response of Swelling Behavior of Weak Branched Poly(ethylene imine)/Poly(acrylic acid) Polyelectrolyte Multilayers to Thermal Treatment. *Langmuir* **2016,** 32, (24), 6020-6027.

175. Fu, J.; Abbett, R. L.; Fares, H. M.; Schlenoff, J. B. Water and the Glass Transition Temperature in a Polyelectrolyte Complex. *ACS Macro Letters* **2017,** 6, (10), 1114-1118.

176. Farhat, T. R.; Schlenoff, J. B. Doping-Controlled Ion Diffusion in Polyelectrolyte Multilayers: Mass Transport in Reluctant Exchangers. *Journal of the American Chemical Society* **2003,** 125, (15), 4627-4636.

177. Wu, B.; Wang, X.; Yang, J.; Hua, Z.; Tian, K.; Kou, R.; Zhang, J.; Ye, S.; Luo, Y.; Craig, V. S. J.; Zhang, G.; Liu, G. Reorganization of hydrogen bond network makes strong polyelectrolyte brushes pH-responsive. *Science Advances* **2016,** 2, (8), e1600579.

178. Tekaat, M.; Butergerds, D.; Schonhoff, M.; Fery, A.; Cramer, C. Scaling properties of the shear modulus of polyelectrolyte complex coacervates: a time-pH superposition principle. *Physical Chemistry Chemical Physics* **2015,** 17, (35), 22552-22556.

179. Liu, Y.; Momani, B.; Winter, H. H.; Perry, S. L. Rheological characterization of liquid-to-solid transitions in bulk polyelectrolyte complexes. *Soft Matter* **2017,** 13, (40), 7332-7340.

180. Cramer, C.; De, S.; Schönhoff, M. Time-Humidity-Superposition Principle in Electrical Conductivity Spectra of Ion-Conducting Polymers. *Physical Review Letters* **2011,** 107, (2), 028301.

181. James, W. D.; Hirsch, L. R.; West, J. L.; O'Neal, P. D.; Payne, J. D. Application of INAA to the build-up and clearance of gold nanoshells in clinical studies in mice. *Journal of Radioanalytical and Nuclear Chemistry* **2007,** 271, (2), 455-459.

182. Gobin, A. M.; Lee, M. H.; Halas, N. J.; James, W. D.; Drezek, R. A.; West, J. L. Near-Infrared Resonant Nanoshells for Combined Optical Imaging and Photothermal Cancer Therapy. *Nano Letters* **2007,** 7, (7), 1929-1934.

183. Rivin, D.; Meermeier, G.; Schneider, N. S.; Vishnyakov, A.; Neimark, A. V. Simultaneous Transport of Water and Organic Molecules through Polyelectrolyte Membranes. *The Journal of Physical Chemistry B* **2004,** 108, (26), 8900-8909.

184. Leroy, D.; Martinot, L.; Mignonsin, P.; Strivay, D.; Weber, G.; Jérôme, C.; Jérôme, R. Complexation of uranyl ions by polypyrrole doped by sulfonated and phosphonated polyethyleneimine. *Journal of Applied Polymer Science* **2003,** 88, (2), 352-359.

185. Guinn, V. P.; Hoste, J., Neutron activation analysis. In *Elemental Analysis of Biological Materials*, International Atomic Energy Agency: Austria, 1980; pp 105-140.

186. Lösche, M.; Schmitt, J.; Decher, G.; Bouwman, W. G.; Kjaer, K. Detailed Structure of Molecularly Thin Polyelectrolyte Multilayer Films on Solid Substrates as Revealed by Neutron Reflectometry. *Macromolecules* **1998,** 31, (25), 8893-8906.

187. Gottlieb, H. E.; Kotlyar, V.; Nudelman, A. NMR chemical shifts of common laboratory solvents as trace impurities. *The Journal of organic chemistry* **1997,** 62, (21), 7512-7515.

188. Berendsen, H. J. C.; van der Spoel, D.; van Drunen, R. GROMACS: A message-passing parallel molecular dynamics implementation. *Computer Physics Communications* **1995,** 91, (1–3), 43-56.

189. Lindahl, E.; Hess, B.; van der Spoel, D. GROMACS 3.0: a package for molecular simulation and trajectory analysis. *Journal of molecular modeling* **2001,** 7, (8), 306-317.

190. Jorgensen, W. L.; Tirado-Rives, J. The OPLS [optimized potentials for liquid simulations] potential functions for proteins, energy minimizations for crystals of cyclic peptides and crambin. *Journal of the American Chemical Society* **1988,** 110, (6), 1657-1666.

191. Jorgensen, W. L.; Gao, J. Monte Carlo simulations of the hydration of ammonium and carboxylate ions. *The Journal of Physical Chemistry* **1986,** 90, (10), 2174-2182.

192. Aqvist, J. Ion-water interaction potentials derived from free energy perturbation simulations. *The Journal of Physical Chemistry* **1990,** 94, (21), 8021-8024.

193. Chandrasekhar, J.; Spellmeyer, D. C.; Jorgensen, W. L. Energy component analysis for dilute aqueous solutions of lithium(1+), sodium(1+), fluoride(1-), and chloride(1-) ions. *Journal of the American Chemical Society* **1984,** 106, (4), 903-910.

194. Qiao, B.; Cerdà, J. J.; Holm, C. Poly (styrenesulfonate)− Poly (diallyldimethylammonium) Mixtures: Toward the Understanding of Polyelectrolyte Complexes and Multilayers via Atomistic Simulations. *Macromolecules* **2010,** 43, (18), 7828-7838.

195. Jorgensen, W. L.; Madura, J. D. Temperature and size dependence for Monte Carlo simulations of TIP4P water. *Molecular Physics* **1985,** 56, (6), 1381-1392.

196. Essmann, U.; Perera, L.; Berkowitz, M. L.; Darden, T.; Lee, H.; Pedersen, L. G. A smooth particle mesh Ewald method. *The Journal of Chemical Physics* **1995,** 103, (19), 8577-8593.

197. Bussi, G.; Donadio, D.; Parrinello, M. Canonical sampling through velocity rescaling. *The Journal of Chemical Physics* **2007,** 126, (1), 014101.

198. Parrinello, M.; Rahman, A. Polymorphic transitions in single crystals: A new molecular dynamics method. *Journal of Applied Physics* **1981,** 52, (12), 7182-7190.

199. Hess, B.; Bekker, H.; Berendsen, H. J. C.; Fraaije, J. G. E. M. LINCS: A Linear Constraint Solver for Molecular Simulations. *Journal of Computational Chemistry* **1997,** 18, 1463-1472.

200. Miyamoto, S.; Kollman, P. A. SETTLE: an analytical version of the SHAKE and RATTLE algorithm for rigid water models. *Journal of Computational Chemistry* **1992,** 13, (8), 952-962.

201. Martínez, L.; Andrade, R.; Birgin, E. G.; Martínez, J. M. PACKMOL: a package for building initial configurations for molecular dynamics simulations. *Journal of Computational Chemistry* **2009,** 30, (13), 2157-2164.

202. Humphrey, W.; Dalke, A.; Schulten, K. VMD: visual molecular dynamics. *Journal of Molecular Graphics* **1996,** 14, (1), 33-38.

203. Zhang, B.; Hoagland, D. A.; Su, Z. Ionic Liquids as Plasticizers for Polyelectrolyte Complexes. *The Journal of Physical Chemistry B* **2015,** 119, (8), 3603-3607.

204. McCormick, M.; Smith, R. N.; Graf, R.; Barrett, C. J.; Reven, L.; Spiess, H. W. NMR Studies of the Effect of Adsorbed Water on Polyelectrolyte Multilayer Films in the Solid State. *Macromolecules* **2003,** 36, (10), 3616-3625.

205. Walrafen, G. E. Raman Spectral Studies of HDO in H2O. *The Journal of Chemical Physics* **1968,** 48, (1), 244-251.

206. Chen, L.; Hallinan, D. T.; Elabd, Y. A.; Hillmyer, M. A. Highly Selective Polymer Electrolyte Membranes from Reactive Block Polymers. *Macromolecules* **2009,** 42, (16), 6075-6085.

207. Dong, B.; Gwee, L.; Salas-de la Cruz, D.; Winey, K. I.; Elabd, Y. A. Super Proton Conductive High-Purity Nafion Nanofibers. *Nano Letters* **2010,** 10, (9), 3785-3790.

208. McAloney, R. A.; Sinyor, M.; Dudnik, V.; Goh, M. C. Atomic force microscopy studies of salt effects on polyelectrolyte multilayer film morphology. *Langmuir* **2001,** 17, (21), 6655-6663.

209. Klitzing, R. v. Internal structure of polyelectrolyte multilayer assemblies. *Physical Chemistry Chemical Physics* **2006,** 8, (43), 5012-5033.

210. O'Neal, J. T.; Wilcox, K. G.; Zhang, Y.; George, I. M.; Lutkenhaus, J. L. Influence of Limited Hydration and Counterion Type on the Glass Transition Temperature of Electrostatic Layer-by-Layer Assemblies. *Manuscript in preparation* **2018**.

211. Volodkin, D.; von Klitzing, R. Competing mechanisms in polyelectrolyte multilayer formation and swelling: Polycation–polyanion pairing vs. polyelectrolyte–ion pairing. *Current Opinion in Colloid & Interface Science* **2014,** 19, (1), 25-31.

212. Kovacevic, D.; van der Burgh, S.; de Keizer, A.; Cohen Stuart, M. A. Kinetics of Formation and Dissolution of Weak Polyelectrolyte Multilayers: Role of Salt and Free Polyions. *Langmuir* **2002,** 18, (14), 5607-5612.

213. Wypych, G., *Handbook of plasticizers*. ChemTec Publishing: 2004.

214. Immergut, E. H.; Mark, H. F., Principles of Plasticization. In *Plasticization and Plasticizer Processes,* AMERICAN CHEMICAL SOCIETY: 1965; Vol. 48, pp 1-26.

215. Hodge, R. M.; Bastow, T. J.; Edward, G. H.; Simon, G. P.; Hill, A. J. Free Volume and the Mechanism of Plasticization in Water-Swollen Poly(vinyl alcohol). *Macromolecules* **1996,** 29, (25), 8137-8143.

216. White, N.; Misovich, M.; Yaroshchuk, A.; Bruening, M. L. Coating of Nafion Membranes with Polyelectrolyte Multilayers to Achieve High Monovalent/Divalent Cation Electrodialysis Selectivities. *ACS Applied Materials & Interfaces* **2015,** 7, (12), 6620-6628.

217. Dressick, W. J.; Wahl, K. J.; Bassim, N. D.; Stroud, R. M.; Petrovykh, D. Y. Divalent–Anion Salt Effects in Polyelectrolyte Multilayer Depositions. *Langmuir* **2012,** 28, (45), 15831-15843.

218. Yu, J.; Mao, J.; Yuan, G.; Satija, S.; Jiang, Z.; Chen, W.; Tirrell, M. Structure of Polyelectrolyte Brushes in the Presence of Multivalent Counterions. *Macromolecules* **2016,** 49, (15), 5609-5617.

219. Barreira, S. V.; García-Morales, V.; Pereira, C. M.; Manzanares, J. A.; Silva, F. Electrochemical impedance spectroscopy of polyelectrolyte multilayer modified electrodes. *The Journal of Physical Chemistry B* **2004,** 108, (46), 17973-17982.

220. Silva, T. H.; Garcia-Morales, V.; Moura, C.; Manzanares, J. A.; Silva, F. Electrochemical Impedance Spectroscopy of Polyelectrolyte Multilayer Modified Gold Electrodes: Influence of Supporting Electrolyte and Temperature. *Langmuir* **2005,** 21, (16), 7461-7467.